

Radiologic Assessment of the Patient with Spine Pain

Timothy P. Maus

Imaging is a significant, but not independent, component of the multifaceted evaluation of the patient with spine or limb pain. Imaging must be interpreted in concert with the history, physical exam, electrodiagnostic evaluation, and responses to image-guided anesthetic or provocative procedures. It does not stand alone, but can only be understood in its proper context: the individual patient's unique syndrome of pain or neurologic dysfunction.

Pain of spinal origin is extremely common; low back pain is the second most common cause of symptomatic office visits in the United States.^{1,2} There is a nearly 75% lifetime prevalence of back pain in the United States,³ and one third of U.S. adults report back pain in the previous 3 months.¹ Advanced imaging is applied to this complaint with ever-increasing frequency; the number of lumbar magnetic resonance imaging (MRI) scans among Medicare beneficiaries rose fourfold from 1994 to 2005.⁴ Over 40% of patients with acute low back pain underwent immediate imaging in a private insurance claims database study.⁵ In another Medicare-based study of low back pain patients without red flags for systemic disease, nearly 30% underwent imaging (radiography or advanced imaging) within 28 days.⁶ In a study in an emergency department environment, the use of advanced imaging (computed tomography [CT] or MRI) for low back pain tripled from 2002 to 2006.⁷ Approximately one third of Medicare low back pain patients who undergo outpatient MRI studies have not received any prior conservative therapy.⁸

Despite this intensity of imaging and the downstream effects of increasing minimally invasive interventions and surgical procedures that flow from them, there is no evidence that patient outcomes are improving. Measures of physical functioning, work/school limitations, and mental health in U.S. adults with back or neck complaints were similar or worse in 2005 than in 1997.⁹ A regional study (North Carolina) demonstrated that the proportion of adults with chronic low back pain causing activity impairment rose from 3.9% in 1992 to 10.2% in 2006.¹⁰ A review article by Chou, Deyo, and Jarvik examined the evidence for our inefficient utilization of imaging in the back pain patient, underlying causal forces and mechanisms for initiating improvements.¹¹ The purpose of this chapter is to foster the rational decision making they advocate in the use of spine imaging, based on evidence, as we in the pain management community seek to improve patient outcomes.

THE GOAL OF IMAGING

The primary goal of imaging in the patient with spine or limb pain is to identify patients who are suffering from an

undiagnosed systemic process causal of the pain/dysfunction syndrome. This is an uncommon phenomenon. An analysis by Jarvik and Deyo¹² suggests that 95% of low back pain is due to benign processes. In patients presenting to a primary care setting with low back pain, only 0.7% suffer from undiagnosed metastatic neoplasm. Spine infection, including pyogenic and granulomatous diskitis, epidural abscess, or viral processes, is present in only 0.01% of subjects. Noninfectious inflammatory spondyloarthropathies, such as ankylosing spondylitis, account for 0.3% of presentations. Osteoporotic compression fractures are the most common systemic pathologic process to present as back pain, accounting for 4% of patients.¹² Imaging seeks to identify the approximately 5% of patients with back or limb pain who have undiagnosed systemic disease as the etiology of their pain. A related imaging goal is to characterize and assist in therapy planning in the very small percentage of patients who have neural compressive disease resulting in radiculopathy or radicular pain syndromes that fail conservative therapy and require surgical or minimally invasive intervention.

SPECIFICITY: ASYMPTOMATIC IMAGING FINDINGS

The low prevalence of systemic disease as a cause of back pain implies that most imaging studies primarily describe what are often, and inappropriately, termed “degenerative” phenomena. These may include anterior and lateral vertebral body osteophytes, loss of T2 signal in the intervertebral disk, and structural changes of facet arthrosis. Degeneration is a pejorative term implying disease; these changes have no relationship to pain syndromes and correlate only with age. They are best referred to as age or age-related change. These age changes are typically relatively uniform across the spine, although the lowest lumbar segments are over-represented. Evidence for the lack of specificity of such imaging findings for spine pain syndromes is evident in cadaver studies, imaging studies in asymptomatic populations, and population studies.

Nathan¹³ described the presence of anterior and lateral osteophytes in 100% of cadavers at the age of 40, whereas posterior osteophytes are present only in a minority of cadavers at 80 years of age. Hult¹⁴ studied adults with spine radiographs and showed that by age 50 years, 87% will have radiographic evidence of disk age-related change (narrowing of the disk space, marginal sclerosis with osteophytes, vacuum phenomena). In a second study including a cohort of asymptomatic workers, Hult¹⁵ noted radiographic evidence of disk

Table 15.1 Imaging Abnormalities in Asymptomatic Subjects

Test	Author (reference), Date	Patients (N)	Age Range (mean)	Disk Herniation	Disk Bulge	Disk Degeneration	Central Canal Stenosis	Annular Fissure
X-ray	Hult ⁽¹⁵⁾ 1954	1200	40-44			56%		
X-ray	Hellstrom ⁽²⁰⁾ 1990	143	14-25			95%		
Myelogram	Hitselberger ⁽¹⁶⁾ 1968	300	(51)	31%		20%		
CT	Wiesel ⁽¹⁷⁾ 1984	51	(40)	20%			3.4%	
MRI	Weinreb ⁽²¹⁾ 1989	86	(28)	9%	44%			
MRI	Boden ⁽¹⁸⁾ 1990	53	< 60	22%	54%	46%	1%	
MRI	Jensen ⁽²²⁾ 1994	98	≥ 60	36%	79%	93%	21%	
MRI	Jensen ⁽²²⁾ 1994	98	(42)	28%	52%		7%	
MRI	Boos ⁽²³⁾ 1995	46	(36)	76%	51%	85%		
MRI	Stadnik ⁽²⁴⁾ 1998	36	(42)	33%	81%	56%		56%
MRI	Weishaupt ⁽²⁵⁾ 1998	60	(35)	60%	28%	72%		20%
MRI	Jarvik ⁽¹⁹⁾ 2001	148	(54)	38%	64%	91%	10%	38%

From Maus T. Imaging the back pain patient. *Phys Med Rehabil Clin N Am.* 2010; 21:725-766, Table 3.

“disease” in 56% of those aged 40 to 44 years, which rose to 95% in subjects 50 to 59 years old. With the evolution of more sophisticated spine imaging techniques, this lack of specificity of degenerative findings has not improved. Hitselberger and Witten¹⁶ studied plain myelography of asymptomatic volunteers and noted that 24% showed abnormalities that would have been considered significant in a clinical context of back or leg pain. A study of lumbar spine CT in asymptomatic volunteers by Wiesel and colleagues¹⁷ showed that in patients older than 40 years, 50% had “significant” abnormalities. Similarly, Boden and colleagues¹⁸ evaluated MRI of the lumbar spine in asymptomatic volunteers; in patients older than 60 years, 57% had abnormalities that would have been considered significant in an appropriate clinical setting. Jarvik and colleagues¹⁹ studied a large patient population with MRI. This study noted that only extrusions, moderate to severe central canal stenosis, and direct visualization of neural compression were likely to be significant and would separate patients with pain from asymptomatic volunteers. Disk protrusions, zygapophysial joint (z-joint or facet joint) arthrosis, and anterolisthesis or retrolisthesis were virtually always asymptomatic findings. Imaging studies of asymptomatic volunteers are compiled in Table 15.1.²⁰⁻²⁵

A study by Kanayama²⁶ in 200 healthy adults (mean age 40, with no current complaint or therapy for back pain nor any history of lumbar surgery) segregated lumbar MRI findings by segmental level (Table 15.2). Asymptomatic T2 signal loss and disk herniations were most common at the L4 and L5 segmental levels; this series also had a high prevalence of asymptomatic high intensity zones (HZ) (24% at L4 and L5). More recent studies have addressed the prevalence of disk “degenerative” imaging findings (T2 signal loss, loss of disk space height) in younger populations, primarily in

Scandinavian countries; these are MRI population-based studies without regard to symptomatology. Kjaer and colleagues,²⁷ studying children age 13 years, found a 21% prevalence of disk “degeneration.” In a study of adolescents, Salminen and colleagues²⁸ found a 31% prevalence of disk “degeneration” in 15-year-olds, which rose to 42% in 18-year-olds. Takatalo and colleagues²⁹ evaluated 558 young adults aged 20 to 22 years. Using the 5-point Pfirrmann classification of disk degeneration, they noted disk degeneration of grade 3 or higher in 47% of these young adults. There was a higher prevalence in males (54%) than in females (42%). Multilevel degeneration was identified in 17%.

As in the lumbar region, age changes in the cervical and thoracic spine are common, asymptomatic, and increase in prevalence with age. Matsumoto studied nearly 500 asymptomatic patients with MRI; he noted a loss of T2 signal within cervical disks in 12% to 17% of patients in their twenties, but in 86% to 89% of patients older than 60 years of age.³⁰ Asymptomatic cervical cord compression was observed in 7.6% of patients, largely over the age of 50. Similarly, Boden studied 63 asymptomatic subjects with MRI and noted cervical disk “degeneration” in 25% of those younger than 40, and in excess of 60% of patients older than 40 years of age.³¹ Asymptomatic subjects older than 40 years of age had a 5% rate of disk herniations and a 20% rate of foraminal stenosis. Teresi studied 100 asymptomatic subjects with MRI and noted asymptomatic cervical cord compression in 7% and either disk protrusion or annular bulge in 57% of subjects older than 64 years of age.³² In the thoracic spine, Wood studied 90 asymptomatic patients with MRI.³³ In this population, 73% of the patients had positive thoracic imaging findings, 37% had disk herniations, 53% demonstrated disk bulges, and asymptomatic cord deformity was present in 29%.

Table 15.2 Segmental Distribution of Asymptomatic Lumbar Age-Related Change

Segment	Disk Herniation	Nuclear T2 Signal Loss	Modic Change	HIZ
L1	0.5%	7%	1%	0%
L2	3.5%	12%	3%	4%
L3	16.5%	15.5%	4%	5%
L4	25%	49.5%	11%	23.5%
L5	35%	53%	10%	24%

Data abstracted from Kanayama M, Togawa D, Takahashi C, et al. Cross-sectional magnetic resonance imaging study of lumbar disk degeneration in 200 healthy individuals. *J Neurosurg Spine*. 2009;11:501-507.

The evidence is deep and overwhelming. The structural spine imaging findings most commonly referred to as “degenerative changes” or “degenerative disk disease,” including anterior and lateral osteophytes, loss of T2 signal in the disk, loss of disk space height, disk bulges and protrusions, and facet arthrosis, are ubiquitous and unassociated with pain syndromes; their only association is with age. They can only be avoided by a youthful death. They are not a disease state and are best referred to as normal age change or age-related change.

A consequence of this high prevalence of asymptomatic age-related changes is that the imager must know the nature of the pain syndrome if he or she is to properly focus on findings significant to the unique patient under consideration. There must be concordance of the imaging finding and the pain syndrome it is postulated to elicit. Imaging cannot prove causation, hence the need for anesthetic and provocative procedures. Communication regarding the nature of the pain syndrome is essential, whether this occurs through a robust electronic medical record, an intake document at the imaging site, or direct interaction of the imager with the patient.

SENSITIVITY: PHYSIOLOGIC IMAGING

There is also a major sensitivity fault associated with spine imaging. The majority of patient symptoms referable to the spine occur in axially loaded positions, either sitting or standing. A substantial portion of radiographs and most advanced imaging (CT and MRI) are obtained in a recumbent position, removing the effects of axial load and physiologic posture. This may fail to reveal the lesion responsible for the index pain.

There is ample evidence of the effect of axial load and physiologic posture on the biomechanical and structural characteristics of the spine, derived from biomechanical, cadaver, and imaging studies. Lumbar intradiskal pressures are higher when sitting or standing than when in a recumbent position.³⁴ The cadaver study of Inufusa demonstrated a reduction in the cross-sectional area of the lumbar central canal and lateral recesses in extension, with an increase in flexion.³⁵ Lumbar neural foraminal cross section is also diminished in extension and increased in flexion. Fujiwara noted a reduction in cadaveric lumbar neural foraminal area with side bending or rotation toward the index foramen; an increase in area was observed with side bending or rotation away from the foramen.³⁶ Studying normal volunteers, Schmid observed a 40-mm² reduction in the cross-sectional

area of the dural sac at the L3-L4 level with movement from flexion to extension.³⁷ The lumbar neural foraminal cross-sectional area was reduced by 23% in moving from an upright neutral to an upright extended position. Danielson³⁸ noted a significant decrease in the dural sac cross-sectional area with axial loading in 56% of subjects, most commonly at L4-L5; this was more common with increasing age. Dynamic reduction in dural sac area with loading was less frequent in normal volunteers than in a population of patients with neurogenic intermittent claudication. Hansson and colleagues identified the ligamentum flavum as the most important structure resulting in dynamic reduction in the lumbar central canal area under physiologic loading.³⁹ Physiologic posture (lumbar lordosis) is likely more important than axial load.⁴⁰ Multiple studies in patients with upright imaging have demonstrated the enlargement of lumbar disk bulges or protrusions with axial load, which may be further exacerbated with extension.^{41,42} Synovial cysts, which may be provocative of radicular pain syndromes or contribute to neurogenic intermittent claudication, may be undetectable on recumbent imaging when synovial fluid remains in the facet joint space. Upon the assumption of axial load and apposition of the facet articular surfaces, the fluid is forced from the joint space into the cyst, where it may act as a neural compressive lesion.

The cervical spine similarly exhibits dynamic physiologic change with posture and load. Cadaveric studies have demonstrated increased disk bulging and buckling of the ligamentum flavum in cervical spine extension; the ligamentum flavum effect was most significant.⁴³ MRI studies of patients^{44,45} noted an increase in central canal stenosis with both extension and flexion of the cervical spine relative to neutral posture; the decrease was most marked in extension. Cervical neural foramina diminish in cross section, width, and height in extension and increase in all these parameters in flexion.⁴⁶

In summary, physiologic extension and axial load reduce the area of all lumbar spine compartments; these are increased in flexion. The cervical central canal is diminished in areas in extension more so than in flexion; it is maximal in the neutral position. Cervical foramina increase in all dimensions in flexion and diminish in extension. These dynamic changes constitute the greatest sensitivity fault in imaging: conventional supine imaging may fail to reveal a lesion that is causal of the patient’s symptoms when that lesion is only expressed in physiologic postures.

Several methods have been devised to overcome this sensitivity fault. Radiographs should always be obtained upright; this allows assessment of sagittal and coronal balance in a physiologic posture. Flexion-extension radiographs may detect instability not observed on neutral upright views, but the yield

of diagnostic information is very low. In studies in both the lumbar and cervical spine segments, less than 1% of flexion-extension radiographic studies provided information over that noted on static upright radiographs.^{47,48} The cost and radiation exposure is best deferred to a presurgical setting, not during an initial evaluation of the back or neck pain patient.

Advanced imaging can be performed with axial loading devices on conventional CT or MRI scanners. These devices can improve the sensitivity to the detection of clinically significant central canal compromise.⁴⁹ The 2011 North American Spine Society's evidence-based guidelines on evaluation and treatment of spinal stenosis suggest axially loaded imaging in the setting of suspected neurogenic intermittent claudication and stenosis unconfirmed by conventional imaging, with a canal diameter of less than 110 mm.^{22,50} Willén and colleagues demonstrated that surgical results of cases of occult lumbar spinal stenosis detected only by axially loaded MRI were comparable to those of stenosis observed in unloaded MRI examinations.⁵¹

MRI scanning in an upright position—sometimes referred to as dynamic, positional, or kinetic MRI—is now commercially available and widely marketed. The practical challenge is that currently available systems are of low field strength (0.6T), with an unavoidable reduction in image quality. This reduction in image quality can have important consequences for clinical image interpretation. If current low field strength dynamic systems were applied selectively to cases where conventional imaging failed to demonstrate a correlative lesion causal of the patient's pain, the patient would likely benefit. All too often, however, the cost of these systems results in their routine use, or even promotion as the best available imaging tool for all spine conditions. This practice could harm patients, as diminished image quality reduces sensitivity to the detection of sinister lesions, which is the primary goal of imaging the back pain patient (Fig. 15.1).

VALIDITY

Spine imaging must be undertaken with a full understanding of the specificity and sensitivity faults inherent in its use. The ultimate question, of course, is one of validity: Does performing an imaging study of the spine segment in question result in improved patient outcomes through a more timely and accurate diagnosis of the process causing the patient's pain? This is well studied, particularly in the application of imaging to the acute presentation of back pain. Chou and colleagues performed a meta-analysis of the six randomized controlled trials (n = 1804) examining the role of imaging in the acute presentation of back or limb pain with no clinical features suggesting systemic disease.⁵² They identified no benefit in pain, function, quality of life, or patient-rated improvement in patients undergoing imaging (radiographs, CT, or MRI) at presentation versus those undergoing clinically directed conservative care. Although routine imaging might have been expected to provide reassurance, imaged patients did not have better psychological outcomes.

Carragee and colleagues elegantly demonstrated the lack of utility of imaging in the acute setting in a 5-year prospective observational study.⁵³ A cohort of asymptomatic subjects deemed to be at risk for back pain resulting from labor-intensive vocations underwent lumbar spine MRI. This patient cohort was followed periodically over the

subsequent 5 years; a subset of these subjects presented to a medical care provider with acute back or leg pain during this 5-year period and a second lumbar MRI was obtained. Less than 5% of the MRI scans obtained at the time of acute presentation with back or leg pain showed clinically relevant new findings; virtually all of the “positive findings” noted on the images at the time of presentation with back/leg pain had been present on the baseline studies obtained when the patient was asymptomatic. Only direct evidence of neural compression in patients with a corresponding radicular pain syndrome was considered to be useful imaging information. Of particular note, psychosocial factors, not the morphology seen on imaging, were the best predictors of the degree of functional disability caused by back or leg pain.⁵³

A study by Modic,⁵⁴ also in the acute presentation of low back pain or radiculopathy, showed no relationship between the extent of disk herniations and presenting signs or symptom. The type, size, or location of a herniation at presentation, or change in size or type over time, did not correlate with clinical outcomes. MRI imaging characteristics did not have measurable value in planning conservative care. The study emphasized that the surgical decisions must be made on clinical grounds, given the inability of imaging to predict outcomes. The Modic study, like that of Carragee, demonstrated that psychosocial factors predict functional disability better than imaging parameters.⁵⁴

Although the depth of evidence regarding the inability of imaging to improve outcomes in back and limb pain patients is most profound in the acute setting, it applies more broadly as well. Chou and colleagues¹¹ explored the seemingly counterintuitive finding that routine imaging does not lead to better outcomes in back or limb pain. This lack of utility can be attributed to the favorable natural history of back and limb pain, the low prevalence of sinister disease as causal of back pain, the weak correlation between imaging findings and symptoms (the specificity fault), and the minimal impact of imaging on clinical decision making. Given the demonstrable modest utility of imaging, the decision to undertake this path must be a carefully reasoned one.

IMAGING RISK/BENEFIT

The decision to proceed with any medical test or procedure should be preceded by a consideration of likely benefit weighed against risk or actual harms. Certainly there are benefits to be derived from imaging. Foremost, imaging may suggest the diagnosis of previously unsuspected systemic disease. In the patient with a radicular pain syndrome or radiculopathy that has not responded to conservative therapy, imaging may supply invaluable information that allows planning of minimally invasive or surgical procedures. Negative imaging should also have value in providing reassurance that there is no sinister disease present and in stopping further workup in appropriate circumstances. Finally, in patients with chronic pain syndromes, imaging may assist in the identification of the structural or inflammatory cause of such pain. Only when a specific pain generator is identified can a specific plan of therapeutic intervention, whether it be conservative or invasive, be developed.

There are direct harms and potential risks associated with imaging, which must be balanced against potential benefits. These include radiation dose, cost, the labeling effect, and

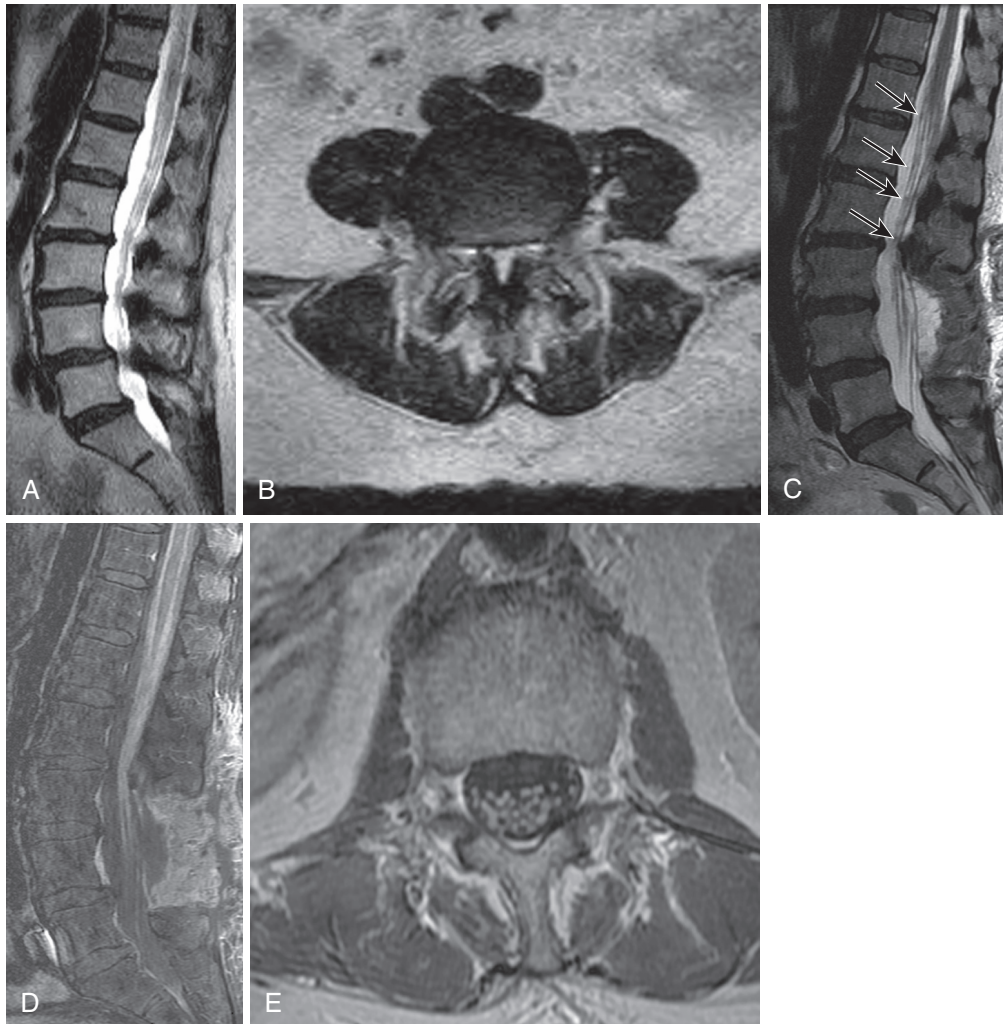


Figure 15.1 Diminished sensitivity of low field strength upright MRI to sinister lesions. A 74-year-old female presented with bilateral lower extremity weakness and pain with a low field strength upright MRI from another institution. Sagittal T2 image (A) and axial T2 image (B) at the L4 level show degenerative spondylolisthesis at L4 with central canal compromise. She underwent an L3-L5 decompression without change in symptoms. A 1.5 Tesla MRI performed 3 weeks postoperatively demonstrated nodularity (arrows) in the cauda equina on a T2 sagittal image (C). Gadolinium-enhanced fat-saturated T1 sagittal (D) and axial (E) images demonstrate diffuse leptomeningeal metastases from breast cancer. She died in 2 months. A high-quality preoperative MRI would have likely led to the diagnosis and avoided an unnecessary operation. (From Khalil JG, Nassr A, Maus TP. Physiologic imaging of the spine. *Radiol Clin North Am.* 2012;50:599-611.)

the downstream risk of provoking minimally invasive or surgical interventions of dubious efficacy.

Radiation dose in radiography, CT or CT/myelography, and nuclear medicine studies constitutes a direct patient harm. Radiation exposure from radiographs, CT, and nuclear medicine studies carries a cumulative risk of neoplasm induction. This risk becomes particularly problematic when serial studies are performed. The biologically effective absorbed radiation dose is measured by the Sievert (Sv); in North America, the average annual natural background exposure is approximately 3 mSv.⁵⁵ A frontal and lateral chest radiograph is often considered the common currency of radiation exposure, incurring a dose of approximately 0.1 mSv. A three-view lumbar spine radiographic series is then worth approximately 15 chest radiographs, or 1.5 mSv; cervical spine radiographs incur a dose 0.2 mSv. A dose of 6 mSv is typical for a lumbar spine CT scan, a value of 60 chest radiographs. Cervical spine CT incurs 2 mSv, or 20 chest radiographs. A technetium bone scan has a dose of 6.3 mSv. The cumulative radiation exposure creates real harm;

the 2.2 million lumbar spine CT scans performed in the United States in 2007 were projected to result in 1200 future cancers.⁵⁶ Although less radiation intensive, lumbar radiography is performed much more frequently than CT and contributes nearly fivefold the cumulative radiation burden to the U.S. population.⁵⁷ The average annual radiation exposure from lumbar radiographs is 75 times that of chest radiography.⁵⁷ Radiation risks of spine imaging are made more acute by the necessary inclusion of radiosensitive tissues, the gonadal structures in the pelvis, and the thyroid in the neck.

Imaging studies of the spine are costly. In the United States, the medical imaging community incurs more than \$100 billion of societal cost per year. The 2012 Medicare reimbursements⁵⁸ for lumbar spine imaging include radiographs: \$41; noncontrast CT: \$264; myelogram: \$506; noncontrast MRI: \$439; whole-body positron emission tomography (PET)/CT: \$1183; bone scan with single-photon emission CT (SPECT): \$261.¹⁸ Nominal fees are typically 3 to 5 times the Medicare reimbursements. It is easy to appreciate how quickly imaging costs can accrue.

The labeling effect refers to the inevitable identification of age-related change, usually described as “degenerative change,” or “degenerative disk disease” on imaging studies obtained in evaluation of back or limb pain. The patient may then perceive that he or she suffers from a degenerative spine condition; the term *degenerative* has only negative connotations. Fearing further damage to their “degenerative” spine, they may give up favorite activities and exercise, resulting in deconditioning and contributing to depression. These fear-avoidance behaviors can be a major impediment to recovery. In a study in which back pain patients were randomized to either receiving or being blinded to the results of their MRI imaging, those who were privy to the results (which were all benign) had a lesser sense of well-being.⁵⁴ A study of subacute or chronic back pain patients showed that those who underwent spine radiography reported more pain, had a diminished global health state, and consumed more follow-up care than those who were not imaged.⁵⁹ These findings emphasize the need for patient education regarding the insignificance of age-related imaging findings; imaging professionals should carefully choose descriptive language in imaging reports and avoid the use of pejorative terms such as “degenerative change.”

Finally, and most ominously, imaging may precipitate interventions that have little evidence of efficacy and expose the patient to harm. Jarvik and colleagues⁶⁰ documented that obtaining advanced imaging (MRI) early in a patient’s spine pain syndrome leads to increased surgical interventions despite equivalent pain and disability profiles, when compared with un-imaged patients. Likewise, Lurie and colleagues⁶¹ examined the dramatic regional variation (12-fold) in the rate of surgical intervention for central canal stenosis. These investigators noted that the rate of surgical intervention correlated directly with the intensity of CT and MRI use. Webster and colleagues, evaluating subjects with acute job-related back pain, noted that undergoing an MRI in the first month of symptoms was associated with an eightfold increased risk for surgery and a fivefold risk for more medical care consumption than that noted for clinically matched, un-imaged subjects.⁶² Many of the interventions directed toward spine pain, both surgical and minimally invasive, have only modest, if any, evidence basis.

IMAGING RECOMMENDATIONS

Imaging is performed to identify sinister disease as a cause of a patient’s back or limb pain. Spine imaging has major specificity and sensitivity faults. The decision to initiate imaging must occur as a reasoned decision, weighting potential benefit against real harms and risk. The evidence is clear that there is no benefit to imaging in the acute presentation of back or limb pain in the absence of signs or symptoms of systemic disease. These principles are firmly based on evidence and have led to the imaging guidelines promulgated by several scientific societies.

These guidelines are not new. In 1994, the Agency for Health Care Policy and Research recommended against imaging patients with back pain within the first month of a pain syndrome in the absence of signs of systemic disease.⁶³ The American College of Radiology (ACR) consensus practice guidelines were restated in 2009.⁶⁴ Imaging is not indicated in the patient who presents with acute low back pain

with or without radiculopathy except in the presence of “red flag” features including the following:

- Recent significant trauma, minor trauma in a patient older than 50 years
- Unexplained weight loss
- Unexplained fever
- Immunosuppression
- History of neoplasm
- Prolonged steroid use or osteoporosis
- Age greater than 70 years
- Known intravenous drug abuse
- Progressive neurologic deficit with intractable symptoms
- Duration longer than 6 weeks

A 2007 joint recommendation from the American College of Physicians (ACP) and the American Pain Society stated that imaging should not be obtained in patients with non-specific low back pain.⁶⁵ Imaging should only be performed when severe or progressive neurologic deficits are present or when serious underlying systemic disease is suspected. Furthermore, patients with signs or symptoms of radiculopathy or spinal stenosis should be imaged only if they are candidates for surgical or minimally invasive intervention (e.g., epidural steroid injection). In a further elaboration on these guidelines, the ACP, in its initiative to promote high-value medical care, provided more specific imaging recommendations based on clinical scenarios (Table 15.3).⁶⁶

There is evidence that of the small proportion of subjects with sinister disease as the cause of their back or limb pain, virtually all have risk factors that trigger imaging under these guidelines. A retrospective study of 963 patients presenting with acute low back pain noted that the 8 subjects with neoplasm all had clinical risk factors.⁶⁷ In a prospective study of 1170 acute low back pain patients without clinical risk factors, no cases of neoplasm were found.⁶⁸ No sinister disease was missed in the absence of clinical risk factors in a subsequent systematic review.⁶⁹

Despite these well-supported, evidence-based guidelines, clinical practice in the United States remains greatly divergent from this ideal. By one estimate, between one third and two thirds of all advanced spine imaging is inappropriate when measured against existing guidelines.⁴ Utilization of spine imaging is accelerating despite a complete lack of evidence of its effectiveness in improving the outcomes of back and limb pain patients. Chou and colleagues have enumerated causes of this overutilization: inappropriate patient expectations, direct and indirect financial incentives on the part of providers, defensive medicine, and provider time constraints.¹¹ These issues present great challenges to imaging professionals and those who utilize imaging to improve the clinical state of their patients. Solutions will undoubtedly be multifactorial, but education of the patient, the imaging professional, and imaging consumers would seem to be at the heart of the matter. It is hoped that the evidence presented here will assist in more rational decision making regarding imaging the spine pain patient (Box 15.1).

RADIOGRAPHS

With the failure of clinically directed conservative care, and having made a reasoned decision to initiate imaging of

Table 15.3 Suggestions for Imaging in Patients with Acute Low Back Pain

Imaging Action and Clinical Situation	Suggestions for Initial Imaging
Immediate Imaging	
Radiography plus erythrocyte sedimentation rate*	Major risk factors for cancer (new onset of low back pain with history of cancer, multiple risk factors for cancer, or strong clinical suspicion for cancer)
Magnetic resonance imaging	Risk factors for spinal infection (new onset of low back pain with fever and history of intravenous drug use or recent infection) Risk factors for or signs of the cauda equina syndrome (new urine retention, fecal incontinence, or saddle anesthesia) Severe neurologic deficits (progressive motor weakness or motor deficits at multiple neurologic levels)
Defer Imaging after a Trial of Therapy	
Radiography with or without erythrocyte sedimentation rate	Weaker risk factors for cancer (unexplained with weight loss or age > 50 years) Risk factors for or signs of ankylosing spondylitis (morning stiffness that improves with exercise, alternating buttock pain, awakening because of back pain during the second part of the night, or younger age (20 to 40 years)) Risk factors for vertebral compression fracture (history of osteoporosis, use of corticosteroids, significant trauma, or older age [> 65 years for women or > 75 years for men])
Magnetic resonance imaging	Signs and symptoms of radiculopathy (back pain with leg pain in an L4, L5, or S1 nerve root distribution or positive result on straight leg raise or crossed straight leg raise test) in patients who are candidates for surgery or epidural steroid injection Risk factors for or symptoms of spinal stenosis (radiating leg pain, older age, or pseudoclaudication) in patients who are candidates for surgery
No imaging	No criteria for immediate imaging and back pain improved or resolved after a 1-month trial of therapy Previous spinal imaging with no change in clinical status

*Consider magnetic resonance imaging if the initial imaging result is negative but a high degree of clinical suspicion for cancer remains. Adapted from Chou R, Qaseem A, Owens DK, et al. Diagnostic imaging for low back pain: advice for high-value health care from the American College of Physicians. *Ann Intern Med.* 2011;154:181-189, Table 4.)

the spine pain patient, imaging should begin with upright, weight-bearing radiographs of the appropriate spine segment. The ACR and the ACP are consistent in their recommendations that patients with “red flag” features of recent trauma, osteoporosis, age greater than 70 years, or clinically suspected inflammatory spondyloarthropathy should initially undergo radiographs; advanced imaging should be reserved for patients with progressive neurologic deficits or a strong clinical suspicion of infection or neoplasm.⁶⁴⁻⁶⁶ Radiographs provide a modest sensitivity screen for sinister conditions, establish spine enumeration, and when performed in physiologic positions allow assessment of sagittal and coronal plane balance.

Spine enumeration is a critical but underappreciated role of radiographs. The typical spine morphology of 24 mobile, presacral spine segments (7 cervical, 12 rib-bearing thoracic, and 5 lumbar type vertebral bodies) is not uniformly present; deviation can result in confusion in establishing the origin of pain syndromes, or wrong segment minimally invasive or surgical interventions. It can be reasonably assumed in the human species that there are 7 cervical vertebrae. There is considerable variation in the number and distribution of thoracic and lumbar segments that may be difficult to appreciate on MRI alone; radiographs can establish this enumeration and serve as the foundation for subsequent advanced imaging description.

In a study by Carrino and colleagues using complete spine radiographs, 91.8% of subjects had 24 presacral vertebral segments: 4.8% had 23 and 3.4% had 25.⁷⁰ Akbar and colleagues, using full spine sagittal MRI localizer images,

Box 15.1 Spine Imaging Principles

- The primary role of imaging is the identification of undiagnosed systemic disease.
- Spine imaging has a significant specificity fault: a high prevalence of asymptomatic age-related “degenerative” findings.
- Significance of imaging findings depends on concordance: the imager must know the pain/dysfunction syndrome.
- Spine imaging may be insensitive to dynamic lesions.
- No imaging is indicated in the acute presentation of back or limb pain in the absence of “red flag” features.
- The decision to undertake imaging must be a reasoned harms and risk/benefit judgment.
- Imaging correlates poorly with clinical presentation and course.

identified 23 presacral segments in 3.3% of subjects and 25 in 3.3%; these anomalies of spine enumeration were not mentioned in the radiology report in nearly 70% of cases.⁷¹ In Carrino’s study, if one considers both anomalous number and distribution (e.g., 13 rib-bearing vertebrae + 4 lumbar type vertebrae) of thoracolumbar spine segments, 10.9% of subjects have nonclassical anatomy.⁷⁰ For the spine interventionist, this implies these situations are in the procedure room regularly; failure of recognition virtually guarantees wrong segment procedures.

Anomalous segmentation is predicted by the presence of transitional thoracolumbar or lumbosacral vertebral bodies,

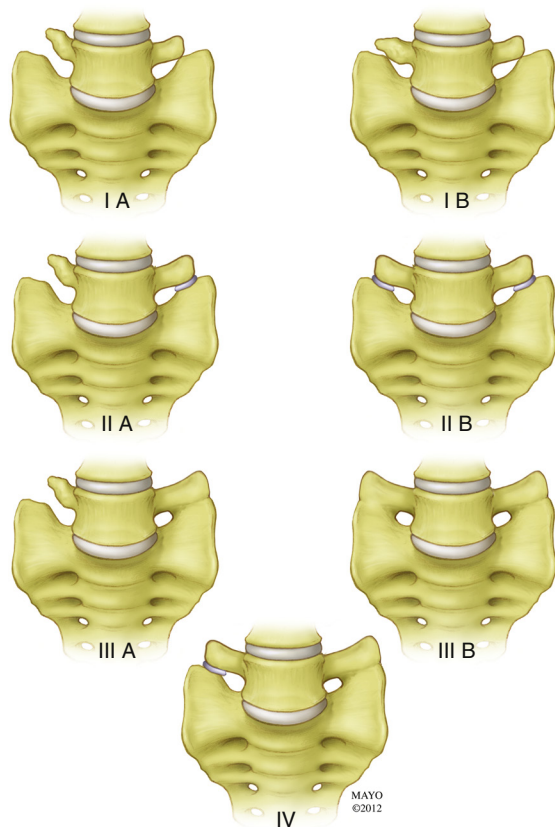


Figure 15.2 Castellvi classification of lumbosacral transitional segments.

which may be a source of confusion in their own right. Thoracolumbar transitional segments have hypoplastic ribs at the lowest rib-bearing segment; they were present in 4.1% of subjects in Carrino's study.⁷⁰ Lumbosacral transitional segments have characteristics of both the L5 lumbar body and the superior sacral segment; their described prevalence ranges from 4% to 30%.⁷² The Castellvi classification (Fig. 15.2) describes the morphologic types, ranging from an expanded (height > 19 mm) dysplastic transverse process (type I), through a pseudoarticulation between the transverse process and sacral ala (type II), to osseous fusion between the transverse process and the sacrum (type III).⁷³ Type IV denotes the presence of a type II transition on one side and a type III on the other. Unilateral (a) and bilateral (b) subtypes are also described. On lateral radiographs or sagittal MRI images, a transitional segment can be suggested in the presence of a perceived narrow S1-S2 disk, which extends for the entire anterior-posterior (AP) width of the sacral body with parallel end plates and a squared upper sacral segment (Fig. 15.3).⁷² The presence of a transitional lumbosacral segment increased by sevenfold the likelihood of an anomalous number of presacral segments. In patients with radicular pain syndromes and lumbosacral transitional anatomy, the pain practitioner must also be aware of the possibility of an extraforaminal nerve entrapment between the enlarged transverse process and sacral ala.

Correlation of pain syndromes with imaging findings can be confounded in patients with transitional anatomy or anomalous segmentation. It is best to consider that, in general, radicular innervation patterns remain relatively constant when counted caudally from the skull base, but

the skeletal anatomy may change about them. For example, the 26th nerve (8 cervical nerves, 12 thoracic, 5 lumbar, 1st sacral nerve) from the skull base most commonly innervates the medial head of the gastrocnemius and the soleus muscles, the basis of the S1 radicular pain pattern. In a patient with 25 presacral vertebral segments, this may exit under the pedicle of the lowest lumbar type vertebral body, creating confusion for the unwary practitioner (Fig. 15.4). There is also variation in typical innervation patterns in the presence of transitional anatomy, which may introduce further localization challenges. Only meticulous attention to spine enumeration, best provided by plain radiographs, sometimes supplemented by total spine MRI localizer images, will protect the spine pain patient and interventionalist from wrong segment invasive procedures (Box 15.2).

When radiographs are obtained, they should be upright, weight-bearing images. Only in a physiologic posture can one assess sagittal and coronal balance (Fig. 15.5). Upright radiographs demonstrate more thoracic kyphosis and lumbar lordosis than do recumbent images.⁷⁴ Weight-bearing images may also demonstrate instability, most commonly L4-L5 degenerative spondylolisthesis, which would be occult on recumbent films.⁷⁵ In spinal deformity patients, the exacerbation of spinal curves with weight bearing can be dramatic. Flexion-extension radiographs in the lumbar or cervical spine are not indicated as part of an initial imaging investigation. There is no role for oblique radiographs of the spine; in the lumbar region they double the gonadal dose and do not provide useful information that will affect clinical decision making.⁷⁵ Cervical spine oblique views similarly serve only to irradiate sensitive tissue (thyroid, lens of the eye) without clinical benefit.

ADVANCED IMAGING MODALITIES

When radiographs are not explanatory of an unremitting pain syndrome or suggest underlying systemic disease, advanced imaging (CT, MRI, nuclear medicine) may be obtained. CT has undergone a revolution since the early 2000s with the advancement of multidetector technology. A data set for the lumbar spine can now be obtained in a few seconds, eliminating motion artifact and dramatically improving patient tolerance. This data set can then be reconstructed in any plane without a loss of spatial resolution or additional radiation exposure. CT provides superior imaging of cortical and trabecular bone when compared with MRI. For this reason, CT may be necessary to characterize primary bone tumors of the spine. CT also provides reasonable contrast resolution and can identify root compressive lesions such as disk herniations or characterize central canal, lateral recess, and foraminal compromise in the majority of cases. CT cannot identify intrathecal pathology and is less sensitive than MRI in the detection of early inflammatory or infectious processes, neoplasm, or paraspinal soft tissue lesions. Radiation dose must always be considered when employing CT, particularly in young patients or in serial studies. One by-product of the rapid technological advance of CT is that the literature contains no comparative studies between MRI and the latest generation of multidetector CT scanners in the detection and characterization of disk herniations.

MRI has been the dominant spine imaging modality since the 1990s, despite modest technological advancement

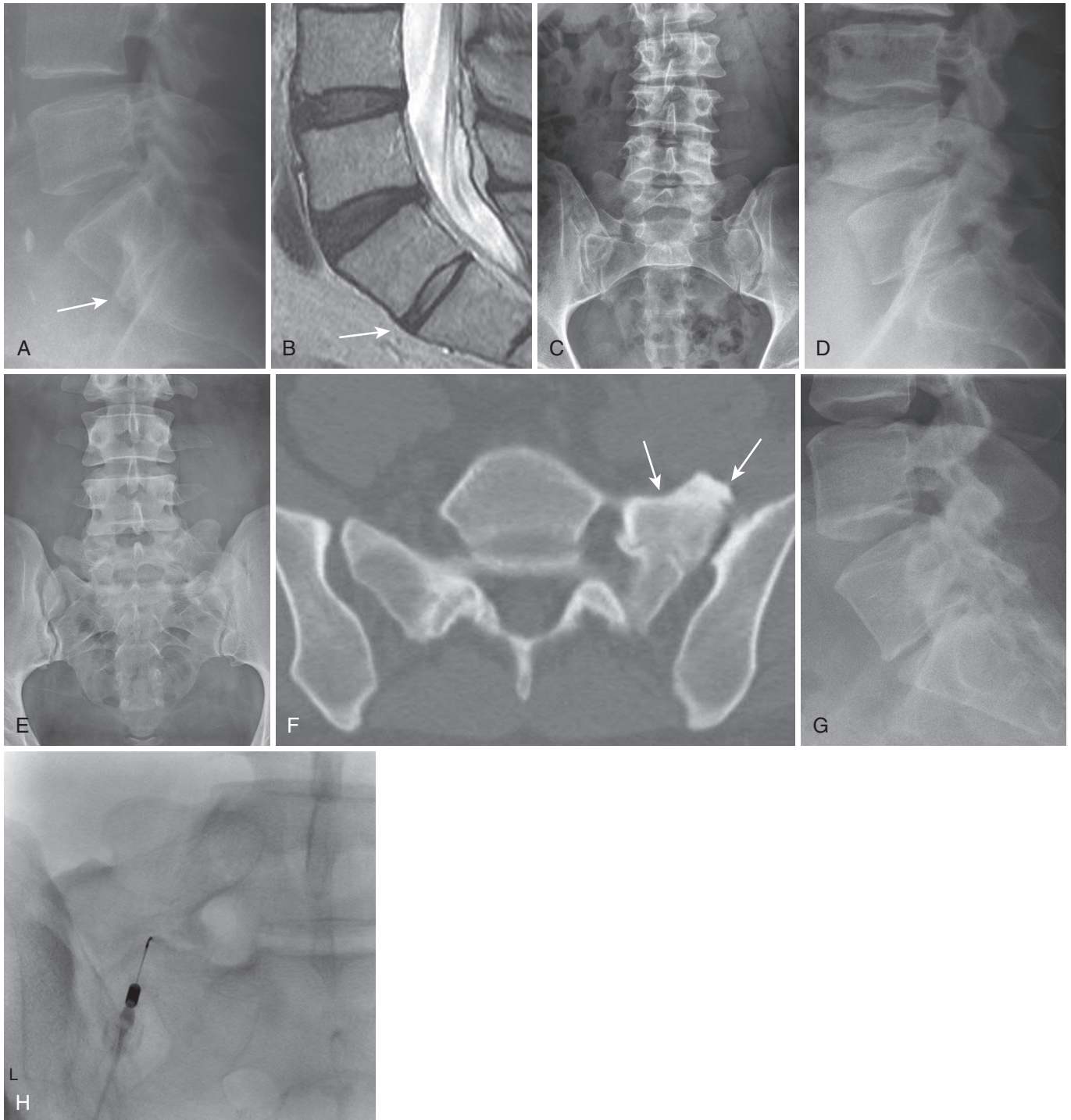


Figure 15.3 Transitional segments. Lateral radiograph (**A**) and sagittal T2 MRI image (**B**) demonstrate typical findings of a transitional segment interspace (*arrows*): a narrow disk space with parallel end plates and normal T2 signal intensity. Castellvi IIA transitional segment is demonstrated in frontal (**C**) and lateral (**D**) radiographs. Note right pseudoarthrosis. In another patient, frontal radiograph (**E**) shows a left-sided pseudoarthrosis, also seen on the axial CT image (*arrows* in [**F**]). Narrow, parallel end plates are visible in the transitional interspace on the lateral radiograph (**G**). This patient had axial pain attributed to the pseudoarthrosis; this was injected (**H**) with relief of the index pain.

in the realm of spine imaging in that time span. MRI has superior contrast resolution and thus the ability to distinguish between soft tissue types, allowing it to detect intrathecal pathology and identify subtle root compressive lesions. MRI has superior sensitivity in the detection of neoplasm and infection. With the use of gadolinium contrast, or heavily T2-weighted imaging sequences (short-tau inversion recovery [STIR] or fast spin echo T2 sequences with fat

saturation), MRI can detect the physiologic parameters of edema, hyperemia, and inflammatory change. It has greater specificity than CT in characterizing the chronicity of fractures. With gadolinium enhancement, MRI can distinguish between recurrent disk herniation and scarring in the post-operative patient. MRI does not evaluate cortical bone well. Patient acceptance remains problematic because of prolonged imaging times and up to 10% examination failures

caused by claustrophobia. Open magnets have improved patient acceptance, but at the cost of image quality. A small percentage of patients are MRI incompatible due to pacemakers, spinal cord stimulators, or other implanted devices. MRI remains costly. The sensitivity challenges imposed by recumbent MRI imaging were discussed earlier; the hope is that the engineering challenges of high field strength, weight-bearing MRI imaging will be met in the near future.

CT myelography retains a problem-solving role in the lumbar spine; it will substitute for MRI in the incompatible

patient. CT myelography has superior spatial resolution when compared with MRI but lacks its soft tissue contrast resolution. It can provide an exquisite demonstration of root compressive lesions and central canal, lateral recess, and foraminal compromise. In the cervical spine, the superior spatial resolution of CT myelography and its ability to discriminate between bone and soft tissue compressive lesions give it a continuing role. CT myelography is minimally invasive, expensive, operator dependent to a degree, and also requires current CT technology to be maximally useful.

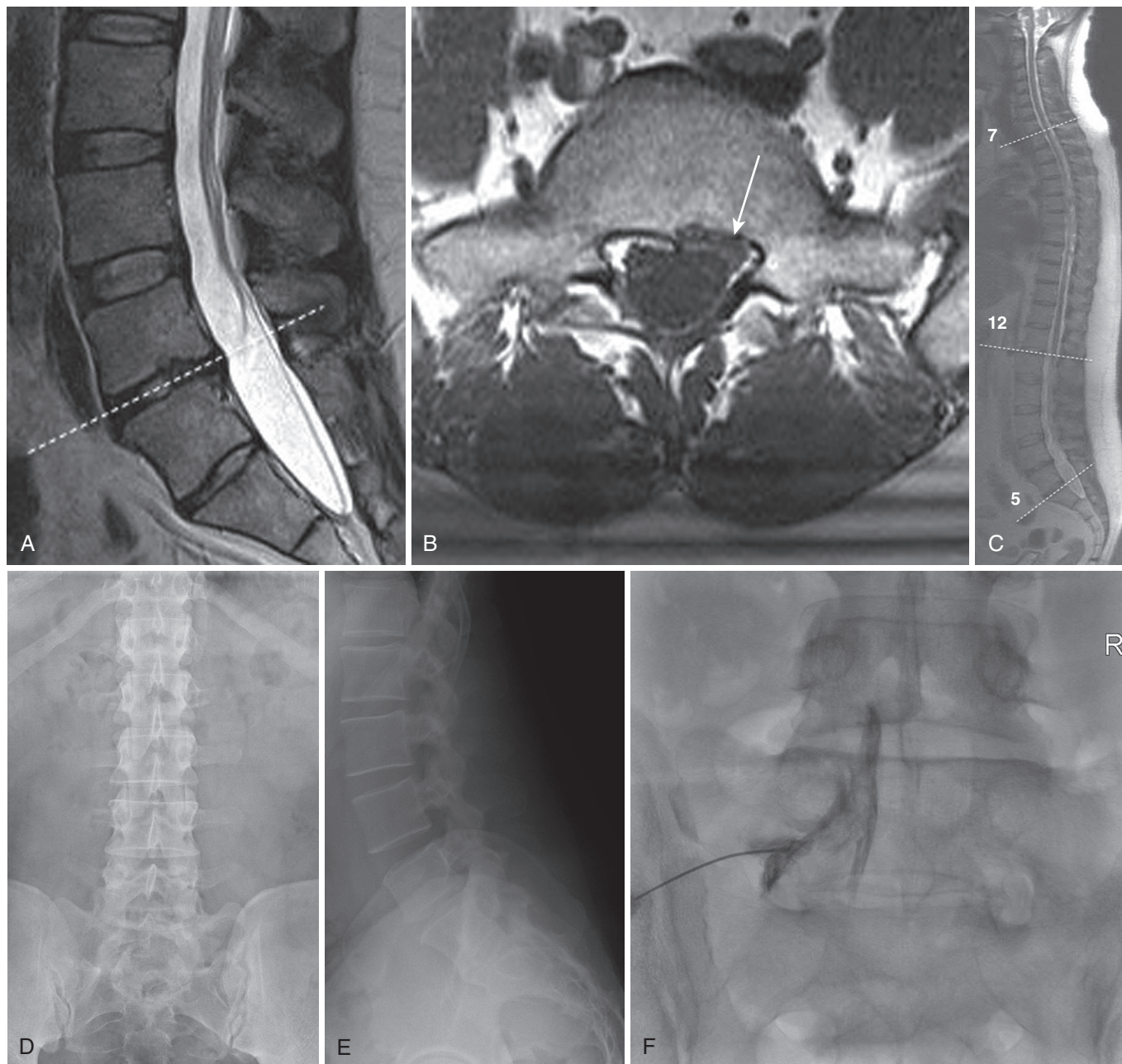


Figure 15.4 The importance of segmental enumeration. This 36-year-old male who has failed conservative care presents with a left-sided L5 radicular pain pattern involving the lateral thigh, lateral calf, and dorsum of the foot. His MRI (sagittal T2 [A] and axial T1 [B] at level of dotted line) shows a subtle disk extrusion in the left lateral recess (arrow in [B]) at the penultimate interspace. The lowest-most disk appears transitional. MRI scout (C) image demonstrates 24 presacral segments. Frontal and lateral radiographs (D and E) may suggest 5 lumbar vertebrae on cursory examination; careful counting at fluoroscopy noted 11 rib-bearing vertebrae. T12 has no ribs and L5 is transitional, Castellvi type 4. The transforaminal epidural steroid injection (F and G) was performed under the pedicle bearing the dysplastic left T5 transverse process and relieved the patient's pain.

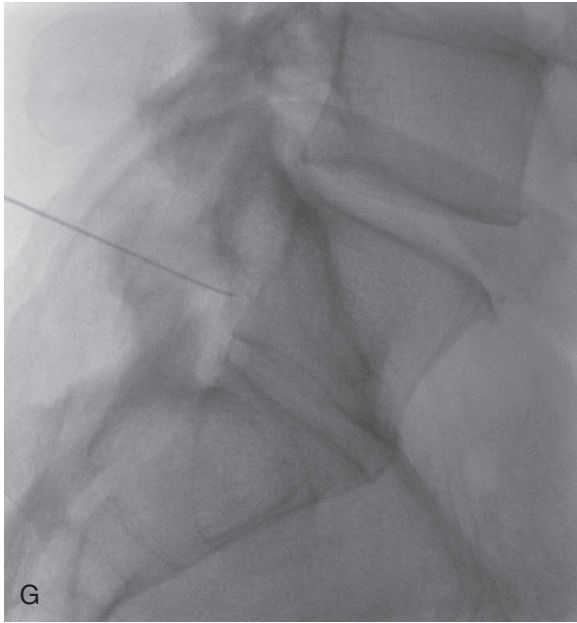


Figure 15.4, cont'd Note (G) the typical appearance of a transitional disk space. Careful enumeration of every case is the only way to avoid wrong segment interventions.

Box 15.2 Spine Enumeration

- Approximately 11% of subjects will have anomalies of number or distribution of thoracolumbar vertebral bodies.
- Anomalous segmentation is predicted by the presence of transitional thoracolumbar or lumbosacral vertebral bodies.
- Ideally, vertebral numbering should occur from the skull base caudally.
- Practically, the human cervical spine is homologous and can be assumed to have seven segments.
- T1 is marked by the first upward inclined transverse process.
- Meticulous enumeration on every case will prevent wrong segment procedures.

Cone-beam CT, weight-bearing myelography holds promise for assessing position-dependent pain syndromes, at least in part defeating the sensitivity fault of recumbent advanced imaging. In this technology, arising from rotational angiography roots, the C-arm rapidly rotates about the standing patient who has had contrast introduced into the thecal sac. A flat panel fluoroscopy detector gathers a data set that can be reconstructed in any plane. Soft tissue contrast does not approach that of true CT, and the longitudinal field of view is limited to the length of the flat panel detector. Despite these limitations, the high inherent contrast among intrathecal contrast, the soft tissue structures of the spinal column, and bone allows for a very good depiction of central canal, lateral recess, and foraminal compromise. This technology will only improve (Fig. 15.6).

Nuclear medicine studies are growing in importance in spine imaging. Technetium pyrophosphate bone scans detect increased blood flow and accelerated bone metabolic activity. With the addition of SPECT and SPECT/CT image fusion, significant additional spatial localization of hyperemia and increased metabolic activity are possible. This imaging is traditionally useful in assessing the burden of metastatic disease but can also be valuable in assessing non-neoplastic inflammatory states such as spondylolysis. SPECT/CT can potentially identify inflammatory synovitis in the facet and sacroiliac joints, which might guide interventions. However, validation studies of these techniques against accepted reference standards such as comparative blocks in the facet joints or intra-articular sacroiliac blocks have not yet been done. When MRI is not technically feasible, technetium bone scanning can be used to characterize the chronicity of vertebral fractures in selecting patients for bone augmentation. The technetium bone scan, in combination with gallium scan, offers sensitivity equal to MRI in the detection of spondylodiscitis. However, these techniques provide less anatomic information and MRI may ultimately be necessary to characterize the degree of central canal compromise that may influence surgical decision making. PET or PET/CT scans have an increasing role in assessing the burden of metastatic disease and in selecting lesions for percutaneous biopsy.

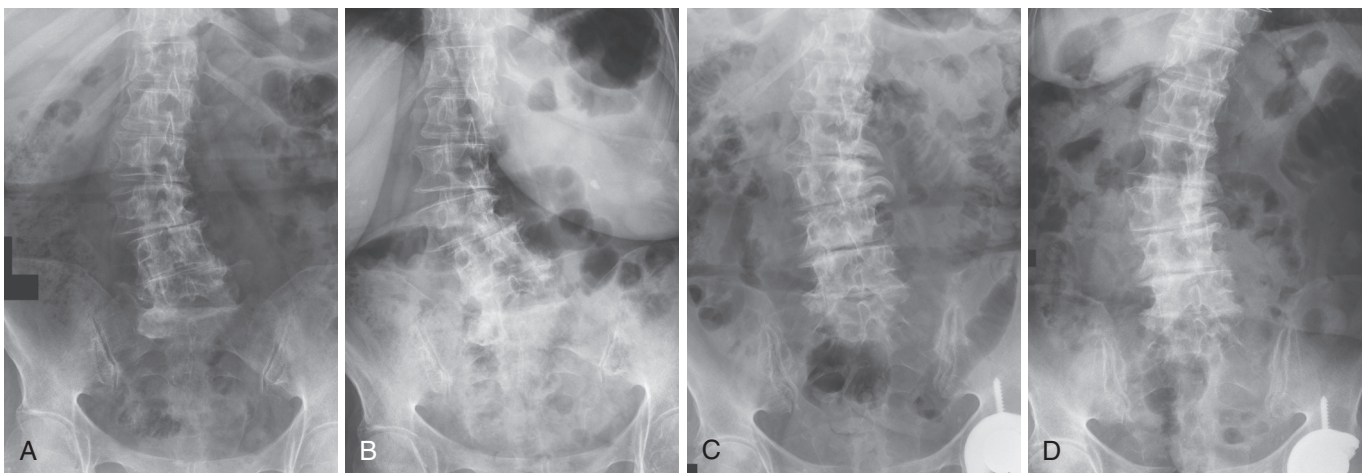


Figure 15.5 The effect of upright weight-bearing radiographs on balance and deformity. Recumbent radiograph (A) shows lumbar scoliosis with a rotatory component, which is significantly exacerbated in a subsequent upright radiograph (B). In another patient, the recumbent radiograph (C) underestimates the true scoliotic curve seen on an upright radiograph (D). Sagittal and coronal balance can only be assessed on upright, weight-bearing imaging.



Figure 15.6 Ligamentum flavum redundancy (buckling) on upright myelography (cone beam CT). A 66-year-old man imaged for neurogenic intermittent claudication. Conventional myelogram in the lateral plane with the patient in the prone position (**A**) and postmyelogram sagittal (**B**) and axial CT at L4-5 interspace (**C**) with the patient in the prone position show minimal redundancy of the ligamentum flavum (*black arrows*) and mild central canal compromise at the L4-5 level. Cone beam CT myelography with the patient in an upright position demonstrates a marked increase in ligamentous buckling (*white arrow*) on the sagittal reconstruction (**D**) and complete effacement of the thecal sac on the axial reconstruction (**E**). (Courtesy of Kent Thielen, MD, Mayo Clinic, Rochester, MN.)

IMAGING OF AXIAL PAIN GENERATORS

Axial pain that may have an imaging correlate derives primarily from stimulation of nociception of the spinal articulations: the intervertebral disk, the zygapophysial or facet joints, and the sacroiliac joint. More broadly, it may include pain originating from the muscular or ligamentous structures in the supporting architecture of the spine. Axial pain is clinically characterized as constant, dull, deep, poorly localized, and aching, located primarily in the paraspinous region with inconstant referral to the

proximal extremities. This is in distinction to the neuropathic pain of radicular character, which is typically sharp, electric, lancinating, and experienced in a bandlike distribution into the more distal extremities. The prevalence of axial spine pain generators has been well described by Depalma (Table 15.4).^{76,77} Intervertebral disk disruption (IDD) was the most common axial pain generator in this series, followed by the facet joint, the sacroiliac joint, and insufficiency fractures of the spine or pelvis. This work also emphasized the age dependence of these pain sources. Patients with diskogenic pain (IDD) were significantly

Table 15.4 Prevalence of Sources of Axial Low Back Pain, Age Correlation

Pain Source	Prevalence (%)	Mean Age (Std Dev)
Intervertebral disk disruption (IDD)	41.8	43.7 (10.3)
Facet joint	30.6	59.6 (13.1)
Sacroiliac joint	18.2	61.4 (17.7)
Vertebral insufficiency fracture	2.9	79 (11.8)
Pelvic insufficiency fracture	1.8	71.3 (11.7)
Baastrup's disease	1.8	75.3 (4.7)
Fusion hardware	2.9	59.6 (19.4)

Data from DePalma MJ, Ketchum JM, Saullo T. What is the source of chronic low back pain and does age play a role? *Pain Med.* 2011;12:224-233.

younger than patients with facet or sacroiliac joint pain. As age increased, the probability of IDD as a pain source decreased and the probability of facet or sacroiliac pain increased, up to approximately age 70.⁷⁶ A later multivariable analysis also showed a gender relationship, with IDD more prevalent in young men.⁷⁸ This echoes the earlier work of Schwarzer, who demonstrated that lumbar facet-mediated pain was uncommon in a population of young workers (~15%) but more highly prevalent in an aged population (~32%).^{79,80}

IMAGING CORRELATES OF DISKOGENIC PAIN

The imaging diagnosis of diskogenic pain is made challenging by the lack of a pathoanatomic gold standard against which to assess imaging parameters. It is not possible to evaluate a disk, either at surgery or upon histologic examination, and deem it painful. The current most stringent reference standard for the diagnosis of diskogenic pain is manometrically controlled provocation diskography with normal control levels as documented in the practice guidelines of the International Spine Intervention Society (ISIS).⁸¹

It is important to observe, however, that examination of the same body of evidence regarding the validity of diskography as the reference standard has resulted in diametrically opposed recommendations regarding its use by different physician societies. The ISIS,⁸¹ the North American Spine Society,⁸² and the International Association for the Study of Pain⁸³ accept diskography as a useful diagnostic tool in back pain patients and recommend its use. The American Pain Society rejects diskography as a diagnostically useful test.⁸⁴ A comprehensive review of diskography in the journal of the American Society of Regional Anesthesia and Pain Medicine notes that whereas CT diskography is the gold standard for the assessment of structural disk alteration, there is no convincing evidence that the use of diskography as a selection tool improves surgical outcomes.⁸⁵ Any analysis of imaging findings in diskogenic pain patients thus remains based on a reference standard (provocation diskography) that is ultimately unproved

against a pathoanatomic gold standard. This is further confounded by evolution of the criteria for a positive diskogram since the 1990s. For the purposes of this discussion, only concordant pain responses were considered to represent a positive diskogram. A significant concordant pain response without a specification of pain intensity or the use of manometry is defined as a Walsh criterion.⁸⁶ Inclusion of the requirement for a normal control disk elevates the criteria to that of the International Association for the Study of Pain (IASP).⁸³ None of the studies reviewed here meaningfully used manometric control or met the ISIS criteria for positive diskography.⁸¹

Although challenging, there is motivation to make the diagnosis of diskogenic pain via noninvasive imaging. Diskography has until recently been considered a minimally invasive and nondestructive test. There is now in vitro and in vivo evidence suggesting that disk puncture or diskography may contribute to disk dysfunction. Korecki and colleagues⁸⁷ noted that in a bovine disk model, single punctures with a 25-gauge needle resulted in biomechanical degradation of disk function with cyclic loading. Carragee and coworkers⁸⁸ demonstrated on 10-year follow-up MR imaging that asymptomatic subjects who had undergone investigational diskography showed more degenerative phenomena than did matched control subjects. Although the clinical significance of these observations remains uncertain, noninvasive diagnosis is desirable.

The specificity fault inherent in spine imaging was previously discussed: manifestations of disk “degeneration” are ubiquitous, usually asymptomatic, and primarily represent normal age change. In a population of symptomatic patients with suspected diskogenic pain, however, are there imaging findings that correlate with positive provocation diskography? The findings evaluated in the literature include (1) loss of disk space height, (2) generalized alterations in T2 signal within the disk, (3) alterations of disk contour, (4) Modic end plate marrow changes, and (5) the presence of high intensity zones (HIZ) or fissures within the posterior disk annulus. These imaging features are examined initially as independent variables with subsequent discussion of the more limited literature in which they are combined in a multivariate analysis. A significant portion of the presented data were drawn from a systematic review of imaging and clinical markers of axial pain generators in the lumbar spine performed by Hancock and colleagues.⁸⁹ Additional studies not included in that report or published subsequent to it have been added.⁹⁰ A common set of measures was compiled from the many studies: sensitivity, specificity, positive predictive value (PPV), negative predictive value (NPV), and likelihood ratios (LRs). When imaging features were quantified (T2 signal loss in the disk was reported as normal, moderate, or severe), a threshold was used. Original data were combined and recalculated to reflect setting a detection threshold as moderate (including moderate and severe cases) or severe only. Because the diagnosis of diskogenic pain may provoke therapeutic interventions (most of which carry risk and have unproved efficacy), emphasis was placed on those measurements that inform about false-positive results: specificity (true negatives/true negatives + false positives) and PPV (true positives/true positives + false positives).

Table 15.5 T2 Signal Loss as a Predictor of Positive Provocation Diskography

Author (ref), Date	Diskogram Criteria	T2 Signal Criteria	Prevalence	Sensitivity	Specificity	PPV	NPV	+LR (CI)	-LR (CI)
Osti ⁽⁹⁵⁾ 1992	Walsh	Moderate + Severe	47%	70%	64%	50%	80%	1.9 (1.3-2.7)	0.49 (0.3-0.8)
		Severe only	13%	23%	92%	60%	70%	2.8 (1.1-7)	0.83 (0.7-1)
Horton ⁽⁹⁶⁾ 1992	Walsh	Moderate + Severe	69%	95%	43%	44%	94%	1.6 (1.2-2.2)	0.18 (0.04-0.9)
		Severe only	20%	37%	88%	58%	74%	2.8 (1.1-7.3)	0.72 (0.5-1)
Ito ⁽⁹¹⁾ 1998	Walsh	Moderate + Severe	63%	96%	46%	34%	97%	1.7 (1.4-2.2)	0.14 (0.03-0.6)
		Severe only	25%	70%	89%	64%	91%	5.7 (3-11)	0.36 (0.2-0.7)
Weishaupt ⁽⁹⁷⁾ 2001	IASP	3-5 of 5-grade Pearce	65%	98%	59%	64%	98%	2.3 (1.8-3.1)	0.05 (0.01-0.3)
Lim ⁽⁹²⁾ 2005	Walsh	4 and 5 of 5-grade Pearce	62%	88%	52%	50%	89%	1.8 (1.4-2.4)	0.25 (0.1-0.6)
Lei ⁽⁹⁸⁾ 2008	IASP	3 and 4 of 4-point Woodward	57%	94%	77%	78%	94%	4 (2.5-6.4)	0.07 (0.02-0.2)
O'Neill ⁽⁹³⁾ 2008	IASP	Moderate + Severe	62%	90%	67%	75%	86%	2.7 (2.2-3.3)	0.16 (0.1-0.2)
		Severe only	15%	24%	96%	87%	54%	6 (3-11.7)	0.79 (0.7-0.9)
Kang ⁽⁹⁴⁾ 2009	IASP	3, 4, and 5 on Pfirrmann 5-point scale	70%	95%	39%	34%	96%	1.6 (1.3-1.8)	0.12 (0.03-0.5)

PPV, positive predictive value; NPV, negative predictive value; LR, likelihood ratio; IASP, International Association for the Study of Pain. From Maus TP, Martin DP. Imaging for discogenic pain. In: Kapural L, Kim P, Deer T, eds. *Diagnosis, Management, and Treatment of Discogenic Pain*. Philadelphia: Elsevier/Saunders; 2012, p 38, Table 3-5.)

DISKOGENIC PAIN

LOSS OF DISK SPACE HEIGHT

The reports of Ito and colleagues,⁹¹ Lim and colleagues⁹² and O'Neill and colleagues⁹³ studied loss of disk space height as an imaging finding that may correlate with positive provocation diskography. The studies of Ito and colleagues and O'Neill and colleagues both suggest that in a population of symptomatic patients with axial pain considered diskogenic in nature, severe disk space narrowing, although an uncommon imaging finding (approximately 10%), is strongly predictive of a painful disk. Specificity of this finding was at least 97% in these studies with PPVs of 78% and 90%, respectively. Lim's study was less supportive. It is reasonable to conclude that in a patient with suspected diskogenic pain undergoing provocation diskography, severe loss of disk space height is a strong predictor of a positive diskogram.

NUCLEAR T2 SIGNAL LOSS

Studies addressing the correlation between MR imaging evidence of disk "degeneration," primarily nuclear T2 signal loss, and diskogenic pain reach back to the 1990s.⁹¹⁻⁹⁸ The challenges in this analysis are well illustrated in Table 15.5.⁹¹⁻¹⁰⁰ Although disk "degeneration" definitions are inconsistent,

original data have been recalculated into threshold values to provide a reasonable basis of comparison. The changes in diskography criteria over time are also noted. Despite these shortcomings, conclusions can be reasonably drawn. The NPV of disks of normal nuclear signal is uniformly high and -LRs are highly informative; disks of normal nuclear signal are rarely painful. Severe, uniform loss of T2 signal, with or without loss of disk space height, is a finding of high specificity (88% to 96% in studies using a three-part classification system) with strongly informative +LR. Disks with severe T2 signal loss are rarely nonpainful. The utility of this finding is reduced by its low prevalence (it is found in 13% to 25% of disks undergoing diskography) and low sensitivity (23%, 24%, 37%, and 70% in the studies with a three-part classification system). Disks with intermediate signal loss may be painful but with less certainty (Fig. 15.7).

DISK CONTOUR ABNORMALITY

The studies of O'Neill and colleagues⁹² and Kang and colleagues⁹³ included data correlating disk contour abnormalities and diskography. Both studies showed a statistically significant correlation of disk contour abnormality with positive provocation diskography. In O'Neill and colleagues' study, a disk bulge was the contour abnormality most predictive of a positive diskogram, with a +LR of 5.3.

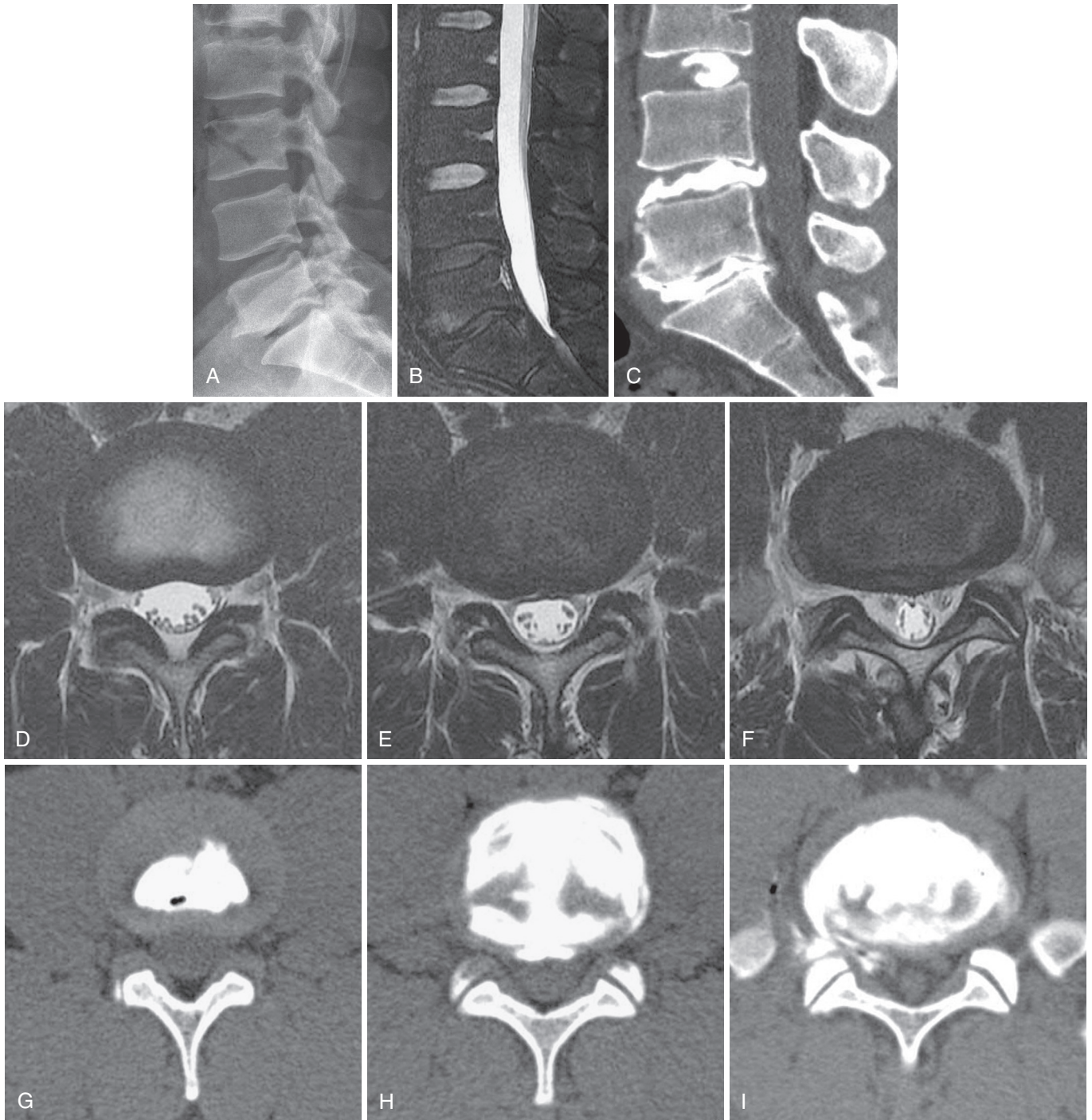


Figure 15.7 Disk height and nuclear T2 signal loss. Lateral radiograph (A) of a 50-year-old male with intractable axial pain. Note loss of height of lumbosacral disk, which contains gas. There is slight retrolisthesis of L4 on L5 and L5 on S1. Sagittal fat-saturated T2-weighted MRI (B) shows loss of T2 signal in the L4-5 and L5-S1 disks; normal upper lumbar disks. Axial T2-weighted images at L3-4 (C), L4-5 (D), and L5-S1 (E) demonstrate normal L3-4 disk, loss of T2 signal in L4-5 with a small central herniation, and a broad bulge at L5-S1. Sagittal CT diskogram (F) and axial images at L3-4 (G), L4-5 (H), and L5-S1 (I) shows normal L3-4 disk, Grade IV annular disruption at L4-5 and L5-S1 with leak of contrast from the right posterolateral annulus at L5-S1. Patient had concordant axial pain at L4-5 and L5-S1 with a normal control disk at L3-4. (From Maus TP, April CN. Lumbar discogenic pain, provocation diskography, and imaging correlates. *Radiol Clin North Am.* 2012;50:681-704.)

MODIC END PLATE CHANGES

The functional unity of the disk and the cartilaginous end plate is manifest in signal changes within the end plate and adjacent subchondral marrow that accompany nuclear matrix degradation. End plate marrow changes were

originally classified by Modic in 1988 (Fig. 15.8).¹⁰¹ Type I change represents ingrowth of vascularized granulation tissue into sub-end plate marrow; it exhibits a hypointense T1 and hyperintense T2 signal on MRI and may enhance with gadolinium. Type II change exhibits elevated T1 and T2

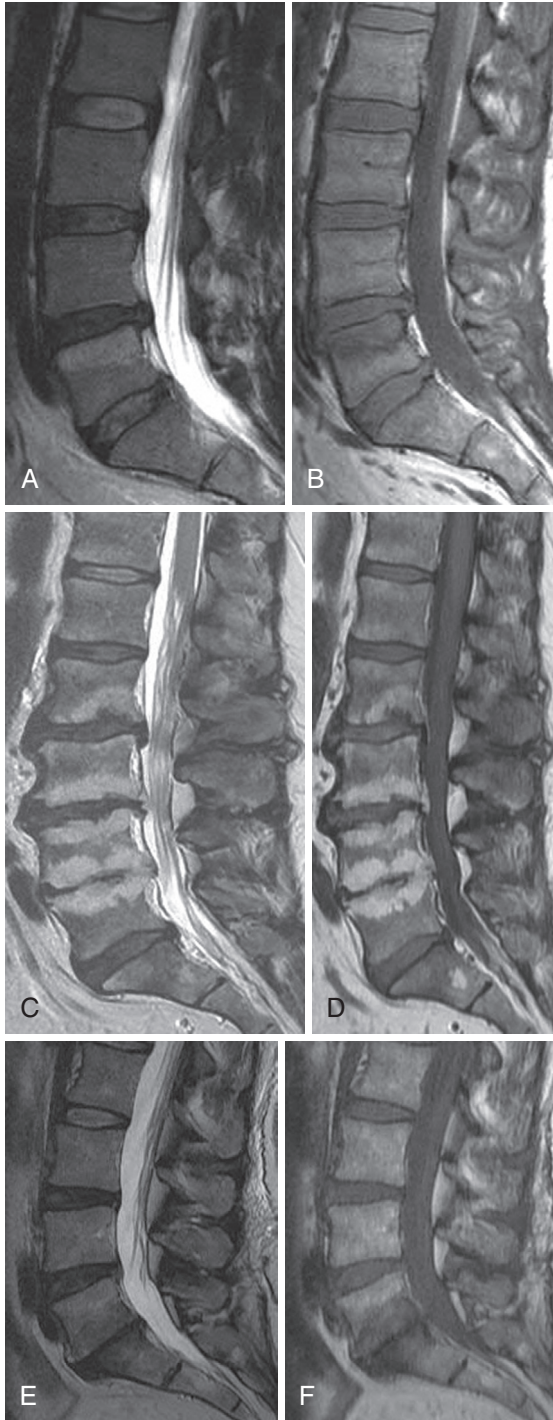


Figure 15.8 Modic end-plate changes. Modic I Sagittal T2 (A) and T1 (B) images demonstrate elevated T2 and diminished T1 signal involving the superior half of the L5 vertebral body. The histologic correlate of Modic I is vascularized granulation tissue. There are disk herniations at the L3-4 and L4-5 disks.

Modic II Sagittal T2 (C) and T1 (D) images reveal elevated T1 and T2 signal in the sub-end plate marrow involving L2-L5. The histologic correlate of Modic II is fatty infiltration.

Modic III Sagittal T2 (E) and T1 (F) images show diminished T2 and T1 signal in the sub-end plate marrow about the L5 interspace. The histologic correlate of Modic III is sclerotic bone.

signal and reflects fatty infiltration of sub-end plate marrow. Type III change is hypointense on T1 and T2; it correlates with bony sclerosis. Type I change is thought to represent an active inflammatory state, with type II more quiescent and type III post-inflammatory. Ohtori and colleagues¹⁰² noted elevated levels of protein gene product 9.5-immunoreactive nerve fibers and TNF- α immunoreactive cells in the cartilaginous end plates of patients with Modic changes. The immunoreactive nerve ingrowth was noted exclusively in patients with diskogenic low back pain. TNF- α immunoreactive cells were more common in type I end plate changes.

Modic end plate changes do carry an association with low back pain, particularly type I change. Toyone and colleagues¹⁰³ found that 73% of patients with type I change had low back pain as opposed to 11% of type II patients. Likewise, Albert and Manniche¹⁰⁴ reported low back pain in 60% of patients with Modic changes but in only 20% of those without Modic changes. Type I change was more strongly associated with low back pain than type II change. Modic type I change may also be associated with segmental instability. Persistent type I change after fusion surgery raises concern for pseudarthrosis; patients with solid fusions more likely have either persistent type II change or resolution of all marrow abnormality.

The data in Table 15.6^{91-94,97,98,105,106} describe Modic-type end plate changes as predictors of diskogenic pain. The studies discussed previously suggested that type I Modic change would be more strongly correlated with positive provocation diskography than type II; that conclusion is not borne out by the data, which suggest that either type I or type II Modic change correlates with positive diskography, although not uniformly. The studies of Braithwaite and colleagues,¹⁰⁵ Weishaupt and colleagues,⁹⁷ Lei and colleagues,⁹⁸ and O'Neill and colleagues⁹³ had few false-positive results (i.e., disks with adjacent type I or type II end plate changes that were nonpainful). The specificity, PPV, and +LRs in these studies were high. The usefulness of the MR imaging findings were only hampered by their infrequency. Other studies were less supportive but may be confounded by technical flaws. The compelling results presented by Weishaupt and colleagues⁹⁷ suggest a significant threshold for marrow change; with a threshold at 25% of vertebral body height, there were no false-positive results in this series. A reasonable conclusion is that Modic type I or II marrow change of this severity (25% of vertebral height) is an infrequent but highly specific finding, with a high PPV for diskogenic pain.

HIGH INTENSITY ZONE (HIZ)

In 1992, Aprill and Bogduk described the HIZ as an imaging marker of a painful disk at provocation diskography.¹⁰⁷ Their definition of the HIZ is a

high-intensity signal (bright white) located in the substance of the posterior annulus fibrosus, clearly dissociated from the signal of the nucleus pulposus in that it is surrounded superiorly, inferiorly, posteriorly and anteriorly by the low intensity (black) signal of the annulus fibrosus and is appreciably brighter than that of the nucleus pulposus. Page 362

This finding was identified on a midsagittal T2-weighted image; it may occur centrally in an otherwise normal

Table 15.6 End Plate (Modic) Change as a Predictor of Positive Provocation Diskography

Author (reference), Date	Diskogram Criteria	Modic Type	Prevalence per Disk	Sensitivity	Specificity	PPV	NPV	+LR	-LR
Braithwaite ⁽¹⁰⁵⁾ 1998	Walsh	I + II	25% imaged 15% tested	24%	96%	91%	47%	6 (1.7-21.2)	0.80 (0.7-0.9)
		I	4% tested	5%	100%	100%	42%	7.4 (0.4-131)	0.95 (0.9-1)
		II	12% tested	18%	96%	89%	48%	4.4 (1.2-16.1)	0.86 (0.8-0.9)
Ito ⁽⁹¹⁾ 1998	Walsh	I + II + III	9%	23%	94%	56%	80%	4 (1.3-12.8)	0.82 (0.7-1)
Weishaupt ⁽⁹⁷⁾ 2001	IASP	I	14%	29%	97%	88%	66%	9.9 (2.4-41.6)	0.73 (0.6-0.9)
		II	9%	19%	99%	90%	63%	12.75 (1.7-97.3)	0.83 (0.7-0.9)
		I + II	22%	48%	96%	88%	72%	10.86 (3.5-34.1)	0.55 (0.4-0.7)
		I + II Mod + Severe	16%	38%	100%	100%	69%	52.1 (3.2-844)	0.63 (0.5-0.8)
Kokkonen ⁽¹⁰⁶⁾ 2002	Walsh	I	17%	19%	85%	41%	65%	1.25 (0.5-3)	0.96 (0.8-1.2)
		II	19%	19%	80%	35%	64%	0.96 (0.4-2.2)	1 (0.8-1.2)
		I + II	36%	38%	65%	38%	65%	1.1 (0.6-1.8)	0.95 (0.7-1.3)
Lim ⁽⁹²⁾ 2005	Walsh	I + II	14%	9%	83%	21%	62%	0.6 (0.2-1.7)	1.1 (0.9-1.3)
Lei ⁽⁹⁸⁾ 2008	IASP	I + II	14%	32%	98%	94%	62%	19.25 (2.7-140)	0.69 (0.6-0.8)
O'Neill ⁽⁹³⁾ 2008	IASP	I	4%	6%	99%	88%	49%	6.94 (1.6-29.9)	0.95 (0.9-1)
		II	4%	7%	99%	90%	50%	8.32 (1.9-35.5)	0.93 (0.9-1)
		I + II	8%	14%	98%	89%	51%	7.63 (2.8-21.2)	0.88 (0.8-0.9)
Kang ⁽⁹⁴⁾ 2009	IASP	I + II	13%	14%	87%	26%	76%	1.08 (0.5-2.6)	0.99 (0.9-1.1)

PPV, positive predictive value; NPV, negative predictive value; LR, likelihood ratio; IASP, International Association for the Study of Pain. From Maus TP, Martin DP. Imaging for discogenic pain. In: Kapural L, Kim P, Deer T, eds. *Diagnosis, Management, and Treatment of Discogenic Pain*. Philadelphia: Elsevier/Saunders; 2012.

annulus, in a bulging annulus, or be located superiorly or inferiorly behind the edge of the vertebral body in a severely bulging annulus. In a series of 500 consecutive patients, the per-patient prevalence was 29%; the per-disk prevalence of an HIZ was 6%. The majority of HIZs were present at the L4 and L5 disk levels, confirmed on later studies.

The relationship of the HIZ to pain production was evaluated in a subset of 41 patients, selected for the presence of an HIZ on prediskography MR imaging.¹⁰⁷ Diskography was performed with the requirement of a nonpainful control disk for a diagnosis of diskogenic pain. Pain responses were tabulated both as “exact” reproduction of pain as well as “similar” pain (Table 15.7). In all, 118 disks were tested in 41 patients; the per-disk prevalence of the HIZ was 34%, reflecting the selection bias. In detecting exact pain, the HIZ had a sensitivity of 82% and specificity of 89%, a 70% PPV, and a +LR of 7.3. When the diskographic criteria were relaxed to exact or similar pain, the specificity rose to 97%

with a PPV of 95%; there were only two false-positive cases where a disk bearing an HIZ was nonpainful. The investigators postulated that the HIZ represents a complex grade 4 fissure where the nuclear material has been trapped within the lamellae of the annulus fibrosis and become inflamed, accounting for the T2 hyperintensity, brighter than that of the parent nucleus. They advanced the HIZ finding as pathognomonic of a symptomatic disk. The publication of these findings elicited considerable interest and many subsequent studies^{91,93,94,97,98,108-113} attempting to verify or refute its conclusions.

Table 15.7 demonstrates informative +LR and high specificity in most of the studies. There are dissenting voices. Carragee and colleagues evaluated the correlation of the HIZ and painful disks at provocation diskography in both symptomatic and asymptomatic subjects. In symptomatic patients, 30% of disks had an HIZ; only 9% of disks in asymptomatic subjects contained an HIZ (significant, $P < 0.0001$).

Table 15.7 High Intensity Zone (HIZ) as a Predictor of Positive Provocation Diskography

Author (reference), Date	Diskogram Criteria	HIZ Criteria	Prevalence per Disk	Sensitivity	Specificity	PPV	NPV	+LR (CI)	-LR (CI)
Aprill ⁽¹⁰⁷⁾ 1992	IASP	Aprill	34%*	82%	89%	78%	91%	7.3 (3.9-13.7)	0.21 (0.1-0.4)
	Exact pain	Aprill		63%	97%	95%	72%	18.4 (4.6-72.7)	0.38 (0.3-0.5)
Schellhas ⁽¹⁰⁸⁾ 1996	IASP	Schellhas [†]	60%*	97%	83%	87%	97%	5.7 (3.5-9.3)	0.03 (0.01-0.11)
Ricketson ⁽¹⁰⁹⁾ 1996	Walsh	Aprill	9%	12%	92%	57%	54%	1.5 (0.4-5.6)	0.96 (0.8-1.1)
Saifuddin ⁽¹¹⁰⁾ 1998	Walsh	Aprill	18%	27%	94%	89%	47%	4.8 (1.7-14.2)	0.77 (0.7-0.9)
Ito ⁽⁹¹⁾ 1998	Walsh	Aprill	20%	52%	89%	60%	87%	4.8 (2.3-10.2)	0.54 (0.4-0.8)
Smith ⁽¹¹¹⁾ 1998	Walsh	Aprill	13%	27%	90%	40%	80%	2.6 (1.2-5.6)	0.82 (0.7-1)
Carragee ⁽¹¹²⁾ 2000	Walsh	Carragee [‡]	30%	45%	84%	73%	62%	2.8 (1.5-5.5)	0.7 (0.5-0.9)
Weishaupt ⁽⁹⁷⁾ 2001	IASP	Aprill	20%	27%	85%	56%	62%	1.8 (0.8-3.7)	0.86 (0.7-1)
Peng ⁽¹¹³⁾ 2006	Walsh	Aprill	12%	NC	NC	100%	NC	NC	NC
Lei ⁽⁹⁸⁾ 2008	Walsh	Aprill	19%	25%	87%	62%	57%	1.8 (0.8-4.1)	0.87 (0.7-1.1)
O'Neill ⁽⁹³⁾ 2008	IASP	O'Neill [§]	28%	44%	89%	82%	60%	4.1 (2.7-6.1)	0.62 (0.5-0.7)
		1+2+3							
		Intensity grades							
		2+3	16%	26%	95%	86%	54%	5.7 (3-10.9)	0.78 (0.7-0.8)
		3	9%	15%	98%	86%	52%	6.8 (2.7-17.1)	0.87 (0.8-0.9)
Kang ⁽⁹⁴⁾ 2009	IASP	Aprill	26%	57%	84%	53%	86%	3.46 (2.2-5.5)	0.52 (0.4-0.7)

*Sensitivity and prevalence values are not meaningful due to this selection bias.

[†]Includes lesions with thin line of T2 hyperintensity within annulus or connecting nucleus to HIZ

[‡]Includes posterolateral lesions, HIZ signal intensity within 10% of CSF T2 signal

[§]Schellhas criteria plus posterolateral and lateral lesions

PPV, positive predictive value; NPV, negative predictive value; LR, likelihood ratio; IASP, International Association for the Study of Pain.

From Maus TP, Martin DP. Imaging for discogenic pain. In: Kapural L, Kim P, Deer T, eds. *Diagnosis, Management, and Treatment of Discogenic Pain*. Philadelphia: Elsevier Saunders; 2012:43, Table 3-7.

The statistics for the symptomatic group are presented in Table 15.7; an HIZ disk had an 84% specificity, a 73% PPV, and a +LR of 2.8 for diskogenic pain. These data are supportive of the HIZ as a useful marker for the painful disk. The investigators, however, point out that the presence of an HIZ disk was strongly predictive of a positive pain response at diskography in both the symptomatic (73%) and asymptomatic (69%) groups. The asymptomatic group had also been stratified by psychometric evaluation; in participants with either chronic pain or abnormal psychometric studies, all HIZ disks produced pain with pressurization. The investigators contend that the similar painful response rate of HIZ disks in symptomatic and asymptomatic subjects devalues the HIZ as a useful finding, because the total weight of diagnosis depends on concordance versus nonconcordance of pain response.

The study by O'Neill and associates⁹³ stratified HIZ lesions by relative signal intensity, and expanded the definition of

the HIZ to include posterolateral and lateral lesions and those that demonstrated a connection to the nuclear compartment. Original data were recalculated to establish a three-part threshold of HIZ intensity: markedly intense cases, markedly and moderately intense cases, and a combination of all three. As the threshold tightened, the specificity and +LR rose; the PPV remained high for all three threshold levels. For only markedly hyperintense HIZs, the specificity was 98%, the PPV was 86%, and the +LR was 6.8. This would support Bogduk's comments that "low intensity zones may well occur in asymptomatic volunteers, but that when activated (ostensibly inflamed), these fissures become painful and assume a higher signal intensity" (Fig. 15.9) page 1260.¹¹⁴

MULTIVARIATE ANALYSIS

The studies of Kang⁹⁴ and O'Neill⁹³ included multivariate analyses. O'Neill and associates showed that the disk

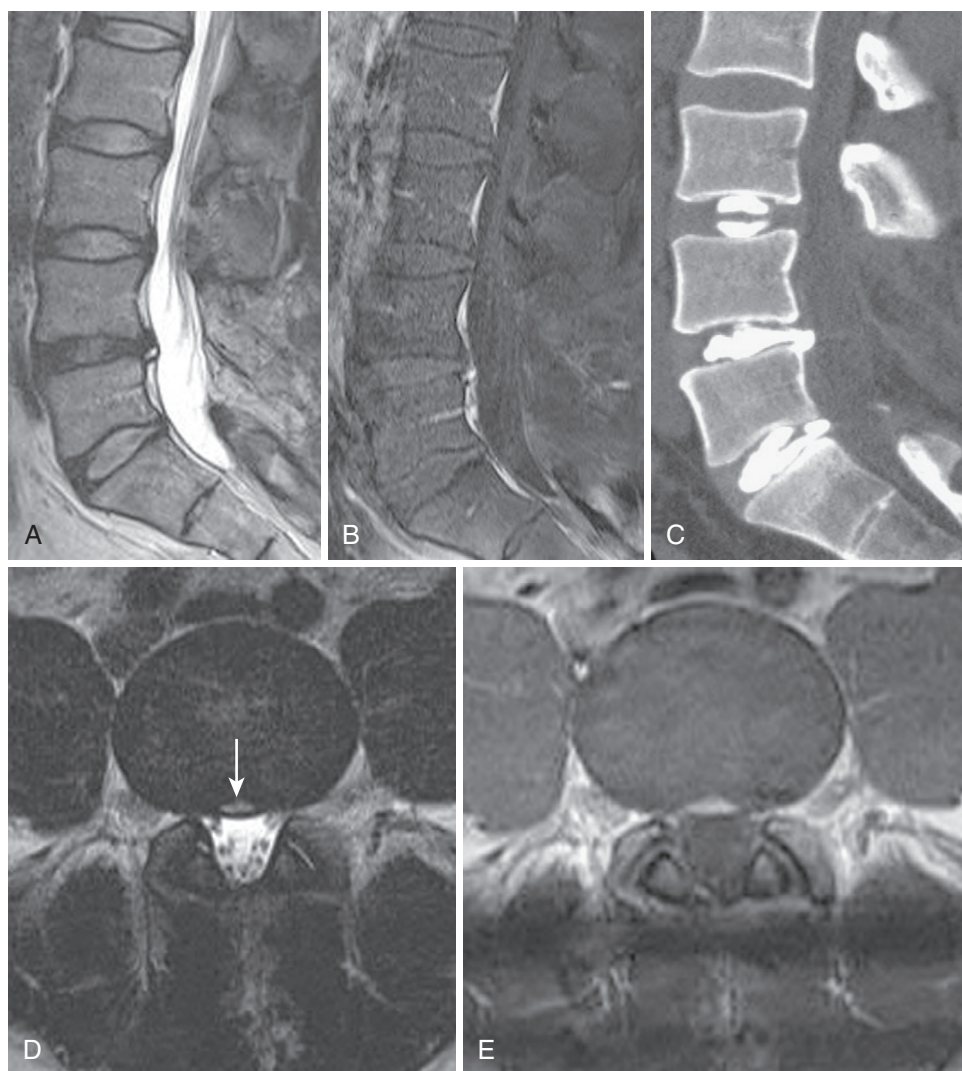


Figure 15.9 High Intensity Zone (HIZ). Middle-aged male has previously undergone L4-5 decompressive procedure, without diskectomy, for back and leg pain. Axial back pain was unrelieved. **A**, Sagittal T2-weighted MRI shows loss of T2 signal in the L4 disk with an HIZ in the posterior annulus. **D**, Axial T2 MRI image at L4-5 interspace demonstrates the HIZ (*arrow*) in the posterior annulus. **E**, Axial enhanced T1 MRI image showing enhancement in the HIZ, also demonstrated in the sagittal fat-saturated T1 image (**B**). Sagittal postdiskogram CT (**C**) demonstrates annular fissure at L4-5 leading to HIZ. Pressurization of the L4-5 disk produced concordant axial pain at < 20 pounds per square inch (PSI) above opening pressure. (From Maus TP, Aprill CN. Lumbar discogenic pain, provocation diskography, and imaging correlates. *Radiol Clin North Am.* 2012;50:681-704.)

structural findings—loss of disk height, loss of nuclear signal, and disk contour abnormalities—correlated strongly with each other; the inflammatory findings, HIZ, and end plate change did not, with the exception of HIZ and disk contour abnormality. The rank correlation of the MRI findings with a positive diskogram was as follows: signal abnormality > disk height > disk contour > HIZ > end plate change. Disk signal change alone was as accurate as other individual parameters or combinations thereof. This was most evident at the two extremes of the receiver operating characteristic (ROC) curve: when disk signal was normal, it was highly unlikely the disk was painful regardless of other findings, and when there was severe signal loss, the disk was highly likely to be painful. Other parameters become useful when disk signal was intermediate. Kang and colleagues⁴⁷ introduced a new MRI classification system combining the findings that were previously addressed as independent variables: class 1, normal or bulging disk without an HIZ; class 2,

normal or bulging disk with an HIZ; class 3, disk protrusion without HIZ; class 4, disk protrusion with HIZ. Disk extrusions and sequestrations were excluded from the analysis. Logistic regression analysis showed that class 4, disk protrusion with HIZ, had the strongest correlation with concordant pain at diskography. This combination had a specificity of 87% and a PPV of 98%. This finding had a prevalence of 13% and a sensitivity of 45%.

IMAGING CORRELATES: CONCLUSION

Imaging identification of diskogenic pain is challenging for a variety of reasons. (1) There is no pathologic or surgical gold standard. (2) The existing standard of comparison, diskography, is ultimately unproven, subjective in its interpretation, and has evolved over time in its criteria for a positive test. None of the studies reviewed earlier use the most current and restrictive criteria, those of ISIS. (3) The

Box 15.3 Imaging Correlates of Diskogenic Pain (IDD)

- The disk structural markers—loss of disk space height, loss of nuclear T2 signal, and disk herniation—correlate strongly with one another; loss of nuclear signal is most significant.
- Severe nuclear signal loss or severe loss of disk space height strongly predicts a painful disk.
- Normal nuclear signal virtually excludes a painful disk.
- When nuclear signal is intermediate, the inflammatory markers of the high intensity zone and end plate marrow change come into play.
- A truly *high*-intensity zone is infrequent but strongly predicts a painful disk.
- When an HIZ is observed in combination with a disk protrusion, it strongly predicts a painful disk.
- Marrow end plate change of type I or type II involving greater than 25% of the vertebral body is uncommon, but it strongly predicts a painful disk.

imaging findings likely have threshold effects, where only a significant expression of the finding (intensity of an HIZ, extent of marrow change) is a useful predictor of diskogenic pain. Most studies do not account for this factor. (4) Imaging findings are likely technique dependent to an unknown degree, and imaging techniques are evolving.

From the tangle of data, useful information can emerge; the imaging correlates of diskogenic pain are summarized in Box 15.3. These imaging predictors of diskogenic pain, when applied to a select population of patients with axial back pain, in whom other pain generators have been excluded, could perhaps be used to initiate a proven therapy possessing a good safety profile. No such therapy exists. Diskography remains the reference standard for the diagnosis of diskogenic pain.

CERVICAL DISKOGENIC PAIN: IMAGING CORRELATES

This discussion has purposely focused on the lumbar spine. The lumbar spine segment is most commonly afflicted with diskogenic pain, and the literature regarding its pathogenesis and evaluation with imaging and provocation diskography, although challenging, is of greatest depth. The cervical intervertebral disk is structurally distinct from the lumbar disk. These is no posterior annulus, and the small nuclear compartment disappears early in life; the residual fibrocartilaginous plate normally develops fissures as mere age-related change.⁸¹ There are no morphologic features at diskography that contribute to a diagnosis of diskogenic pain. Diagnosis is reliant entirely on the provocation of concordant pain, with the requirement of nonpainful control disks.

As in the lumbar segment, structural age changes (loss of T2 signal, loss of disk space height, contour abnormality) are ubiquitous on cervical MRI studies. The Matsumoto³⁰ study cited earlier examined 2480 cervical disks in asymptomatic subjects and noted loss of T2 signal in 17% of males and 12% of females between ages 20 to 30, and 89% of males and 86% of females over 60 years of age. In another study by Okada,¹¹⁵ 89% of asymptomatic subjects (mean age 49)

exhibited structural age changes on MRI; another group of patients (mean age 46) with symptomatic lumbar disk herniations but asymptomatic of neck pain showed cervical disk age-related change in 98%. There is a paucity of literature addressing the correlation of imaging findings with cervical diskography. An early study by Parfenchuck (1994) showed only a modest ability of MRI findings of T2 signal loss or disk contour abnormality to predict a positive cervical diskogram (sensitivity = 73%, specificity = 67%).¹¹⁶ Schellhas' 1996 study suggested that MRI cannot reliably predict a positive cervical diskogram.¹¹⁷ A more recent study by Zheng¹¹⁸ again demonstrated only a modest predictive value of MRI using parameters of T2 signal loss and disk contour abnormality (sensitivity = 73%, specificity = 49%). The inflammatory disk parameters that proved to have such high specificity in the lumbar region are either unusual or little studied (Modic change) or have no anatomic existence (HIZ) in the cervical region. Occasionally foci of elevated T2 signal are observed in the posterior cervical disk, but in the absence of a posterior annulus, the anatomic correlate is unclear. Imaging identification of diskogenic pain in the cervical spine remains elusive. Cervical diskography remains the reference standard in diagnosis of cervical diskogenic pain.

The imaging investigation of diskogenic pain highlights a theme common to this chapter: physiologic parameters have greater significance in pain syndromes than purely structural alteration. To be ultimately valuable in the diagnosis of diskogenic pain, imaging must move beyond macroscopic descriptions of morphology to the realm of biochemical imaging, quantifying the change in nuclear constituents over time. In addition to characterizing biochemical nuclear matrix degradation, imaging will also need to more precisely identify inflammatory mediators in the disk and adjacent cartilaginous end plate. Perhaps then we will truly be capable of the noninvasive diagnosis of diskogenic pain.

IMAGING OF AXIAL PAIN GENERATORS

ZYGAPOPHYSIAL JOINT (Z JOINT, FACET JOINT)

The supporting structure of the posterior column of the spine includes the paired facet joints with their associated capsules, the ligamentum flavum, the intraspinal and supraspinal ligaments joining the spinous processes, and the intertransverse ligaments. The inferior articular process of the facet joint faces anteriorly and is convex in configuration; on axial images the inferior articular process is the more posterior component of the joint. The superior articular process (SAP) has a concave articular surface that faces posteriorly and medially; on axial images it appears as the anterior component of the joint. In an erect standing position, the lumbar facet joints bear approximately 16% of the compressive load; in a flexed sitting position they bear essentially no load. With loss of disk space height, the lumbar facet joints will bear proportionally more axial load. The fibrous joint capsule has been demonstrated to be richly innervated by nociceptors and proprioceptive fibers.¹¹⁹ In a normal state, nociceptors such as those seen in the facet joint capsule have a high threshold and would not be expected to discharge unless loads are suprathysiologic. However, in the presence of pathologic joint inflammation, synovitis,

chemical mediators may sensitize these nociceptors and supraphysiologic levels of stress may no longer be required to stimulate pain. Such inflammatory mediators (substance P, bradykinin, phospholipase A2) have been detected in the facet joint capsule.¹²⁰

There is thus a pathoanatomic basis for facet joint-mediated pain, particularly in the presence of facet synovitis. The imaging challenge in identifying a potentially painful joint lies in the well demonstrated specificity fault, that imaging changes of morphologic facet arthrosis (subchondral sclerosis, erosions, or cyst formation, osteophytes, joint space narrowing, vacuum phenomena) are age related change and do not correlate with pain. The reference standard for facet pain is positive comparative dual medial branch blocks, as there are no reliable physical exam or historical features allowing a confident diagnosis of Z-joint pain.⁸¹ Schwarzer and colleagues semi-quantitatively scored CT finding of structural facet arthrosis and found no relationship to Z-joint pain as determined by placebo controlled medial branch blocks.¹²¹ More recently, Cohen and associates showed no association between MRI findings of structural facet arthrosis and pain relief with dual medial branch blocks and subsequent radiofrequency rhizotomy.¹²² These structural changes become universal by the sixth or seventh decade of life; they do not represent active inflammatory disease causal of pain.¹²³

Rather, imaging must look to identify physiologic, not structural, markers of active facet synovitis. Imaging techniques that may be applicable include the technetium pyrophosphate bone scan (including its technologic evolution SPECT and SPECT/CT) and the MRI physiologic imaging parameters of T2 hyperintensity and gadolinium enhancement. Technetium pyrophosphate bone scans detect hyperemia and accelerated bone turnover, which may be considered manifestations of active inflammation. Dolan and associates¹²⁴ compared the response to intra-articular facet joint injection guided by clinical exam versus positive SPECT studies; there was a significantly greater short term (1- to 3-month) clinical response in the SPECT-guided injections. A similar study by Holder and colleagues, using response to uncontrolled intra-articular injections as the reference standard, identified a 100% sensitivity and 71% specificity for SPECT scans in the detection of facet joint-mediated pain.¹²⁵ Pneumatics and colleagues prospectively studied patients undergoing intra-articular injections in three groups: injections guided by positive SPECT scans, injections in patients with negative SPECT scan guided by clinical exam, and injections in patients without SPECT studies guided by clinical exam.¹²⁶ The patients whose injections were directed to SPECT-positive joints had significantly better clinical outcomes than the other two groups, as well as lower costs as fewer joints were injected. McDonald used SPECT/CT to identify joints for injection in 37 patients with clinical facet joint lumbar pain. The mean visual analog score (VAS) dropped from 7.2 to 2.8, with an average duration of benefit of 2.2 months; only 1 in 37 patients did not report benefit. The fused SPECT/CT images were useful in distinguishing the L4-5 and L5-S1 facet joints.¹²⁷

There is no correlation between the degree of morphologic facet arthrosis and the intensity of SPECT activity.¹²⁴ Rather, the phase of active synovitis correlating with pain production may occur relatively early in the progressive development of structural changes of facet arthrosis. Kim

and colleagues correlated MRI findings in the facet joints with SPECT; they noted that the MRI appearance of T2 hyperintensity in the synovium, intrasynovial fluid, and cartilage disruption best correlated with a positive SPECT, here used as a reference standard for active facet synovitis.¹²⁸ More extensive structural manifestations of facet arthrosis did not demonstrate the physiologic finding of SPECT activity. Cervionke and colleagues have demonstrated an indirect association of T2 hyperintensity within and about the facet joint with axial pain.¹²⁹ T2 hyperintensity in the adjacent pedicle has also been associated with axial pain of facet origin; this finding can also be seen in pedicle or pars stress fractures. T2 hyperintensity accompanying facet synovitis may also be seen in the surrounding multifidus muscle, occasionally sufficiently extensive as to raise concern for a sinister process. Gadolinium enhancement in and about the facet joint is also suggestive of facet synovitis. Ultimately, the physiologic parameters of edema, hyperemia and accelerated metabolic activity as detected by increased SPECT or SPECT/CT activity, and T2 hyperintensity and gadolinium enhancement on MRI must be evaluated as predictors of facet joint pain against the current reference standard, comparative medial branch blocks. Prevalence studies of these parameters in populations asymptomatic of back pain are also needed for researchers to understand the specificity of these imaging observations. Despite the lack of absolute validation, if the patient is going to undergo an MRI for evaluation of axial pain, a fat-saturated or short tau inversion recovery (STIR) sequence should be performed, as it represents the best chance of demonstrating physiologic findings (T2 hyperintensity), which may identify an axial pain generator (Fig. 15.10).

SPACE OF OKADA

A tissue pathway between same segment, contralateral facet joints was initially described in the cervical region by Dr. Kikuzo Okada in 1981; 80% of cervical facets demonstrated a communication between the joint capsules via a space situated dorsal to the ligamentum flavum in the axial plane and in the interlaminar space in the coronal plane.¹³⁰ This communication is frequently observed in intra-articular injections of cervical facet joints that are structurally normal on imaging or exhibit only modest evidence of synovitis or structural arthrosis. In the lumbar region, this communicating pathway is commonly observed only in the face of advanced facet arthrosis; it may also be observed in the presence of defects in the pars interarticularis. This lumbar retroligamentous pathway also commonly communicates with an adventitious bursa within the interspinous ligament (i.e., Baastrup's disease).¹³¹

This pathway may serve as a means of transmission of infection or, more commonly, noninfectious inflammatory change between multiple joints and tissue compartments.¹³¹ In patients with lumbar axial pain and spondylolytic defects, this posterior element inflammatory complex may involve four facet joints, the bilateral pars defects, and the interspinous ligament. It may have a capacity of 4 to 6 cc of fluid in the author's experience. It is also a potential confounding space in interlaminar epidural steroid injections. This space may provide a false loss of resistance superficial to the dorsal epidural space; contrast injection may subsequently

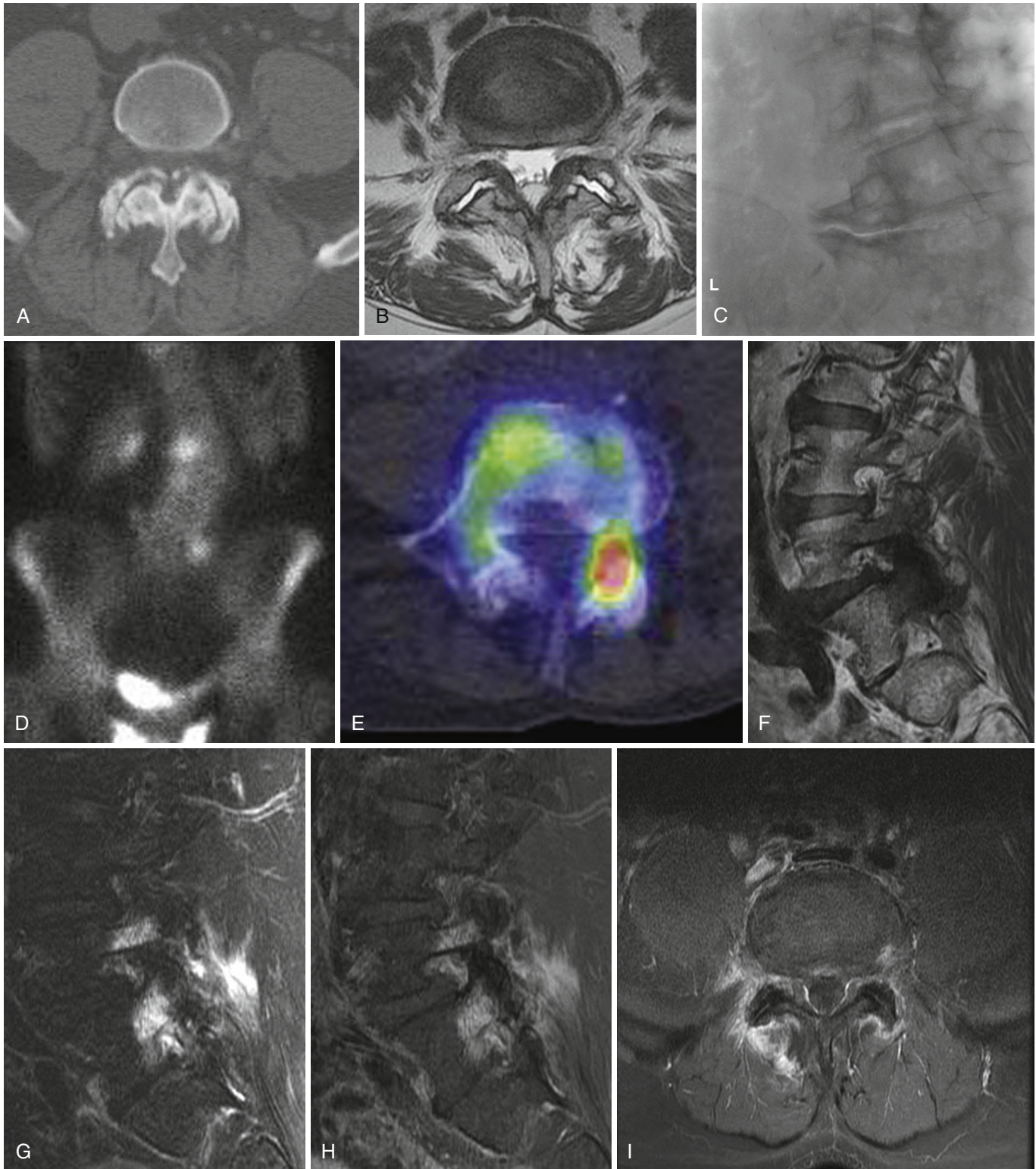


Figure 15.10 Imaging of facet arthrosis and synovitis. The changes of arthrosis (i.e., joint space narrowing, osteophytes, subchondral cysts, or sclerosis) as seen in the CT image (A) the T2 MRI image (B) or the radiographic image (C) do not correlate with pain. Planar bone scan image (D) of the same patient as (C) shows increased uptake near the lumbosacral junction on the left in this patient with left-sided axial pain. SPECT/CT image (E) provides better anatomic localization to the left L4-5 facet. In another patient with right-sided axial lumbar pain, T1 MRI image (F) shows low signal in right L5 pedicle, right L4-5 facet. Fat-saturated T2 sagittal image (G) demonstrates T2 hyperintensity in L4 and L5 pedicles, L4-5 facet, and adjacent soft tissues. Enhanced T1 sagittal (H) and axial (I) images also demonstrate the extensive inflammatory response in this patient with active synovitis. T2 hyperintensity or enhancement in pedicles can occur in facet synovitis or stress fractures of the pars or pedicle.

fill either facet joint at that segment level or the interspinous ligament (Fig. 15.11).

SACROILIAC JOINT

The sacroiliac joint is a large irregular synovial joint lined by thick hyaline cartilage on its sacral surface and thinner fibrocartilage on its iliac surface. The inferior and

antero-superior aspects of the radiographically perceived joint are synovial; its superior and posterior aspect is ligamentous. The posterior surface of the joint is covered by thick interosseous and dorsal sacroiliac ligaments. There is minimal movement of the joint, except under the hormonal influences of pregnancy. This modest mobility is, however, vital to appropriate gait. The synovial portion of the joint is uniformly present in young adults, with a cartilage thickness

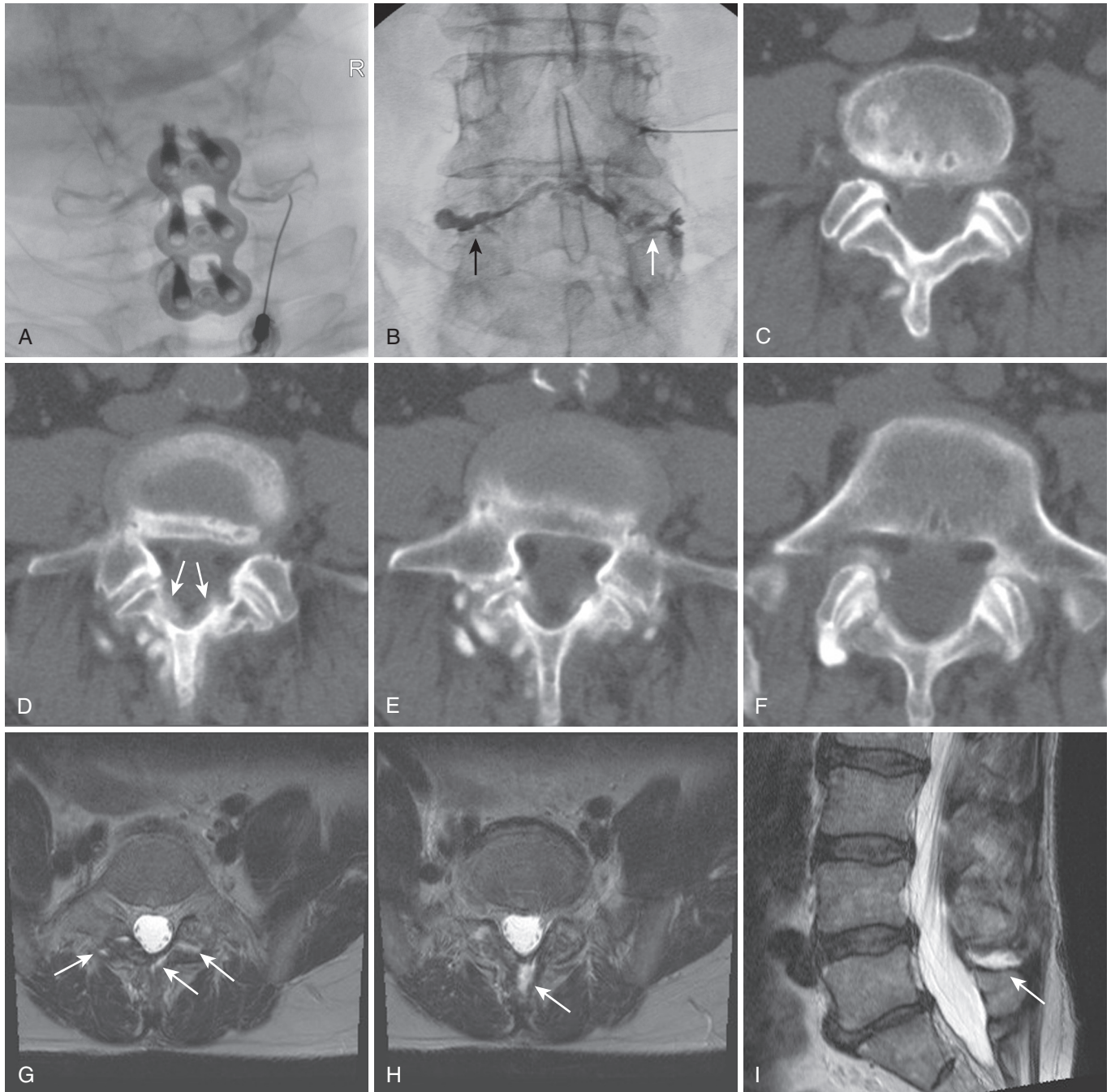


Figure 15.11 The Space of Okada. Frontal fluoroscopic image (A) demonstrates the space of Okada providing communication between the bilateral C6-7 facets via the right-sided injection. In another patient (B), an attempted right L4 transforaminal injection opacified the superior recess of the L4-5 facet, traversed an L5 pars defect (white arrow) to the right L5-S1 facet, and opacified the space of Okada to a left L5 pars defect (black arrow) and the left L4 and L5 facets. Subsequent CT (C, D, E, F) confirms opacification of all these structures. The space of Okada is marked by the white arrows in (D). The space of Okada may contain a small amount of fluid, which appears as T2 hyperintensity (white arrows, G, H, I). Note continuity with interspinous ligament (arrow in [H] and [I]).

Continued

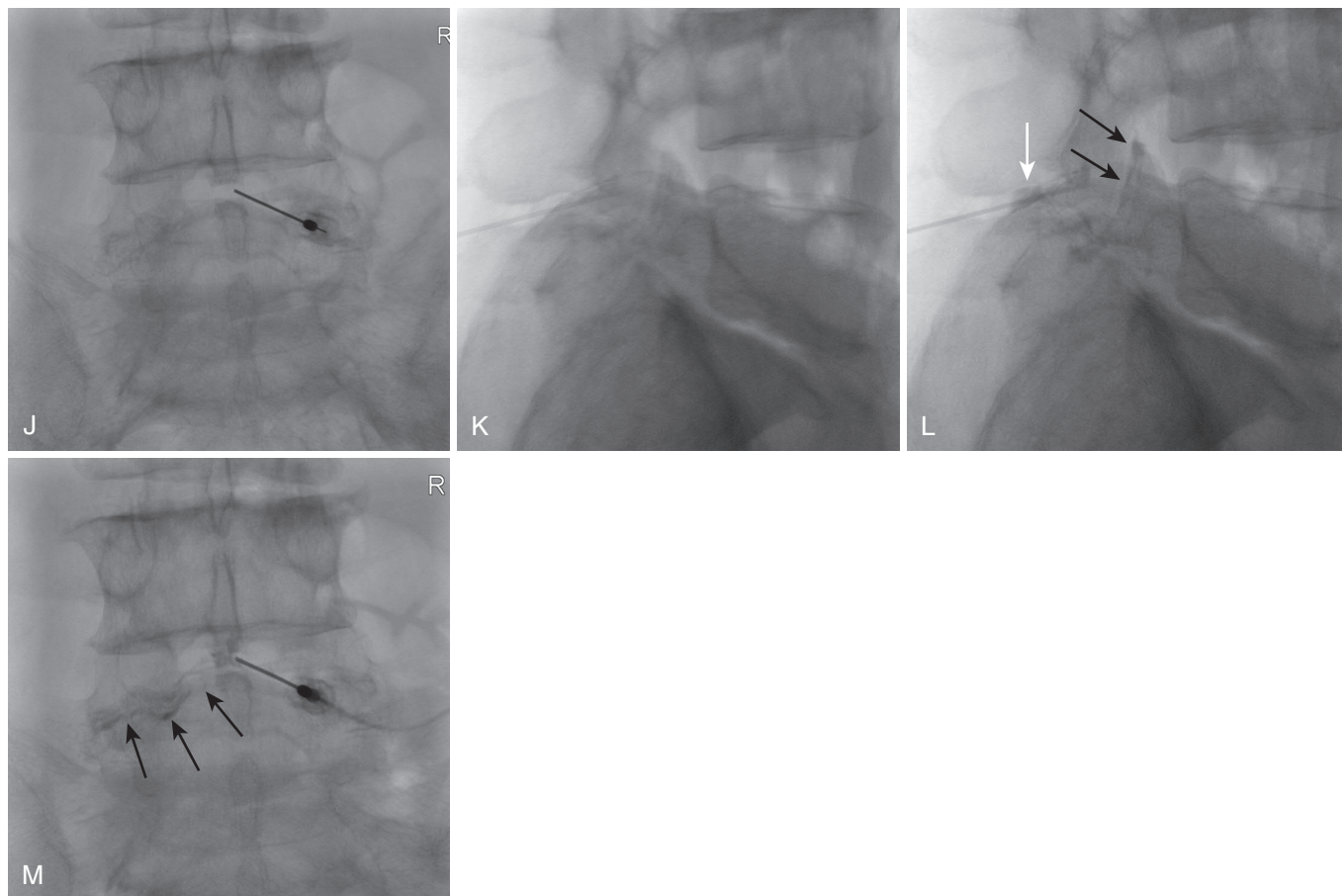


Figure 15.11 cont'd. In a final patient, an attempted interlaminar injection (needle placement images **J**, **K**) opacified the interspinous ligament (*white arrow* in **[L]**) and the left L4-5 facet (*black arrows* in **[L]**) via the space of Okada. This space (*black arrows* in **[M]**) is posterior to the ligamentum flavum; the needle was advanced ventrally into the epidural space without incident. (From Murthy NS, Maus TP, Aprill C. The retrodural space of Okada. *AJR Am J Roentgenol.* 2011;196:W784-W789.)

of 2 to 5 mm; the synovial space may be attenuated in older adults by fibrous adhesions, but fusion across the joint is not a normal change of aging. Potential communications between the synovial space and the dorsal sacral foramina, the L5 epidural sheath, and the ventrally situated lumbosacral plexus have been observed.¹³² These could explain radicular pain associated with sacroiliac joint dysfunction. Although the surface area of the joint is large, its synovial space is of small volume, ranging from 1 to 2.5 cc.^{133,134} Innervation of the sacroiliac joint is complex and remains controversial. Consensus suggests a dominant dorsal innervation from the L5 and S1-S4 dorsal rami.

Osteoarthritis of the sacroiliac joints may be seen in pathologic specimens of young adults, but it is not generally appreciable radiographically until middle age. Changes of cartilage degeneration are more prominent on the iliac side of the joint. Beyond age 40, many subjects have detectable narrowing of the sacroiliac joint, especially in its inferior portion. This may be accompanied by subchondral sclerosis and osteophyte formation, most prominent anteriorly and inferiorly. A vacuum phenomenon may be seen. As in the facet joint, changes of osteoarthritis are a normal aging phenomenon and are not predictive of pain.

Evaluation of imaging features predictive of sacroiliac joint pain is yet again confounded by the lack of a pathoanatomic

gold standard. Medical history and physical exam provocative maneuvers are not capable of consistently identifying painful sacroiliac (SI) joints.¹³⁵ The reference standard for sacroiliac joint pain is relief of index pain with an intra-articular anesthetic block; this should ideally be either placebo controlled or a comparative block paradigm. Potential leakage from the joint capsule may complicate diagnostic specificity. Schwarzer¹³⁶ studied patients with chronic low back pain experienced below the lumbosacral junction. Using response to single blocks as the diagnostic criteria for sacroiliac pain yielded a prevalence of 30%. Requiring a positive block and a ventral capsular tear on postarthrographic CT yielded a prevalence of 21%; adding pain provocation with joint distension to the criteria lowered prevalence to 16%. The Maigne study using double blocks suggested a prevalence of 18.5%.¹³⁷ More recent work by DePalma⁷⁶ identified a prevalence of 18%; sacroiliac joint pain increased in prevalence with age up to approximately 70 years.

Structural changes of osteoarthritis in the sacroiliac joint are poor predictors of pain. Elgafy and colleagues¹³⁸ scored CT features of arthrosis in SI joints and noted a sensitivity of 58% and a specificity of 69%. Physiologic imaging parameters suggesting the presence of hypervascularity, edema, or inflammation are more likely to predict pain. In the studies of Maigne¹³⁹ and Slipman,¹⁴⁰ technetium bone scans

Box 15.4 Zygapophysial (Facet) and Sacroiliac Joint Pain

- Structural arthrosis as seen by radiographs, CT, or MRI does not predict pain.
- Physiologic parameters of hyperemia, edema, and increased metabolic activity may predict pain.
- These physiologic parameters may be assessed by T2 hyperintensity (STIR or fat-saturated T2 images), gadolinium enhancement, or increased uptake on SPECT or SPECT/CT.
- There are no validation studies of physiologic parameters against accepted reference standards (dual, comparative blocks).
- There are no studies addressing specificity—that is, the prevalence of these findings in asymptomatic subjects.

achieved specificities of 89.5% and 100%, although with low sensitivity, for sacroiliac pain as referenced by uncontrolled intra-articular injections. The MRI physiologic parameters of T2 hyperintensity and gadolinium enhancement have been studied primarily in the context of inflammatory spondyloarthropathies. MRI evidence of active inflammation (sacroiliitis) is intrinsic to the diagnoses of spondyloarthropathies and correlates well with clinical disease activity and therapeutic response to disease modifying agents (TNF α inhibitors) (Box 15.4).

BAASTRUP'S DISEASE

Baastrup's disease, the apposition of the lumbar spinous processes resulting from hyperlordosis, segmental instability, or loss of disk space height, may degrade the interspinous ligament with formation of a pseudarthrosis or pseudobursa.¹⁴¹ This may be a cause of focal midline lumbar pain. Such pseudobursa may have a synovial membrane and can communicate with facet joints or pars defects via the retroligamentous space of Okada.¹³⁰ The pseudobursa may extend anteriorly through a midline cleft in the ligamentum flavum and present on MRI or CT as a midline posterior epidural cyst, causing neural compression and contributing to radicular or claudicatory pain. It may be mistaken for a synovial cyst of facet origin but is distinguished by its midline posterior location, the relative absence of facet degeneration, and inflammatory change in the interspinous ligament.

Baastrup's disease may be identified on radiographs as contact between adjacent spinous processes with sclerosis, flattening, and enlargement. Not surprisingly, this structural change is commonly observed in asymptomatic individuals; in one study it was present in 81% of individuals greater than 80 years of age.¹⁴² The authors also noted that "Baastrup's phenomenon" was observed in 41% of patients undergoing CT imaging for non-low-back pain indications.¹⁴² MRI findings of edema, inflammation (T2 hyperintensity, gadolinium enhancement), or a cystic fluid collection in the interspinous ligament are more likely to represent symptomatic disease, although this has not been well validated against anesthetic blocks. DePalma's study suggested that Baastrup's disease accounted for approximately 2% of axial low back pain.⁷⁶ In an MRI study by

Maes and associates, imaging evidence of Baastrup's disease was present in 8.2% of subjects, most commonly at the L4-5 segment; nearly half of the patients had multiple-level involvement.¹⁴³ Baastrup's disease may also be identified as hyperemia and increased metabolic activity on technetium pyrophosphate SPECT or SPECT/CT studies as well as Fluorodeoxyglucose (FDG)-PET/CT scans. Focal uptake in the spinous processes is most likely to be inflammatory and should not be misinterpreted as metastatic disease; the distinction should be obvious when correlated with the simultaneously obtained CT images, which will show typical structural changes of arthrosis.

BERTOLOTTI'S SYNDROME

Bertolotti's syndrome describes the controversial association of transitional lumbosacral segments with mechanical back pain. It does not imply a specific mechanism of pain production. Transitional lumbosacral segments occur in 4% to 30% of the general population.⁷² In a large study of 4000 patients, Tini found no correlation between the presence of a transitional segment and low back pain.¹⁴⁴ The disk at the level of the transitional segment is often rudimentary, with little nuclear material; disk herniations seldom occur at this level.⁷² Rather, stresses may be accentuated at the supra-adjacent disk level, where accelerated disk degeneration and an increased incidence of disk herniations have been reported.

Axial low back pain in the presence of an asymmetric transitional segment has also been attributed to abnormal unbalanced motion at this level, with the neoarticulation of the transverse process with the sacral ala or the contralateral facet as the specific pain generator. Jonsson reported 11 cases of mechanical pain attributed to the neoarticulation despite normal bone scans. Nine of 11 patients obtained pain relief with local anesthetic injection in the neoarticulation; a similar proportion of patients had improvement in pain with resection of the neoarticulation.¹⁴⁵ Physiologic imaging parameters (MRI T2 fat-saturated or STIR images, SPECT/CT) are more likely to be useful than structural changes, although no systematic studies have been performed. Brault reported a case of an adolescent athlete with focal mechanical pain consistently relieved by intra-articular injection of the facet contralateral to the neoarticulation. Interestingly, bone scan showed increased uptake at the neoarticulation, but not at the contralateral facet. Surgical resection of the neoarticulation resulted in complete relief of the contralateral pain at 1 year.¹⁴⁶ This may represent a case of pain generated by excessive facet capsular stresses caused by the asymmetric motion at this level, without detectable facet synovitis.

Transitional lumbosacral segments thus may be associated with axial pain, related to a neoarticulation, the contralateral facet at the level of an asymmetric neoarticulation, or IDD in the at-risk disk above a transitional segment. Radicular pain may be caused by a herniation in the adjacent segment disk or an extraforaminal entrapment at a neoarticulation. The presence of a transitional segment should always prompt meticulous attention to segmental enumeration, because of both its intrinsic capacity for confusion and the sevenfold increased likelihood of an anomalous number of mobile presacral segments (Fig. 15.12).⁷²

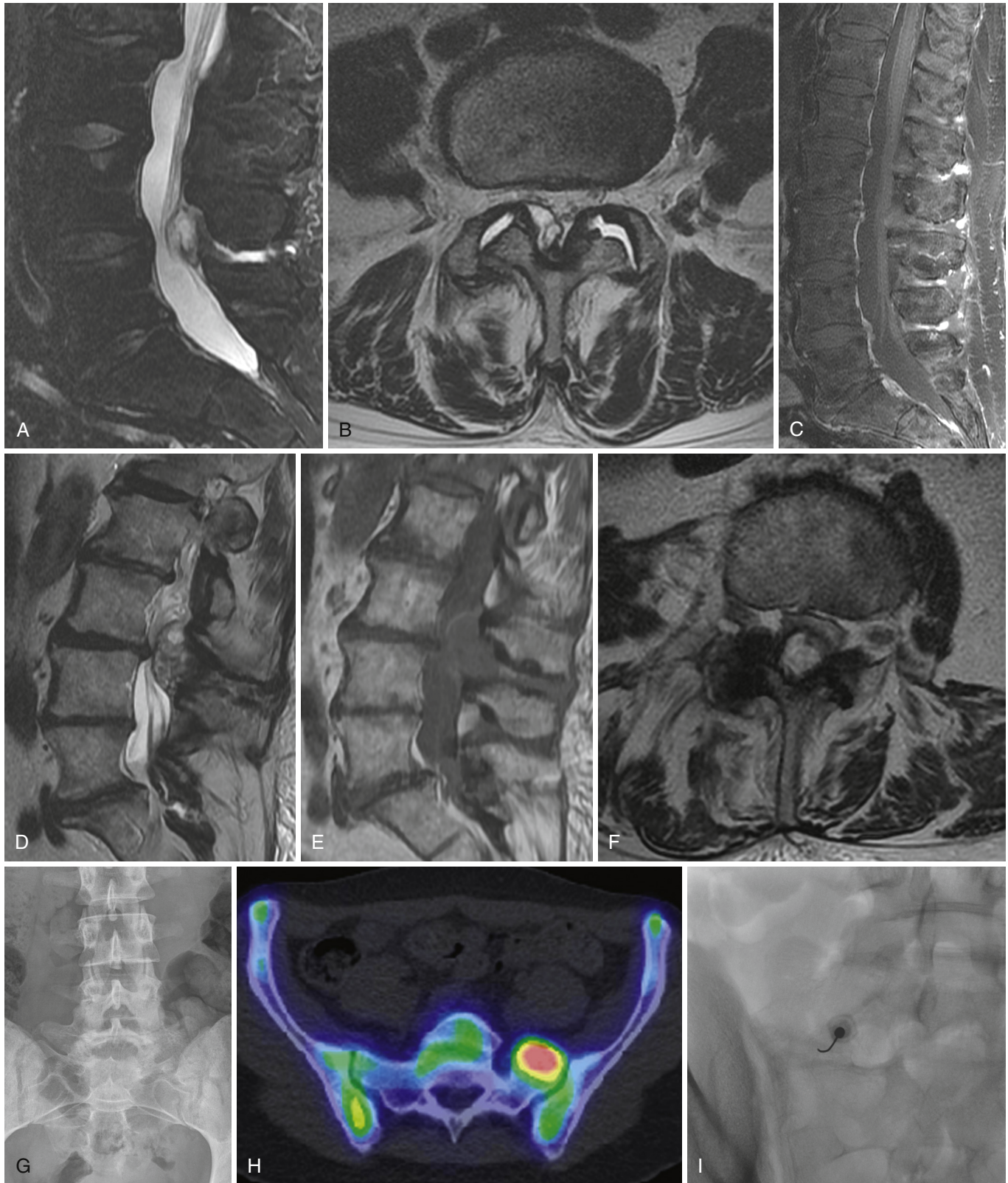


Figure 15.12 Baastrup's disease and Bertolotti's syndrome as posterior element pain generators. An elderly male presents with neurogenic intermittent claudication. T2 fat-saturated sagittal image (**A**) and axial T2 image at the L4-5 interspace (**B**) demonstrate that the compressive lesion is a right paramedian dorsal cyst in continuity with the interspinous pseudobursae of Baastrup's disease. There are also facet joint effusions. In another patient with axial pain (**C**), a fat-saturated, enhanced T1-weighted image shows inflammatory enhancement in the interspinous ligaments of T12-L4. Sagittal T2 (**D**) and T1 (**E**) images of another patient demonstrate a large complex midline dorsal cyst emerging from an interspinous pseudobursae at the L3-4 interspace (axial T2 image [**F**]). A 17-year-old female (frontal lumbar spine radiograph [**G**]) presented with intractable left lumbosacral junction region pain. Note left pseudoarthrosis (Bertolotti's syndrome). SPECT/CT image (**H**) shows markedly increased uptake at the pseudoarthrosis; pain was relieved with injection into this site (fluoro image [**I**]; note that the patient is prone).

COCCYDYNIA

The radiographic evaluation of the sacrococcygeal region in patients with coccydynia remains controversial. This largely female pain syndrome is probably multifactorial in origin with contributions by somatic and neuropathic pain.¹⁴⁷ A single lateral view of the coccyx to evaluate for destructive bony lesions is a reasonable screening study. Maigne has described a dynamic radiographic study to more fully evaluate the mobility of the coccyx.¹⁴⁸ This consists of a lateral radiograph with the patient standing for 10 minutes to visualize the coccyx without load, followed by a sitting lateral view, with the patient altering the pelvic position to that which stimulates the usual pain. Maigne and colleagues have studied coccygeal mobility and suggested that a normal coccyx may undergo from 5 to 25 degrees of angulation in moving from a standing to a sitting position. Flexion of the coccyx by more than 25 degrees with sitting as well as posterior subluxation of the coccyx with sitting and reduction with standing are considered pathologic and may be the anatomic basis of coccydynia.¹⁴⁸ Aggressive treatment decisions based on this evaluation are controversial. Advanced imaging has little role in this setting unless there is clinical suspicion of underlying systemic disease.

PSEUDARTHROSIS, POSTOPERATIVE AXIAL PAIN

Patients with posterior fusion instrumentation may develop pain related to pseudarthrosis, infection, implant fracture or loosening, or at the interface between the metal and the overlying soft tissue. Radiographs should be scrutinized for integrity of the implant construct, loosening of pedicle screws (which will manifest as a halo of lucency surrounding the screws), or imaging evidence of pseudarthrosis. Anesthetic injection about prominent hardware may be useful in identifying this as a pain generator.

Despite advances in surgical technique and fixation hardware, fusion remains an imperfect procedure. Pseudarthrosis is defined as the failure to achieve a solid bony fusion 1 year after attempted surgical fusion. It is manifested as persistent motion at the segment and absence of bony trabeculae bridging the vertebrae. Approximately 15% of lumbar spinal fusions result in pseudarthrosis; the range of successful reported technical and clinical outcomes spans 16% to 95%.¹⁴⁹ Rates of pseudarthrosis increased with the increasing number of fused levels and with risk factors including prior surgery, instability, deficient bone graft quality and quantity, and nicotine use (Fig. 15.13).

Detection of pseudarthrosis with imaging is of significance, as it is a cause of persistent or recurrent pain following surgery. The correlation is not exact; patients with radiographic pseudarthrosis may be pain free and patients with solid fusions by all imaging techniques may have persistent pain arising from other factors. The clinical questions, therefore, are twofold: Is a pseudarthrosis present, and, if so, is it the cause of persistent or recurrent pain? The ultimate gold standard for fusion is surgical exploration; even this is not foolproof, as patients who have had hardware removal after intra-operative evaluation of stability have subsequently gone on to develop progressive deformity.¹⁵⁰

Weight-bearing radiographs are the primary tool in assessing stability and adequate fusion. In this setting,

flexion-extension views likely add value. Radiographic evidence of instability includes translation of 3 mm or more at L1-L4 or 5 mm at L5-S1. Radiographic fusion may take 6 to 9 months, with ongoing remodeling for up to 2 years. Criteria for a radiographic solid interbody fusion are as follows:¹⁵¹

- No motion, or less than 3 degrees of intersegment position change on lateral flexion and extension views
- Lack of a lucent area around the implant
- Minimal loss of disk height
- No fracture of the implant, bone graft, or vertebrae
- No sclerotic change in the bone graft or adjacent vertebrae
- Visible osseous formation in or around the cage

CT will provide greater sensitivity in the detection of pseudarthrosis, which manifests as lucent fracture lines with adjacent sclerosis or fragmentation of the bone graft, and fracture or lucency about implants. Ideally, to verify solid fusion, one would like to be able to confirm the presence of continuous bony trabeculae across the site of fusion. In patients with intervertebral cage devices, bony trabeculae should be seen bridging the interspace through the cage and external to the cage.

Technetium bone scans with SPECT may be helpful. The fusion mass will be metabolically active for a prolonged period after surgery, and increased tracer uptake diffusely in the fusion mass is expected for several months. In normal healing, studies with serial bone scans have shown a steady decrease in tracer uptake after 3 months, with only minimal increased uptake at 1 year.¹⁵² Increased uptake within the fusion mass beyond 1 year after surgery, or new increased uptake not present on prior studies, should raise concern for pseudarthrosis. On MRI, solid bone graft should exhibit signal characteristics of normal marrow. Focal zones of T1 hypointensity, T2 hyperintensity, and gadolinium enhancement may indicate a site of pseudarthrosis with ongoing motion and inflammation. This requires careful inspection.

With disk arthroplasty, postoperative evaluation can occur by radiography or CT; radiography is more conservative of cost and radiation for serial follow-up. The implant should be centered between the pedicles on AP images without penetration of the end plates. On lateral or sagittal images, the center of rotation should be in the posterior half of the disk space, but the implant should not extend beyond the posterior vertebral line.

The clinician and imager must also be aware of symptomatic adjacent segment disease as a cause of recurrent pain in the post fusion patient. Although controversial, this likely occurs at a rate of approximately 3% per year following lumbar fusion;¹⁵³ a similar rate has been associated with cervical fusion. The imaging findings will be those of diskogenic pain. Radiographic evidence of adjacent segment disease may or may not be clinically symptomatic.

Pseudarthrosis and adjacent segment disease are two primary causes of pain in the post-operative patient, sometimes labeled the “failed back.” Although conventionally considered a dread diagnosis, studies have shown that careful clinical evaluation, augmented by high-quality imaging and provocation and anesthetic interventions, can identify the specific cause of pain in the majority of cases. Waguespack and Slipman have each published large series of patients with so-called failed back syndrome.^{154,155} A specific diagnosis identifying the pain generator was achieved in over

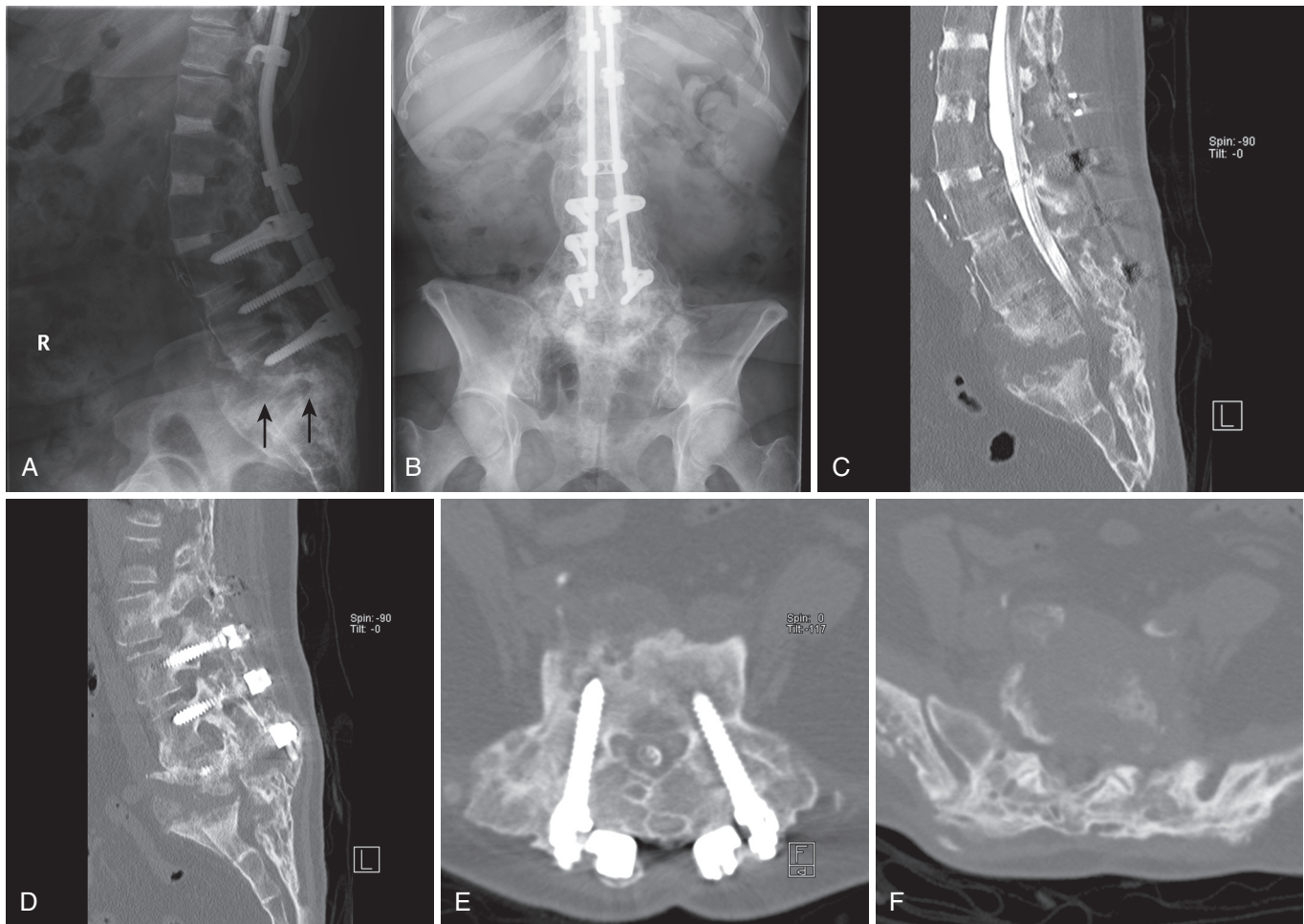


Figure 15.13 Pseudarthrosis on CT Myelography. This 71-year-old female is post multiple spine surgeries and has an instrumented fusion from the upper thoracic region to L5. She presents with bilateral leg pain in an L5 radicular distribution. Radiographs (**A, B**) show lucency with surrounding sclerosis at the L5 level. CT myelography sagittal reconstructions (**C, D**) reveal a pseudarthrosis at L5-S1 with Charcot or infectious features. Cultures were negative. Despite the instrumentation, the thecal sac is well demonstrated; it is patent at the L5 vertebral level (**E**) but obliterated at the L5-S1 disk level (**F**). (From Thakkar RS, Malloy JP, Thakkar SC, et al. Imaging the postoperative spine. *Radiol Clin North Am.* 2012;50:731-747.)

90% of patients in both of these series. The most common diagnoses were foraminal stenosis (> 20%), diskogenic pain (20%), pseudarthroses (14%), neuropathic pain (10%), and recurrent disk herniation (7% to 12%), with lesser contributions from facet and SI joints. Each of these morphologic lesions has been individually addressed in preceding sections. The imaging challenge is to systematically evaluate each segmental level for these potential pain generators despite the confusion of the surgically altered anatomy.

IMAGING OF RADICULAR PAIN, RADICULOPATHY, AND MYELOPATHY

DISK HERNIATION

Radicular pain, or radiculopathy or myelopathy, has as its substrate neural compression and inflammation. Degradation of the nuclear matrix of the disk may occur in response to a variety of insults, including end plate infraction, genetically determined apoptotic chondrocyte cell death, diabetes

mellitus, ochronosis, smoking, or infection. The nuclear compartment of the disk can no longer bear axial load, shifting its burden to the posterior annulus, which may undergo structural failure in the form of radial fissures, the anatomic basis of IDD. In addition to potentially causing axial pain, these fissures may allow herniation of nuclear material into the outer annular lamellae as a contained protrusion or breach the annulus and pass into the epidural space as an extrusion. The mechanical compression of neural tissue and an induced inflammatory response conspire to provoke radicular pain or radiculopathy.

Mixer and Barr initially described the disk herniation as the cause of sciatica in 1934; this observation, and the ability to relieve pain and neurologic dysfunction by surgical extirpation of the offending herniation, provided the basis for the first 70+ years of spine imaging. Myelography, CT, CT/myelography, and MRI were deemed useful in the patient with radicular pain or radiculopathy in the ability to first indirectly and later directly visualize the disk herniation and neural compression. The pathogenesis of radicular pain or radiculopathy is more complex than the simple

compression of neural elements; an inflammatory response is also necessary to produce pain. The evidence supporting an inflammatory component in radicular pain was summarized by Mulleman and colleagues.^{156,157} Neural compression in isolation produces nerve dysfunction, but not pain; exposure of compressed neural elements to the inflammatory response induced by disk nucleus pulposis results in radicular pain. This inflammatory response is mediated by phospholipase A2, interleukins 1 and 6, TNF α , and nitric oxide. The necessity of an induced inflammatory response for pain production provides a measure of understanding for the glaring specificity fault of disk herniation imaging: large disk herniations are often asymptomatic, and the severity of symptoms bears no relationship to herniation size.

The imaging description of disk herniations has historically been chaotic, with significant disparities among medical specialties and regionally. Clarity was restored by a lexicon of nomenclature produced as a cooperative venture between multiple spine societies in 2001.¹⁵⁸ In this construct, spondylosis deformans describes those changes thought to be due to normal aging. Degradation of the nuclear matrix may occur without structural failure of the annulus, hence there is preservation of disk space height and normal cartilaginous end plate and subchondral marrow. Anterior and lateral osteophytes are observed. MRI imaging shows loss of the normal intranuclear cleft and mild to moderately diminished T2 signal within the disk. Small concentric and transverse annular tears may be seen in spondylosis; radial tears are not considered a normal aging phenomenon. Small amounts of gas may be present within the disk that may be detected on plain films.

In this lexicon, pathologic discovertebral change is termed intervertebral osteochondrosis. This includes the changes of IDD, radial and large circumferential fissures extending to the outer annulus. They may be accompanied by the development of posterior osteophytes that encroach on the central canal. In addition to posterior osteophytes, plain film manifestations of intervertebral osteochondrosis include large amounts of gas within the interspace, loss of disk space height, and end plate irregularity. On T2-weighted MRI images, the disk is of markedly diminished signal intensity. Disk herniations are common.¹⁵⁸

The inclusive term for displacement of disk material is *herniation*. A localized herniation is defined as involving less than 50% of the disk circumference; generalized disk displacement of more than 50% of the circumference is a bulging disk. Localized herniations are further subdivided: displacement of the disk over less than 25% of its circumference is called a focal herniation, and disk displacement between 25% and 50% is called a broad-based herniation. The distinction between protrusion and extrusion is one of shape (Fig. 15.14). In a protrusion, the width of displaced disk material, in any plane, does not exceed the width of its base against the normal ring apophysis. In an extrusion, the width of the displaced disk material exceeds its base in any plane. The presence of an extrusion shape suggests that there has been complete disruption of the outer annulus and disk material has entered the epidural space. *Sequestration* is the term for loss of continuity of a disk fragment with the parent disk from which it arose. Displacement of disk material away from the parent disk is termed *migration*. Migration can occur caudally or cranially. A herniated disk

can further be classified as contained or uncontained. A contained disk herniation is one in which the outer annulus fibrosis is intact, whereas an uncontained herniation is one in which the annulus is completely disrupted. The shape definitions of protrusion and extrusion speak to this, but only by implication, not direct observation. CT or MRI can only rarely directly establish containment; post-CT diskography can make this distinction.

Description of displaced disk material (Fig. 15.15) in the axial plane is defined by zones: the central zone defined by the medial margins of the facets, the subarticular zone extending from the medial facet margin to the medial pedicle margin, the foraminal zone extending from the medial to lateral margins of the pedicle, and the extraforaminal zone peripheral to the lateral pedicle margin. A right-sided focal disk herniation may therefore be described as right central, right subarticular, right foraminal, or right extraforaminal. Similarly, the location in the sagittal plane (superior-inferior) is defined by levels in relationship to the vertebral end plate and pedicle margins. Extending from superior to inferior, the designations include the disk level, suprapedicular level, pedicle level, infrapedicular level, and the subsequent disk level. Although an element of subjectivity remains inherent in any usable system of terminology, careful adherence to these descriptors should allow a more coherent discussion of disk pathology.

Imaging of patients with radicular pain or radiculopathy should begin with upright radiographs of the involved spine segment. This will establish the enumeration, assess balance and stability, and act as a low-sensitivity screen for sinister disease. Advanced imaging may be needed in the setting of intractable radicular pain or progressive neurologic deficit. MRI has long been considered the primary imaging modality in the evaluation of disk herniations, but this has little basis in evidence. There are no studies comparing current generation CT with MRI technology in the detection and characterization of disk herniations. MRI remains the initial modality of choice largely because of its superior sensitivity and specificity in the detection of sinister disease causal of back or limb pain, which, it must be remembered, is the primary goal of imaging. CT myelography retains a problem-solving role in the lumbar region, but it plays a more prominent role in the cervical spine, where its ability to distinguish disk from bone may impact surgical planning.

IMAGING RELIABILITY

MRI has shown good reliability in the assessment of disk herniations. Lurie and colleagues¹⁵⁹ analyzed MRI studies of patients with disk herniations from the Spine Patient Outcomes Research Trial (SPORT) trial; interobserver reliability was high ($\kappa = 0.81$) for disk morphology when classified as normal/bulge, protrusion, and extrusion/sequestration. There was moderate inter-observer agreement for thecal sac ($\kappa = 0.54$) and nerve root compression ($\kappa = 0.47$). Pfirrmann and colleagues¹⁶⁰ proposed a grading system for nerve root compression. The authors divided the relationship of the herniated disk and the nerve root into four categories: no compromise, contact with the nerve root, deviation of the nerve root, and compression of the nerve root. The intra-observer ($\kappa = 0.62$ to 0.67) and intra-observer ($\kappa = 0.72$ to 0.77) reliability results were good. The correlation for a higher grade of nerve root involvement (compression) was better than for low-grade nerve root involvement.

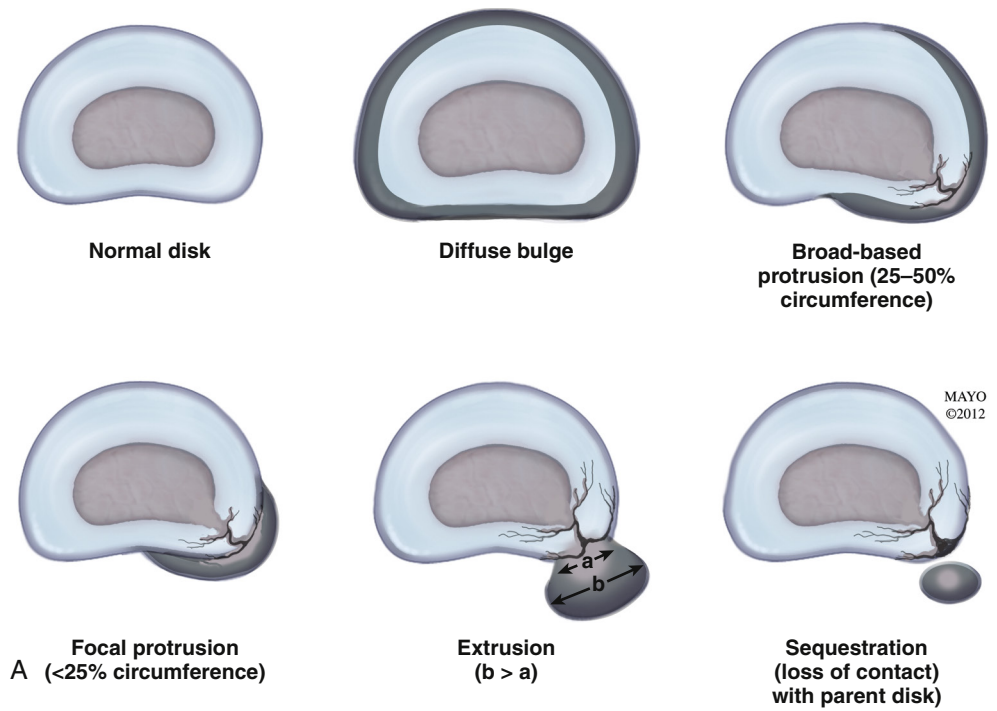


Figure 15.14 Disk herniation definitions. Disk herniation definitions are depicted in the axial (A) and sagittal (B) planes. Note that the normal L1-L4 disks, shown here, are not round, but an oblate structure whose dorsal margin is convex anteriorly. The L5 disk is normally oval in configuration, convex posteriorly. The definitions are elaborated in the accompanying text.

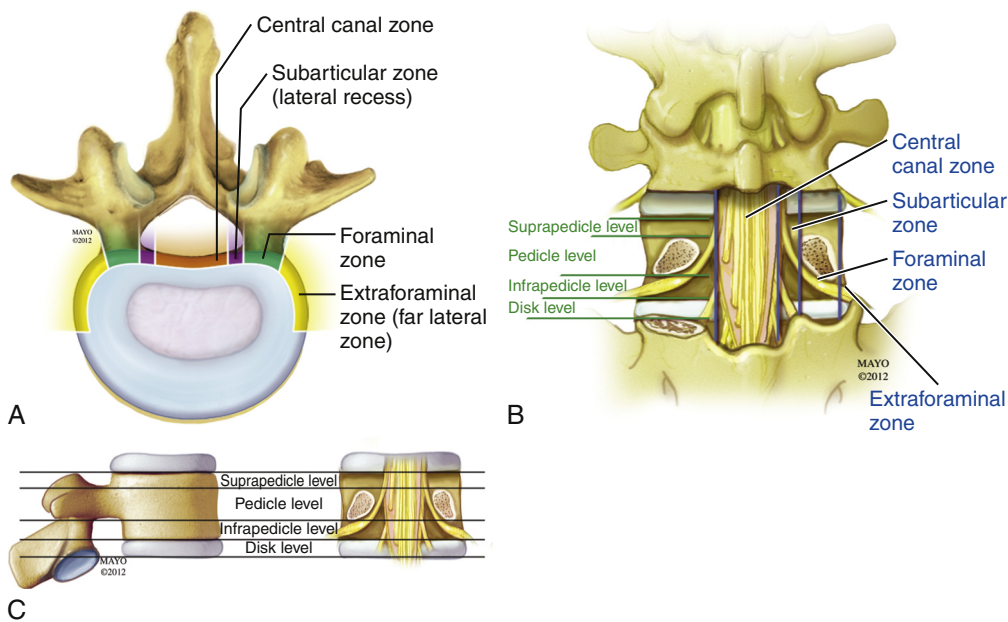
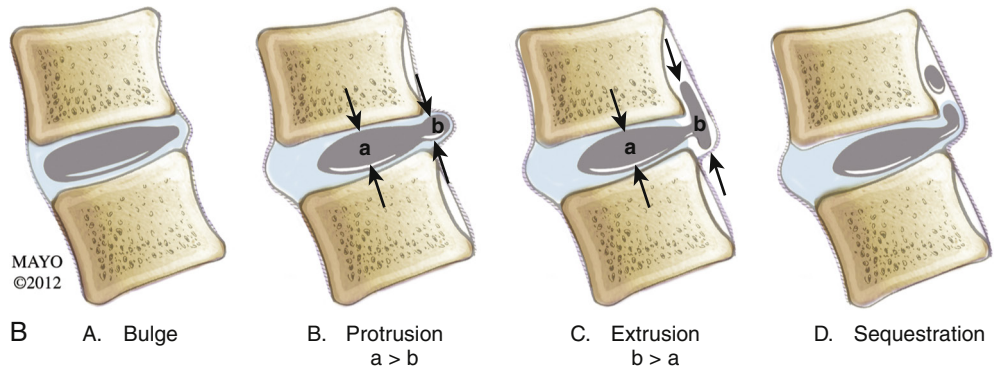


Figure 15.15 Zones and levels of disk displacement. In the axial plane (A) the location of displaced disk material is described by zones. Moving from the midline laterally, these zones are the right or left central zone, demarcated by the medial margins of the facet joints; the subarticular zone (lateral recess), bounded by the medial aspect of the facet joint and the medial aspect of the pedicle; the foraminal zone, bounded by the medial and lateral aspects of the pedicle; and the extraforaminal or far-lateral zone, peripheral to the lateral margin of the pedicle. These zones are also illustrated in the coronal plane (B). The displacement of disk material in the cephalocaudal dimension is described by levels, as illustrated in (B) and (C).

IMAGING OBSERVATIONS

MRI T2-weighted images can well display the interface between disk herniations and the thecal sac. The herniated material may be of low T2 signal intensity comparable to the parent disk that has undergone nuclear matrix degradation, but not uncommonly extruded disk material is of higher T2 signal than its parent disk. This may in part reflect inflammatory reaction surrounding extruded material; it can make detection of extruded material in the lateral recesses or foramina challenging on Fast Spine Echo, Turbo Spin Echo (FSE, TSE) T2-weighted images in which fat is also bright. Comparison with matched T1-weighted images will identify the now dark disk material against the bright fat in the lateral recess or foramina. Occasionally, disk herniations may be associated with a small amount of hemorrhage in the epidural space, which may manifest itself as an epidural process of high T1 and variable T2 signal intensity. This hemorrhage may be related to the pathogenesis of discal cysts, relatively rare cystic lesions in the epidural space, which may present with radicular pain and be the result of prior disk extrusion and hemorrhage with incomplete resorption.¹⁶¹

Ninety percent of lumbar disk herniations occur at the L4 or L5 interspace levels. The vector of disk displacement in most herniations is posterolateral. In the lumbar spine, the exiting nerve passes immediately inferior to the vertebral pedicle and exits the foramen above the interspace level. Therefore, most disk herniations do not affect the exiting nerve, but rather impinge on the traversing nerve, which exits under the next lower vertebral pedicle. For example, a posterolateral L4-L5 disk herniation results in an L5 radicular pain syndrome or radiculopathy. For a lumbar disk herniation to affect the like numbered nerve, it must be an extrusion with lateral and cephalad migration of disk material into the neural foramen. The greater spatial resolution of CT myelography may identify subtle lateral recess or foraminal lesions less well seen on MRI.

Contrast material is not typically used when MRI is undertaken to evaluate for causes of radicular pain or radiculopathy except in the presence of red flag features raising concern for infection of neoplasm, or prior surgery. Unenhanced imaging can primarily detect the mechanical compression of a nerve, not the inflammatory response, which is also necessary to provoke radicular pain. T2 hyperintensity on STIR or fat-saturated images may identify this reaction. If gadolinium is given, it is often observed that the soft tissue seen on unenhanced images, thought to be herniated disk material, is largely enhancing inflammatory/granulation tissue about a small disk fragment. When confronted by a patient with clinically evident radicular pain or radiculopathy and no evidence of a neural compressive lesion on standard imaging, an enhanced exam may reveal an inflammatory process associated with a disk whose annulus is incompetent.¹⁶² This is described as chemical radiculitis. The neural compressive component of the lesion may only be present on imaging with axial load and physiologic positioning (Fig. 15.16).

POSTOPERATIVE IMAGING

Gadolinium-enhanced MRI does have a well-defined role in the evaluation of the postoperative patient. Plain films, CT, and CT myelography are relatively uninformative in

the postoperative patient, as they cannot reliably distinguish recurrent disk herniation from epidural fibrosis/scar. Following discectomy, extensive anatomic changes evolve over time, confounding imaging interpretation. Great caution must be used in interpreting MRI within 6 weeks of surgery.¹⁶³ In this time frame, MRI is most useful in the evaluation for hemorrhage, pseudomeningocele, or diskitis; evaluation for recurrent disk herniation is tenuous. The diagnosis of postoperative diskitis is also complicated by the normal linear enhancement that may be observed in the postoperative disk.¹⁶³ As postoperative tissue disruption and edema stabilize, MRI with gadolinium enhancement has been reported to be 96% to 100% accurate in distinguishing recurrent disk herniation from scar.¹⁶³ Scar or epidural fibrosis enhances rapidly and uniformly following gadolinium administration; disk material does not enhance for the first 20 to 30 minutes. Early post-gadolinium images in the postoperative patient will show recurrent disk herniation as a nonenhancing zone; enhancing epidural fibrosis may surround this. Extensive scar or epidural fibrosis is in itself a negative prognostic sign, associated with an increased incidence of postoperative radiculopathy.¹⁶⁴ In the postoperative setting, the thecal sac should be examined for evidence of arachnoiditis. In this condition, the roots of the cauda equina are either clumped together or adherent to the dural tube. The dural tube may even appear empty of roots, which are smoothly scarred to its wall. Roots may exhibit enhancement in this condition.

IMAGING NATURAL HISTORY

The imaging natural history of disk herniation is resolution.¹⁶⁵ Large disk herniations, extrusions, and sequestrations, which have entered the highly vascular epidural space, are most likely to undergo resorption mediated by macrophage produced metalloproteases.¹⁶⁶⁻¹⁶⁸ This inflammatory response is integral to the profound pain these patients feel, but it will ultimately resorb the extruded disk material. If the inflammatory response can be attenuated by the targeted administration of corticosteroids, thus allowing the patient to remain functional, over time natural history will bear out with resolution of the herniated disk material and the radicular pain syndrome. Contained protrusions and bulges, with intact outer annulus shielding the herniation from the full fury of the immune system, tend not to change over time.

VALIDITY OF DISK HERNIATION IMAGING: CORRELATION WITH SYMPTOMS/SIGNS

The fundamental specificity fault of spine imaging is very evident in the imaging of disk herniations. Modic⁵⁴ demonstrated that there was no relationship between herniation type, size, or change over time and patient outcome. Most of the imaging findings observed on an imaging study obtained at presentation with radicular pain will have been present at a time when the patient was asymptomatic.⁵³ In another study by Masui, disk herniations treated conservatively were followed over 7 years.¹⁶⁹ Clinical outcomes were unrelated to the size of the herniation or age changes in the disk. To assign causality to a disk herniation, there must be concordance, a perfect match of the patient's pain or dysfunction syndrome, and the expected detriment caused by

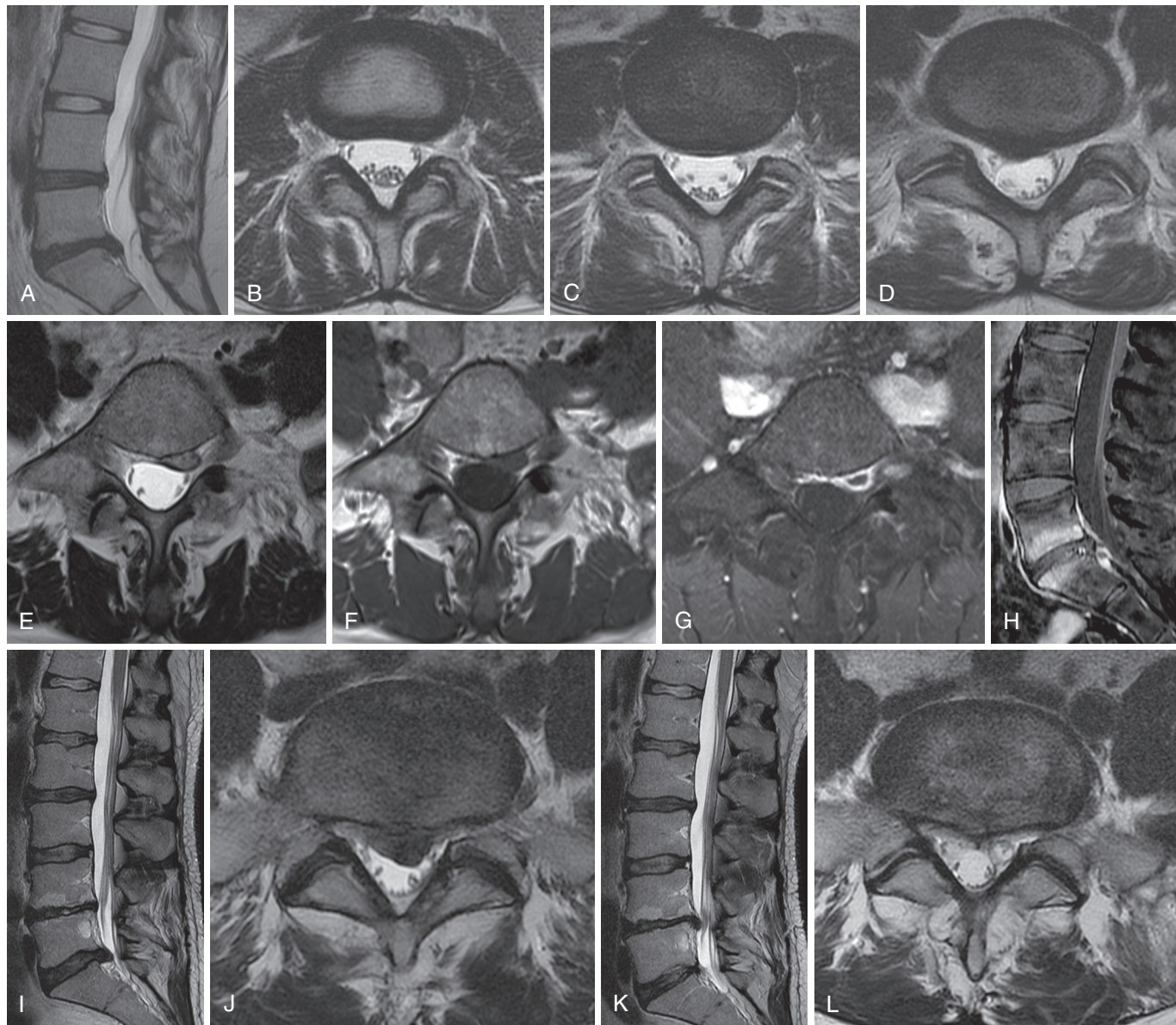


Figure 15.16 Disk herniations. Sagittal T2 MRI (A) and axial T2 images at L3-4 (B), L4-5 (C), and L5-S1 (D) disks demonstrate a normal L3-4 disk, a central protrusion at L4-5, and a right central extrusion with caudal migration at L5-S1. Axial T2 (E) and T1 (F) MRI images at the S1 end plate level demonstrate a left-sided sequestered disk fragment contacting the thecal sac. Fat-saturated T1 axial image (G) and sagittal image (H) show that much of the apparent disk herniation enhances and is inflammatory reaction about a small disk fragment. Enhancing Modic I change is present. Another patient with left S1 radicular pain due to an L5-S1 disk extrusion (I, J) was treated with a transforaminal epidural steroid injection with resolution of pain. He returned 4 years later with new L5 distribution pain and was reimaged (K, L). Note that the L5-S1 extrusion has completely resolved; (L) is at the identical level as (J) and a new L4-5 extrusion has developed. The natural history of disk extrusion is resolution.

an observed herniation. The imager must know the nature of the pain syndrome to identify its likely cause among the distracters of asymptomatic findings. The sensitivity fault is also evident; disk herniations that do not appear to contact neural tissue on recumbent imaging may be compressive under axial load and physiologic posture. Willén and Danielson demonstrated that significant additional information was demonstrated in 14% of sciatica patients on images obtained under extension and axial load, including accentuation of disk herniations, increasing lateral recess or foraminal stenosis, and distension of synovial cysts that contributed to root compression (Box 15.5).¹⁷⁰

RADICULAR PAIN

LATERAL RECESS, FORAMINAL STENOSIS

As the nerve root exits the common dural sac into its root sleeve, it leaves the central canal, passing caudally and laterally into the lateral recess or subarticular zone. Compromise of the lateral recess may be causal of radicular pain or radiculopathy. Lateral recess stenosis is primarily a product of facet joint arthrosis with overgrowth of the superior articular process. This encroaches on the posterior aspect of the lateral recess, impinging on the exiting nerve root. This is

Box 15.5 Disk Herniations and Radicular Pain

- Radicular pain requires both compression of neural tissue and an inflammatory response, likely mediated by TNF α .
- Standard imaging can only detect nerve root displacement or compression, which are necessary but insufficient to cause symptoms.
- This is in part the basis of the specificity fault: many disk herniations are asymptomatic.
- Assignment of causality of symptoms to a disk herniation requires concordance: there must be a key in lock match of the lesion and the syndrome of pain and neurologic dysfunction.
- The imager must know the nature of the radicular pain/radiculopathy syndrome to consider ascribing symptoms to a disk herniation.
- The natural history of disk herniations is resolution; larger herniations, extrusions, and sequestrations are more likely to resolve.
- There is no relationship between the size, type, or change in disk herniations over time and patient outcomes.
- Decisions regarding surgical intervention must be based on clinical grounds, not imaging appearance.

best demonstrated on axial MRI or CT myelographic images (Fig. 15.17). These images should be scrutinized to be certain that the nerve root in question is indeed entrapped within the lateral recess rather than simply displaced medially into the central canal. The minimum normal A-P dimensions of the lateral recess have been variably reported as 3 mm to 4 mm.¹⁷¹ The lumbar level most commonly involved with lateral recess stenosis is the L4-5 interspace level.

As the exiting nerve root continues to progress caudally and laterally under its similarly numbered lumbar pedicle, it enters the foraminal zone. The intervertebral foramen is an inverted teardrop-shaped orifice; the exiting root is situated in the larger, superior aspect of the foramen. An annular bulge or lateral protrusion may intrude into the inferior portion of the neural foramen without causing neural compression. A disk extrusion with cranial migration of disk material into the foramen may compress the exiting root. Other degenerative phenomena causing foraminal stenosis include osteophytes arising from the posterior margin of the vertebral body or superior articular process, synovial cysts, or abnormalities of vertebral alignment, including the concavity of a scoliotic curve or spondylolisthesis resulting from spondylolysis or facet arthropathy. Foraminal stenosis is best demonstrated on sagittal MRI images (see Fig. 15.17). The low signal nerve root and accompanying small veins should always be surrounded by high-signal fat on T1- or T2-weighted sagittal MRI images. Axial MRI images may also demonstrate foraminal stenosis, although to less advantage.

SYNOVIAL CYSTS

Synovial cysts may accompany facet osteoarthritis and may be a cause of radicular pain, neurogenic claudication, and may be associated with axial low back pain. Synovial cysts are thought to originate with a degenerative or traumatic defect in the fibrous facet joint capsule, with subsequent

herniation of the synovial membrane through the defect. Expansion of the synovial outpouching, no longer constrained by the joint capsule, results in a cystic lesion, which may impinge on adjacent neural structures or simply serve as an imaging marker of capsular pathology. Synovial cysts may retain or potentially lose their communication with the facet joint. Ganglion cysts may have a similar gross appearance but histologically lack a synovial lining; they may be indistinguishable on imaging studies.

Although relatively unusual, synovial cysts are not rare: the series of Doyle and associates¹⁷² demonstrated a prevalence of nearly 10% in a population of patients undergoing MRI for back or leg pain. In this series, anterior or intraspinal cysts, often arising from the superior recess, had a prevalence of 2.3%; posterior or extraspinal cysts were more common with a 7.3% prevalence. Synovial cysts are prevalent in an elderly population, with an average age of 63 in Metellus' study,¹⁷³ 61 in Apostolaki's¹⁷⁴ study population, and 66 years in the large surgical series of Lyons.¹⁷⁵ Reported male-to-female ratios are inconsistent, varying from a 1:1 ratio in the Lyons series to 1.2:1 in the Metellus series to 1:2 in the Apostolaki study; Doyle noted a female predominance in posterior cysts only. Synovial cysts are far more common in the lumbar region than in the thoracic or cervical spine. The literature has consistently shown that 60% to 70% of lumbar synovial cysts will be at L4/5 level, followed in relative order by L5/S1, L3/4, and L2/3. Anterior or intraspinal synovial cysts most commonly occur posterolateral to the thecal sac in close association to the facet joint. They may be embedded in the ligamentum flavum. Uncommonly, cysts may be located directly dorsal to the thecal sac, laterally within the neural foramen, or in a far lateral or extraforaminal site. Far lateral synovial cysts typically arise from the superior recess of the joint, which extends over the superior margin of the superior articular process; the communication with the joint will not be seen on an axial image but may be apparent on sagittal images.

Synovial cysts often arise from facet joints exhibiting significant arthrosis, with sclerosis, osteophytes, and increased joint fluid, although most joints with arthrosis do not produce cysts. Segmental hypermobility is postulated as an underlying cause of synovial cysts. This is supported by the strong association with the most mobile lumbar segment (L4/5) and the frequent (42% to 65%) association with degenerative spondylolisthesis.¹⁷⁴ Disk age-related changes are commonly present at the level of the cyst. Metellus¹⁷³ also noted that most cysts arise from joints with a predominant sagittal orientation; this orientation is also associated with segmental instability.

Synovial cysts may be detected by CT, CT myelography, or MRI; MRI is thought to be most sensitive (Fig. 15.18). Calcified cysts may rarely be seen on plain radiographs. Synovial cysts have great variation in their histology, with corresponding variety in their imaging appearance. Synovial cysts may be thin-walled collections of pure synovial fluid, or they may be complicated by varying degrees of chronic or acute hemorrhage and inflammation. Pure cysts have a high T2 signal, equal to or exceeding that of cerebrospinal fluid (CSF), with a thin, low-signal wall. With chronic hemorrhage, cyst contents may develop a high T1 signal (methemoglobin) and a variable T2 signal; the wall often enhances with gadolinium. In the presence of chronic inflammation and calcification,

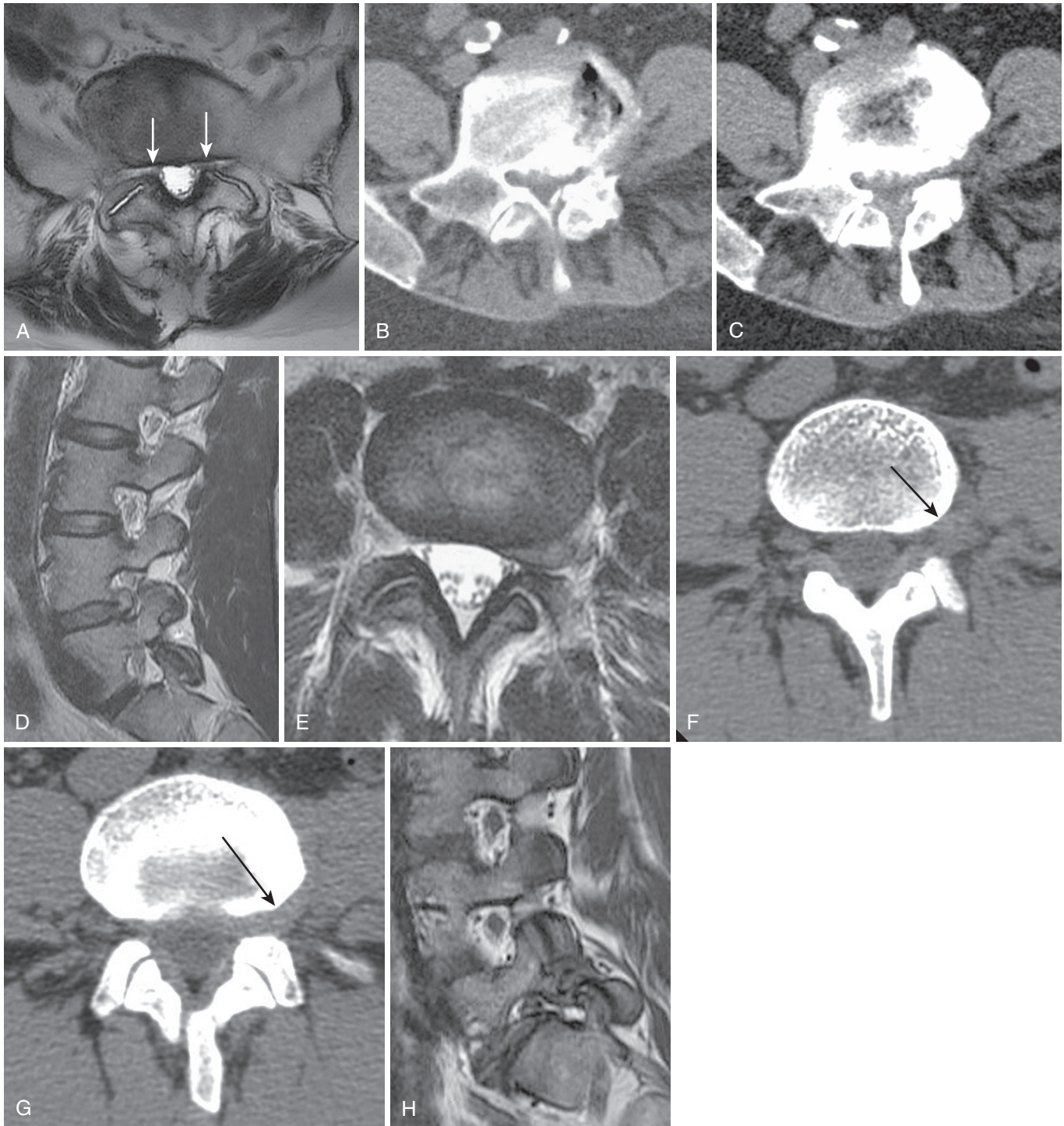


Figure 15.17 Subarticular zone (lateral recess) and foraminal compromise. Axial T2 MRI image (**A**) at the S1 superior end plate demonstrates a widely patent central canal, but severe bilateral subarticular zone stenosis (*arrows*) resulting from facet hypertrophy. Consecutive CT images (**B**, **C**) at the L5 pedicle level in another patient show severe central canal stenosis, but also severe subarticular zone stenosis primarily caused by end plate osteophytes. T2 sagittal and L4-5 disk axial images (**D**, **E**) in a patient with left anterior thigh pain reveal a left foraminal disk extrusion, displacing the dorsal root ganglion (DRG) superiorly and laterally. Axial CT images (**F**, **G**) in another patient with left L4 radicular pain also demonstrate a left L4 foraminal and extraforaminal extrusion (*arrows*) effacing the fat about the exiting L4 DRG and ventral ramus. A final patient with L5 spondylolysis (**H**) demonstrates the typical S-shaped foraminal stenosis at L5-S1 seen in this setting. Note normal foramina at L3-4 and L4-5 with abundant fat surrounding the DRG and small veins.



Figure 15.18 Synovial cysts. Typical bilateral L4 intraspinal synovial cysts (**A**) compress the thecal sac on a T2 axial image. A different patient (**B**) demonstrates a synovial cyst in the left L5-S1 neural foramen as well as a posterior extraspinal cyst. Another patient with right L5 radicular pain demonstrates an L4-5 synovial cyst on sagittal (**C**) and axial (**D**) T2 images. The patient underwent a right L5 transforaminal epidural steroid injection and an intra-articular injection of the facet joint/cyst. Her pain resolved. She presented 4 years later with axial pain. MRI T2 sagittal (**E**) and axial (**F**) show a new L5 compression fracture; the synovial cyst has resolved. A final patient demonstrates an irregular thick-walled cyst (arrows) arising from the left 3-4 facet (**G, H, I**). Note the T1 hyperintensity (**H**). CT (**J**) shows the cyst is calcified (arrow).

the wall may become quite thick, with a very low T1 and T2 signal. On CT, calcification is variably observed and cyst contents range from hypodense to slightly hyperdense relative to muscle. Changes of arthrosis in the adjacent facet joint are typical, including abnormal marrow signal (T2

hyperintensity, T1 hypointensity) in the articular processes and pedicle. A direct communication with the facet joint is not always demonstrable on either CT or MRI. Synovial cysts may not be evident on recumbent CT or MRI imaging, as the synovial fluid recedes into the joint space, collapsing the

cyst; when the patient assumes axial load, the joint surfaces are opposed, driving the fluid into the cyst, which then exerts mass effect on neural elements. Not infrequently synovial cysts will fill when the joint is pressurized by intra-articular injection, despite no evidence of their existence on recumbent advanced imaging. The imaging differential diagnosis includes conjoined nerve root sleeves, sequestered disk fragments, cystic nerve sheath tumors, and degenerative cysts of other origins, such as pseudobursae in Baastrup's disease.

Anterior or intraspinal synovial cysts often present as lesions causing unilateral radicular pain or contributing to neurogenic claudication. Anterior synovial cysts may cause focal neural compression in the lateral recess, foramen, or extraforaminal space, or they may contribute to central canal stenosis. Posterior cysts do not cause neural compression but may be associated with axial pain and be an imaging sign of facet capsular disease. Synovial cysts may regress spontaneously. Radicular pain resulting from synovial cysts may be treated by an injection of corticosteroid into the facet joint bearing the cyst, with a transforaminal epidural steroid injection at the same procedural setting. This strategy successfully allowed 50% of patients to avoid surgical injection in a series by Sabers and colleagues.¹⁷⁶ Other nonoperative therapies have included aspiration, fenestration, or rupture of cysts under CT or fluoroscopic guidance. A large case series ($n = 101$) of percutaneous cyst rupture showed surgical sparing in about 50% of cases.¹⁷⁷ Surgical resection of synovial cysts generally has a favorable outcome, but it may require facetectomy, laminectomy, and possible fusion.

CERVICAL DISK HERNIATIONS

The cervical intervertebral disks differ structurally from the lumbar disk. The cervical disks are thicker anteriorly than posteriorly and have a less well defined nuclear/annular structure. There is no discrete annulus at the posterior disk margin. The cervical disks function less to disburse axial load. They undergo maturational change with age; intradiscal T2 signal loss is a poor predictor of axial pain. Cervical radicular pain or radiculopathy is less common than lumbar symptomatology. Cervical radicular pain is most commonly caused by foraminal compromise of multifactorial origin: uncovertebral joint and facet hypertrophy, loss of disk space height, and less frequently disk herniation. In a population-based study in Rochester, Minnesota, disk herniations were causal of only 22% of cervical radiculopathies.¹⁷⁸ The C6 and C7 nerves were most commonly affected. As in the lumbar region, the vector of herniation is usually posterolateral, but as the cervical nerves exit low in the foramen, a herniation will likely affect the exiting nerve, not the traversing nerve. The C6 nerve exits low in the C5-6 neural foramen; a herniation at this segment will most likely impinge on the C6 nerve.

The natural history of cervical disk herniations parallels the lumbar region. Cervical disk herniations may undergo spontaneous regression. As in the lumbar region, extrusions, migrated disk material, and laterally situated disk herniations are more likely to undergo spontaneous regression. As most lesions causing cervical radicular pain are not purely soft disk but are, at least in part, bony, overall regression of

the root compressive lesion is less likely than in the lumbar region. MRI remains the primary advanced imaging modality, but CT myelography may play a larger role. It provides the best spatial resolution, critical in the narrow confines of the cervical region, and excels at discriminating bone from soft disk, which may alter the surgical approach (Fig. 15.19).

THORACIC DISK HERNIATIONS

Symptomatic thoracic disk herniations are rare; only 1% to 2% of all disk surgeries are performed in the thoracic segment.¹⁷⁹ The expected specificity fault applies; disk age-related changes are ubiquitous, and herniations are often asymptomatic. The majority of disk herniations occur in the mid and lower thoracic region. In the surgical series of Stillerman,¹⁸⁰ the T8 to T11 levels were most commonly affected. In this series, 76% of patients presented with pain, 61% with either motor or sensory dysfunction, and 24% with bladder dysfunction. Nearly two thirds of the disk herniations showed evidence of calcification on CT imaging. At surgery, 7% showed intradural extension. Thoracic disk herniations involving the conus can mimic lumbar radicular pain; MRI studies of the lumbar spine should always extend to the conus on the sagittal sequences.

Imaging of thoracic radicular pain should involve MRI or CT myelography. CT myelography has the greatest spatial resolution and may better demonstrate the presence of calcification within thoracic disks. MRI can detect signal abnormality within the cord, which may identify cord edema or venous hypertension, verifying the physiologic significance of a disk herniation. All imaging evaluation for thoracic disk disease must include careful enumeration of the segmental level involved. If a lesion that may require surgical or percutaneous intervention is detected, the imaging study should be extended to include sagittal images from the sacrum to the skull base. Communication between radiologist and surgeon or spine interventionalist is critical to avoid wrong segment interventions.

DEGENERATIVE SPONDYLOLISTHESIS

Spondylolisthesis refers to the abnormal anterior or posterior displacement of one vertebral body relative to another. Displacement caused by defects in the pars interarticularis (spondylolytic spondylolisthesis) will be discussed later. Degenerative anterolisthesis is the anterior displacement of a vertebral body relative to the body immediately caudal to it. The etiology of degenerative anterolisthesis is primarily facet joint arthrosis, often with a relative sagittal orientation of the facets. Disk structural failure is also necessary. Degenerative anterolisthesis may be present in 4% to 14% of elderly patients.¹⁸¹ Anterolisthesis is most frequent at the L4 level, with less common occurrence at L5, followed by L3. It is significantly more common in women than in men.¹⁸¹ Radiographic findings of degenerative anterolisthesis include the obvious displacement itself, joint space narrowing and sclerosis in the associated facets, and findings of intervertebral osteochondrosis, including a loss of disk space height, gas within the disk, and subchondral sclerosis.

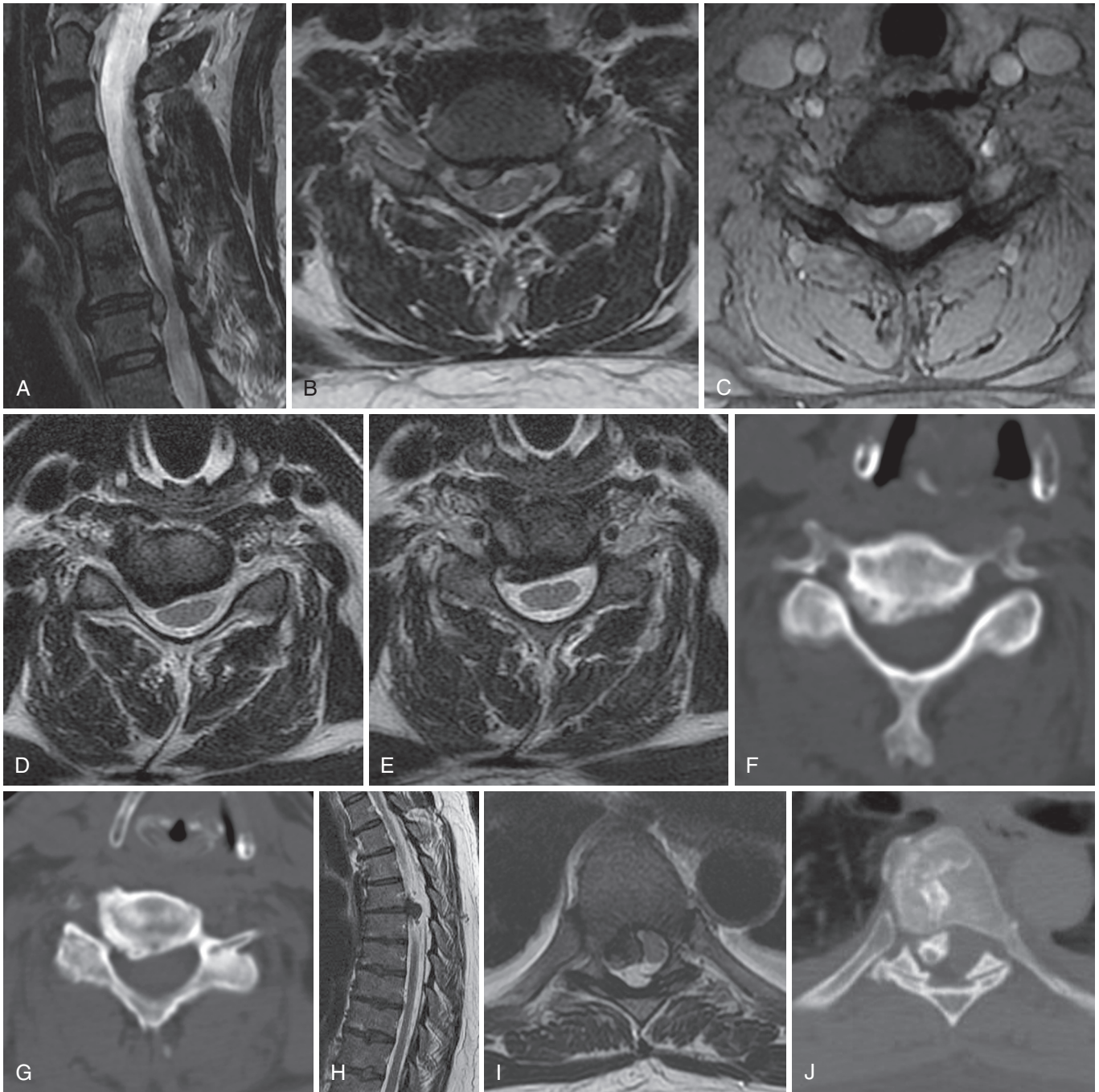


Figure 15.19 Cervical and thoracic disk herniations. A patient with prior C5-6 anterior cervical discectomy and fusion presents with new right C7 distribution radicular pain. Sagittal T2 image (**A**) shows disk extrusion with caudal migration from the adjacent C6-7 segment. Note that the extruded material has higher T2 signal than parent disk, perhaps a reflection of the inflammatory response. Axial fast spine echo (FSE) T2 (**B**) and gradient echo (**C**) axial images at the C6-7 interspace well demonstrate the extrusion. In another patient with a right C6 radiculopathy axial FSE T2 images (**D**, **E**) at the C5-6 interspace suggest a disk-osteophyte complex and uncovertebral joint osteophytes compromise the right C5-6 foramen. The primary bony nature of the process is confirmed on CT images (**F**, **G**). In the cervical spine, compressive lesions are more likely to be osseous than soft disk alone. Thoracic disk extrusion in a 51-year-old woman with progressive thoracic myelopathy is shown in images **H**, **I**, and **J**. Sagittal T2 MR image (**H**) shows large T5-6 disk extrusion. Low T2 signal suggests calcification. The cord is displaced and compressed by the right-sided extrusion on T2-weighted axial MR image (**I**). Axial CT image (**J**) demonstrates coarse calcification in the disk extrusion. Note the linear defect with marginal sclerosis in the end plate, a finding often accompanying disk herniations.

Degenerative retrolisthesis describes the posterior displacement of the index vertebral body relative to that below it; the primary causative process is intervertebral osteochondrosis. As there is a loss of disk space height, the oblique orientation of the facet results in the more

superior vertebral body gliding posterior relative to its inferior counterpart. Degenerative retrolisthesis is most commonly seen at the L2 interspace level, with less common occurrence at L1, followed by L3. There is no significant gender difference.

Degenerative spondylolisthesis may be associated with axial low back pain. The Kauppila study showed that patients with degenerative spondylolisthesis had a higher prevalence of daily low back symptoms.¹⁸¹ There was, however, no increased disability in spondylolisthesis patients relative to controls. In this study, the overall incidence of degenerative spondylolisthesis approached 20%. Degenerative spondylolisthesis carries with it the risk of neural element compromise with secondary central canal stenosis, lateral recess stenosis, or foraminal compromise.

SPINAL STENOSIS: LUMBAR NEUROGENIC INTERMITTENT CLAUDICATION (NIC)

Lumbar spinal stenosis is an imaging observation; it may give rise to the clinical syndrome of NIC. NIC is the most common cause of spine surgery in patients over 65 years of age.¹⁸² The hallmark is the induction of gluteal and lower extremity pain with upright exercise or specific postural positions, and palliation by forward flexion, sitting, or recumbency. The most common symptoms in patients with lumbar spinal stenosis are back pain (prevalence of 95%), claudication (91%), leg pain (71%), weakness (33%), and voiding disturbances (12%).¹⁸³ There may be a paucity of physical findings, even in the presence of symptoms.

Despite its significance, few prevalence or natural history data are available for NIC. Kalichman and colleagues utilized data from the Framingham study to establish the prevalence of congenital and acquired lumbar central canal stenosis in a community population.¹⁸⁴ Using the anterior-posterior dimension of the central canal derived from CT studies (12 mm = relative stenosis, 10 mm = absolute stenosis), they noted congenital central canal narrowing of relative degree in 4.7% of the population and absolute stenosis in 2.6%. Acquired stenosis was identified in 22.5% (relative) and 7.3% (absolute) of individuals. Their review of the literature noted that the prevalence of acquired lumbar stenosis ranged from 1.7% to 13.1%. The prevalence of acquired stenosis (absolute) increased from 4% in patients younger than 40 years of age to 14.3% in patients older than 60. The North American Spine Society (NASS) 2011 evidence-based guidelines on the diagnosis and treatment of spinal stenosis suggest, in the absence of reliable evidence, that the natural history of patients with clinically mild to moderately symptomatic degenerative stenosis is favorable in one third to one half of patients.¹⁸⁵ In patients with mild to moderately symptomatic stenosis, rapid or catastrophic neurologic decline is a rare phenomenon.

PATHOPHYSIOLOGY

The pathogenesis of NIC in lumbar spinal stenosis has been a subject of investigation for half a century. Verbiest initially described mechanical compression of the nerve roots of the cauda equina as a cause of NIC in 1954.¹⁸⁶ Subsequent investigators have postulated that arterial and venous ischemia, perhaps exacerbated by restriction of CSF flow (which participates in nerve root nutrition), are contributors to the clinical syndrome. The current preponderance of evidence favors venous congestion secondary to mechanical compression. This hypothesis emphasizes the importance of multiple

levels of compression and the physiologic effects of lumbar extension. Both of these observations have significant relevance to imaging.

The animal work of Takahashi and Olmarker demonstrated that two zones of modest compression in the cauda equina would dramatically reduce blood flow to the intervening nerve segment because of venous congestion; this venous congestion could precipitate neural dysfunction.^{187,188} Kobayashi examined cauda equina histology after the application of a modest stenosis (30% of cross-sectional area) to the dural tube.¹⁸⁹ The cauda equina demonstrated congestion and dilatation of intraradicular veins and an inflammatory cellular infiltrate. There was disruption of the blood-nerve barrier, both at the site of the compression and also in more distant sites of Wallerian degeneration. The necrotic debris created by Wallerian degeneration stimulated macrophage activity generating inflammatory molecules such as interleukin-1 and TNF α . Macrophages stimulate cytotoxic activity by the release of nitric oxide and proteases. They are considered the chief effector cells causing an inflammatory neuritis that results in aberrant ectopic neural discharge and conduction disturbance leading to the pain and neural dysfunction of neurogenic intermittent claudication.¹⁸⁹

Multiple sites of venous congestion are key to this model of NIC; it is supported by clinical studies. Sato demonstrated that patients with two-level central canal stenosis were significantly more likely to exhibit NIC than were patients with a single level of canal compromise. In two-level stenosis, the symptomatic expression most closely matched the radicular distribution of the more caudal of the two stenotic levels; in patients with compromise at the L3 and L4 disk levels, the pain pattern matched that of the traversing L5 roots.¹⁹⁰ Porter and Ward noted that the sites of compression may be either in the central canal or in the neural foramina.¹⁹¹ In their cohort of 49 patients with NIC, 94% had either multilevel central canal stenosis or central canal plus neural foraminal stenosis. The work of Morishita emphasized the importance of the neural foramen as a potential zone of compression, particularly with dynamic changes in posture.¹⁹² Even without demonstrable foraminal compromise by imaging in a neutral position, in lumbar extension intraforaminal pressures exceeded venous pressure and neural dysfunction was documented by electromyography (EMG). All levels of neural compromise, central, lateral recess, and foraminal, are potentially significant and must be detected by imaging.

CONGENITAL CENTRAL CANAL STENOSIS

A small proportion of patients with clinical NIC will have developmental narrowing of the lumbar central canal, with only modest spondylotic changes necessary to produce clinical symptoms. Singh and colleagues studied the morphologic characteristics of a cohort of surgically treated patients carrying the clinical diagnosis of congenital lumbar stenosis.¹⁹³ They noted that these patients had a significantly shorter pedicle length and, as a result, a smaller cross-sectional spinal canal area when compared with age- and sex-matched controls. The patients with a congenitally narrowed lumbar central canal typically exhibit these morphologic characteristics over several vertebral segments,

maximal at the L3 level. This contrasts with purely acquired stenosis, which is often more focal, particularly at the L4 disk level. Congenital central canal stenosis patients tend to present at a younger age (40 to 50 years old) and with less spondylotic change than typical.

ACQUIRED SPINAL STENOSIS

The great majority of patients presenting with neurogenic intermittent claudication have acquired spondylotic change as their primary cause of central canal, lateral recess, or foraminal compromise. The changes that result in compromise of the central canal are rooted in the three-joint structure of the spine motion segment: the disk and the paired facet joints. In the anterior column, degradation of the disk nuclear matrix places excessive load on the posterior annulus, and annular failure results in posterior end plate osteophytes and disk herniation. These changes encroach on the ventral aspect of the central canal or lateral recesses. Loss of disk space height obligates narrowing of the neural foramina and contributes to increased facet load and ultimately arthrosis; facet capsular hypertrophy and superior articular process osteophytes compromise the lateral recesses. Synovial cysts, particularly at the L4 level, may contribute to central canal, lateral recess, or foraminal compromise. The reduced height of the segment and the loss of elasticity of the ligamentum flavum result in its buckling centrally as a dominant cause of the loss of cross-sectional area of the central canal. The ligamentum flavum may also thicken, although it is unclear if this represents true hypertrophy. These several anterior and posterior column phenomena conspire to narrow the central canal most commonly at the L4-5 disk level, followed by L3-4, L5-S1, and L1-2.¹⁹⁴

There are a number of measurable parameters that could quantify the degree of stenosis depicted by radiography, myelography, CT, or MRI. Verbiest, in his early descriptions of the entity of spinal stenosis, suggested that a 10- to 12-mm anterior-posterior diameter of the dural sac on conventional myelography constituted relative stenosis, with a measurement of < 10 mm denoting absolute stenosis.¹⁸⁶ Steurer, in a 2011 review, surveyed the numerous measurements applied by various authors in the intervening decades in 25 unique studies and four systematic reviews.¹⁷¹ The most common descriptors of central stenosis include the anterior-posterior (AP) dimension of the osseous canal or the dural sac and the cross-sectional area of the dural sac. A dural sac AP dimension of < 10 mm or a dural sac cross-sectional area of < 100 mm² constitutes stenosis. Descriptors of lateral recess (LR) or subarticular stenosis include the height and the lateral recess angle. Height is defined as the shortest distance between the most anterior point of the superior articular process (SAP) and the posterior vertebral body, and the LR angle is the angle formed by the posterior vertebral body and the pars interarticularis. LR stenosis is typically defined as height < 3 mm or angle < 30 degrees. Descriptors of foraminal stenosis most commonly used suggest a diameter of ≤ 2 to 3 mm as indicative of stenosis.

The multiplicity of quantitative parameters suggests that no single measurement has proven satisfactory. Indeed, the very notion of a readily quantifiable measure of stenosis may be flawed. There is a wide normal variation in central canal and dural tube diameters; an assessment of stenosis must

address not simply diameter or cross-sectional area but the crowding or compression of neural tissue. The semiquantitative criteria advanced in 2001 by Fardon and Milette¹⁵⁸ simply defines reduction in expected area by less than one third as mild, by one third to two thirds as moderate, and by greater than two thirds as severe. This allows a subjective judgment of neural compression at the potential cost of reliability. Lurie and associates studied the reliability of the subjective grading of stenosis of the central canal, lateral recesses, and neural foramina and measurement of central canal and dural sac area aided by specific definitions and imaging examples of the criteria.¹⁹⁵ Stenosis was subjectively rated as none, mild, moderate, and severe using the Fardon and Milette definitions; nerve root compromise in the foramen was categorized as none, touching, displacing, or compressing. Inter-reader reliability in assessing the central canal was substantial, with a $\kappa = 0.73$. There was moderate to substantial reliability for foraminal stenosis and nerve root impingement ($\kappa = 0.58, 0.51$, respectively). Reliability for subarticular stenosis was only moderate at $\kappa = 0.49$. These results emphasize the importance of a clear definition of criteria for reliably grading stenosis by subjective scales.

Other imaging observations have been employed in an attempt to identify significant stenosis. The observation of nerve root redundancy as a qualitative marker of central canal compromise dates from the original description of the entity of spinal stenosis by Verbiest.¹⁸⁶ This is presumed to originate from mechanical entrapment of the root at the site of compression, with subsequent elongation of the nerve above this site under the tensile stress of physiologic flexion and extension motion. Some of these prominent structures may also represent dilated veins. Although frequently observed, this sign has been subjected to little study. Redundant nerve roots are present in 34% to 42% of surgical candidates with clinical NIC.¹⁹⁶ In a 2007 study by Min and colleagues, redundant nerve roots were more commonly observed in older patients, but there was no significant association with duration of symptoms, diameter of the spinal canal, preoperative symptom intensity or surgical outcomes.¹⁹⁶ There was a nonsignificant trend toward poorer surgical outcomes in patients with redundant roots.

A 2010 study by Barz described the “nerve root sedimentation sign” as a marker of symptomatic NIC.¹⁹⁷ In patients without central canal compromise, the roots of cauda equina lie in the dorsal aspect of the dural sac on supine MRI imaging. A positive sedimentation sign was defined as the absence of nerve root sedimentation to the dorsal dural sac on at least one axial MRI image at a level above or below the zone of compression; the two nerve roots leaving the dural sac at the next most caudal segment are exceptions. This retrospective study utilized a total of 200 patients: 100 patients with low back pain but without clinical NIC, and a dural cross-sectional area (DCSA) of > 120 mm² and a cohort of 100 patients with clinical NIC, a maximum walking distance of less than 200 m, and a DCSA of less than 80 mm² on at least one level. There was no correlation between the smallest DCSA and patient disability as measured by the Oswestry Disability Index (ODI). The sedimentation sign, however, was identified in 94 of the patients in the NIC cohort but in none of the low back pain group. It remains to be demonstrated that this sign provides additional specificity over a quantitative measurement of the DCSA.

Given the specificity challenges of purely anatomic imaging, the more physiologic parameter of gadolinium enhancement may have a role. This is not a new observation; in 1993, Jinkins observed abnormal intrathecal nerve root enhancement at the site of stenosis on enhanced MRI in patients with NIC.¹⁹⁸ He postulated that this represented a breakdown of the blood-nerve barrier at sites of nerve root injury with subsequent Wallerian degeneration. This has been elegantly confirmed in a canine model by the work of Kobayashi.¹⁸⁹ Histologic examination demonstrated congestion and dilatation of intra-radicular veins and an inflammatory cellular infiltrate at sites of gadolinium enhancement. Gadolinium enhancement may provide added specificity in the correlation of imaging and the clinical symptomatology of NIC; this remains to be proven in clinical studies (Fig. 15.20).

SPECIFICITY OF IMAGING FINDINGS

The ultimate challenge in establishing the utility of diagnostic imaging in the diagnosis of NIC is the lack of a gold standard against which to measure imaging parameters. Surgical findings may be subjective. Clinical outcomes are highly dependent on the technical success of the instituted surgical therapy and the outcome instruments used in any such measurement.

The specificity fault in imaging of central canal stenosis can be seen in studies of asymptomatic volunteers. Boden and associates noted significant central canal stenosis on MRI in 21% of asymptomatic subjects over the age of 60.¹⁸ Jarvik and colleagues demonstrated that asymptomatic stenosis on MRI increases in prevalence with age: moderate to severe central canal stenosis was observed in 7% of subjects < 45; in 6% of subjects age 45 to 55; in 11% of subjects age 55 to 65, and in 21% of subjects over age 65.¹⁹

Against this background of asymptomatic central canal narrowing, numerous conflicting studies have attempted to establish a relationship between imaging quantitation of central canal or dural size and clinical expression of NIC. For example, Hamanishi and colleagues showed that a decrease in the DCSA to less than 100 mm² at more than two of three lumbar levels (L2-3, L3-4, L4-5) was highly associated with the presence of clinical NIC.¹⁹⁹ For each study showing such an association, several others refute it. Sirvanci examined patients undergoing decompressive surgery for NIC.²⁰⁰ Morphologic stenosis was assessed by DCSA (> 100 mm²: normal; 76 to 100 mm²: moderately stenotic; < 76 mm²: severely stenotic) and a 4-point grading of subarticular and foraminal stenosis. There was no correlation between any of the measured parameters in any spine compartment and patient disability as measured by the Oswestry Disability Index (ODI). This applied both to patients with multilevel central stenosis and to a subset with degenerative spondylolisthesis. The NASS guidelines¹⁸⁵ conclude that there is insufficient evidence to recommend for or against a correlation between clinical symptoms or function and the presence of anatomic narrowing of the spinal canal on cross-sectional imaging.

SENSITIVITY OF IMAGING FINDINGS

There is also a basic sensitivity flaw in advanced imaging. NIC is by definition intermittent; most patients with NIC

report exacerbation of symptoms with extension and weight bearing. It is well known that the cross-sectional area of the central spinal canal, subarticular zone or lateral recess, and neural foramina is maximized with flexion positioning; the dimensions of these structures diminish with extension and axial load. Intradiskal pressures are significantly lower when one is in a recumbent position than when sitting or standing. A 2009 study by Hansson and associates identified the ligamentum flavum as the greatest dynamic contributor to central canal compromise with axial load and extension.³⁹ The average cross-sectional area of the central canal diminished by 23 mm² at the L3 disk level and 14 mm² at the L4 level under load. The ligamentum flavum was responsible for 50% of the reduction at the L3 level and 85% of the reduction at the L4 level. Madsen and associates attempted to distinguish between the effects of axial load and extension; their work suggested that lumbar spine extension is the dominant cause of reduction in DCSA in the standing patient.⁴⁰ Mechanisms circumventing this flaw include upright axial loading devices, the technologically immature upright MRI, and cone beam CT myelography (Box 15.6).

THORACIC SPINAL STENOSIS

Symptomatic central canal stenosis in the thoracic segment of the spine resulting from age-related change is far less common than in the cervical and lumbar regions, likely because of the added mechanical stability imparted by the rib cage. Systemic disease accounts for a correspondingly greater proportion of cases. Systemic processes leading to thoracic central canal compromise include achondroplasia, osteochondrodystrophy, Scheuermann's disease, diffuse idiopathic skeletal hyperostosis (DISH), and Paget's disease.

Compromise of the thoracic spinal canal may be manifest clinically as myelopathy, radiculopathy, or a mixed presentation. The segmental level of canal compromise is most commonly reported to be in the lower thoracic region. Thoracic spine mobility, particularly flexion-extension motion, is greatest near the thoracolumbar junction, likely the biomechanical underpinning to this distribution of age-related pathology. Posterior element age-related changes play a greater role in the genesis of thoracic central canal compromise. This takes the form primarily of unilateral or bilateral facet joint hypertrophy. Thoracic disk herniations or disk-osteophyte complexes may also contribute. Both the ventral and dorsal contributions to thoracic central canal compromise are clearly visible on CT, CT/myelography, and MRI.

Other causes of thoracic central canal stenosis include ossification of the thoracic ligamentum flavum (OLF), a well-recognized cause of thoracic stenosis in an Asian population, but rare among Caucasian subjects. Epidural lipomatosis is a rare cause of central canal compromise in the thoracic or lumbar spine. It may be idiopathic or secondary to endogenous or exogenous steroid excess. Obesity is a common factor in both groups. Excess epidural fat acts as a mass compressing the dural sac, most commonly from a dorsal vector in the thoracic region; it is more likely to be circumferential in the lumbar region.

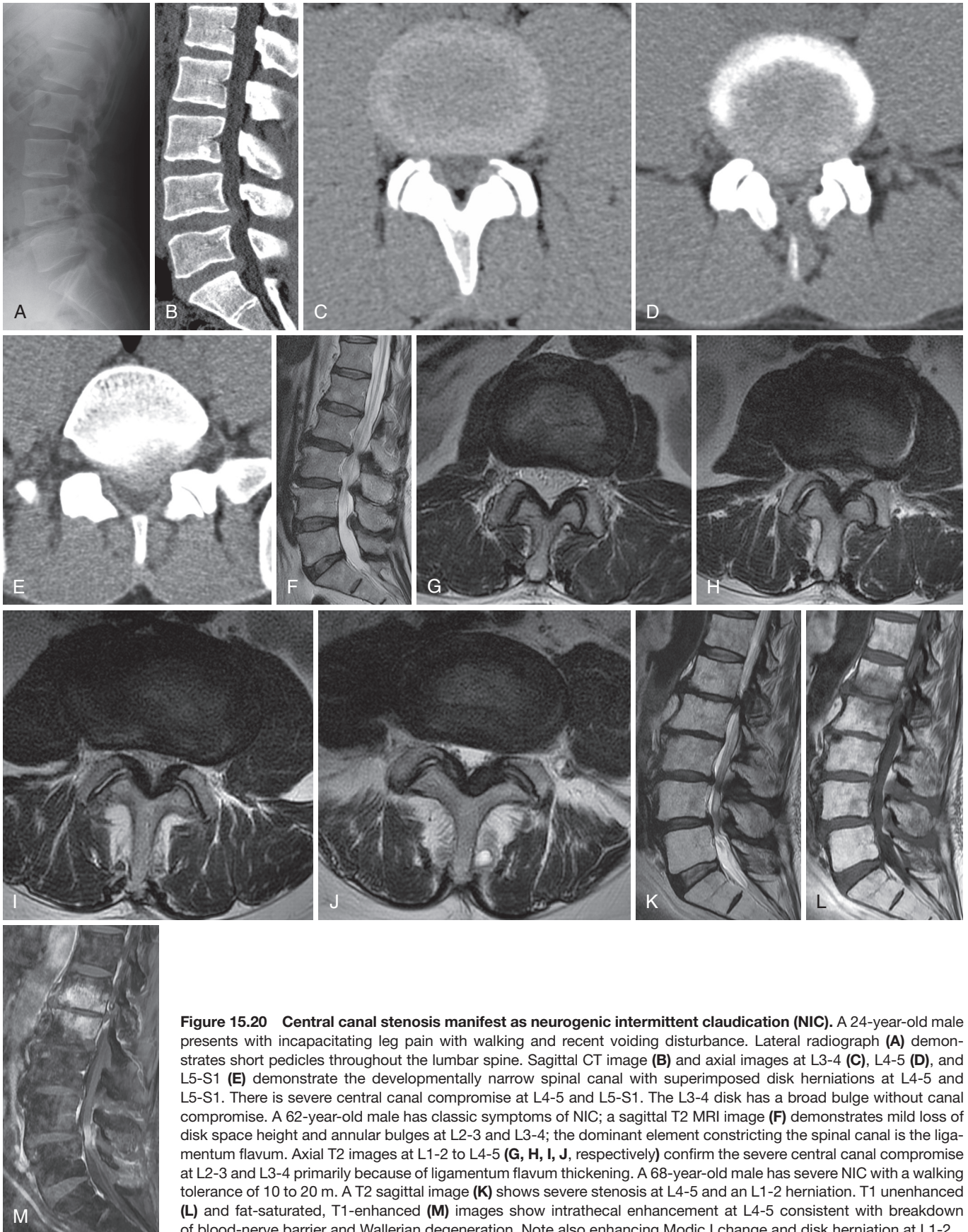


Figure 15.20 Central canal stenosis manifest as neurogenic intermittent claudication (NIC). A 24-year-old male presents with incapacitating leg pain with walking and recent voiding disturbance. Lateral radiograph (A) demonstrates short pedicles throughout the lumbar spine. Sagittal CT image (B) and axial images at L3-4 (C), L4-5 (D), and L5-S1 (E) demonstrate the developmentally narrow spinal canal with superimposed disk herniations at L4-5 and L5-S1. There is severe central canal compromise at L4-5 and L5-S1. The L3-4 disk has a broad bulge without canal compromise. A 62-year-old male has classic symptoms of NIC; a sagittal T2 MRI image (F) demonstrates mild loss of disk space height and annular bulges at L2-3 and L3-4; the dominant element constricting the spinal canal is the ligamentum flavum. Axial T2 images at L1-2 to L4-5 (G, H, I, J, respectively) confirm the severe central canal compromise at L2-3 and L3-4 primarily because of ligamentum flavum thickening. A 68-year-old male has severe NIC with a walking tolerance of 10 to 20 m. A T2 sagittal image (K) shows severe stenosis at L4-5 and an L1-2 herniation. T1 unenhanced (L) and fat-saturated, T1-enhanced (M) images show intrathecal enhancement at L4-5 consistent with breakdown of blood-nerve barrier and Wallerian degeneration. Note also enhancing Modic I change and disk herniation at L1-2.

Box 15.6 Lumbar Spinal Stenosis: Neurogenic Intermittent Claudication

- Decompression procedures for lumbar spinal stenosis are the most common spine surgery in the elderly.
- Neurogenic intermittent claudication (NIC) is a clinical syndrome; spinal stenosis is an anatomic observation.
- The best evidence of NIC pathophysiology suggests venous congestion from multiple sites of compression initiates an inflammatory reaction and Wallerian degeneration with blood-nerve barrier disruption and intra-radicular edema.
- Clinically, multiple sites of compression, at different segment levels or different spine compartments (central, lateral, foraminal) are necessary for NIC.
- Beware the specificity fault: The correlation between quantitative measures of central canal or dural sac size and patient symptoms or function is poor.
- Beware the sensitivity fault: Dynamic lesions, present only with extension and axial load, may make recumbent imaging insensitive.

CERVICAL STENOSIS: CERVICAL SPONDYLOTIC MYELOPATHY (CSM)

Cervical spondylotic myelopathy (CSM) is the most common cause of spinal cord dysfunction in patients over 55 years of age.²⁰¹ Stookey originally described cervical spondylotic myelopathy in 1928.²⁰² Although its pathophysiology remains incompletely understood, it is widely acknowledged to involve static factors causing stenosis of the cervical canal and dynamic factors causing repetitive cord injury.²⁰¹ These mechanical factors both directly injure neural tissue and initiate secondary ischemia, inflammation, and apoptosis. The histologic characteristics in the cord in CSM include cystic cavitation and gliosis of the central gray matter and demyelination of the medial portions of the white matter long tracts. There is Wallerian degeneration in the posterior columns and posterolateral tracts cephalad to the site of compression. Loss of anterior horn cells and corticospinal tract degeneration are visible at and caudal to the site of compression.

The developmentally narrow spinal canal is a more universal substrate for CSM than is the case with NIC in the lumbar region. The sagittal diameter of the adult spinal cord is nearly constant, measuring about 8 mm from C3-C7; the cervical cord enlargement occurs primarily in the transverse plane.²⁰¹ The normal cervical spinal canal sagittal diameter (posterior vertebral body to spinolaminar line) is 17 to 18 mm (C3-C7) in a Caucasian population; these subjects rarely develop sufficient age-related change to provoke CSM. Edwards and LaRocca observed that patients with developmentally narrowed midcervical sagittal diameters of < 10 mm were often myelopathic, patients with canals of 10 to 13 mm were at risk for CSM, canals of 13 to 17 mm were noted in patients with symptomatic spondylosis but rarely myelopathy, and subjects with canals > 17 mm were not prone to develop spondylosis.²⁰³ Morishita studied the kinematics of subjects with congenitally narrowed canals; there is hypermobility in the lower cervical region, providing a biomechanical explanation for the significantly

greater age-related change seen in this setting.²⁰⁴ Hence, the individual with a congenitally narrowed canal is at risk because of both the limited space available for the cord and a greater propensity to age-related spondylotic change.

Acquired cervical central canal stenosis encompasses age-related spondylotic change (most common), ossification of the posterior longitudinal ligament (OPLL), and OLF. Disk degradation results in a loss of disk space height, excess loading of the uncovertebral joints with osteophyte formation, excess facet loading causing hypertrophy, and central buckling of the ligamentum flavum. These processes circumferentially narrow the canal and directly compress the cord, exiting nerves, and the anterior spinal artery. The most common levels of compromise were C3-4 (27%), C4-5 (37%), and C-5/6 (29%) in a surgical series.²⁰⁵ This series included patients with spondylosis only and those with OPLL. It is also known that the cross-sectional area of the cervical canal diminishes in both extension and flexion, with greater effects during extension.^{44,45} Ventral compression of the cord compromises flow through the arterioles arising from the anterior spinal artery in the ventral sulcus of the cervical cord; dorsal compression reduces perfusion to the central gray matter. Oligodendrocytes are extremely sensitive to ischemic injury; resultant apoptotic cell death may cause the demyelination characteristically observed in CSM.²⁰¹ Animal evidence further supports the role of an inflammatory cascade in apoptotic cell death.²⁰⁶

IMAGING

Historically, radiographic assessment of cervical anatomic stenosis relied on the anterior-posterior dimension of the central canal as measured from the posterior vertebral body to the spinolaminar line. The normal sagittal diameter from C3 through C7 is considered to be 17 to 18 mm; Edwards and LaRocca noted that a cervical canal with a sagittal diameter of less than 13 mm was at risk for myelopathy; absolute stenosis was defined as being less than 10 mm.²⁰³ The advent of cross-sectional imaging has allowed us to directly measure the diameters and cross-sectional areas of the cervical spinal canal and the cervical cord. MRI has also given us the ability to evaluate physiologic parameters: T2 hyperintensity, T1 hypointensity, gadolinium enhancement, and, with diffusion tensor imaging (DTI), fractional anisotropy (FA), and apparent diffusion coefficient (ADC).

A 2010 study by Naganawa and associates demonstrated good intra- and inter-observer reliability in evaluation of the cross sections of the cervical canal and spinal cord with both CT/myelography and MRI.²⁰⁷ They noted that dural sac diameter and cross-sectional area measurements were slightly but significantly larger with CT/myelography than fast spin echo T2-weighted MRI; conversely, the diameters and cross-sectional areas of the spinal cord were slightly but significantly larger with MRI. MRI graded the stenosis as slightly, but significantly, more severe than CT/myelography. A 2009 study by Song and associates found no significant difference in inter-observer or intra-observer reliability between CT/myelography and MRI.²⁰⁸ With its superior spatial resolution, CT/myelography was somewhat better in assessing foraminal stenosis and much better in discriminating bony versus soft tissue lesions. MRI was more reliable in identifying direct nerve root compression (Fig. 15.21).

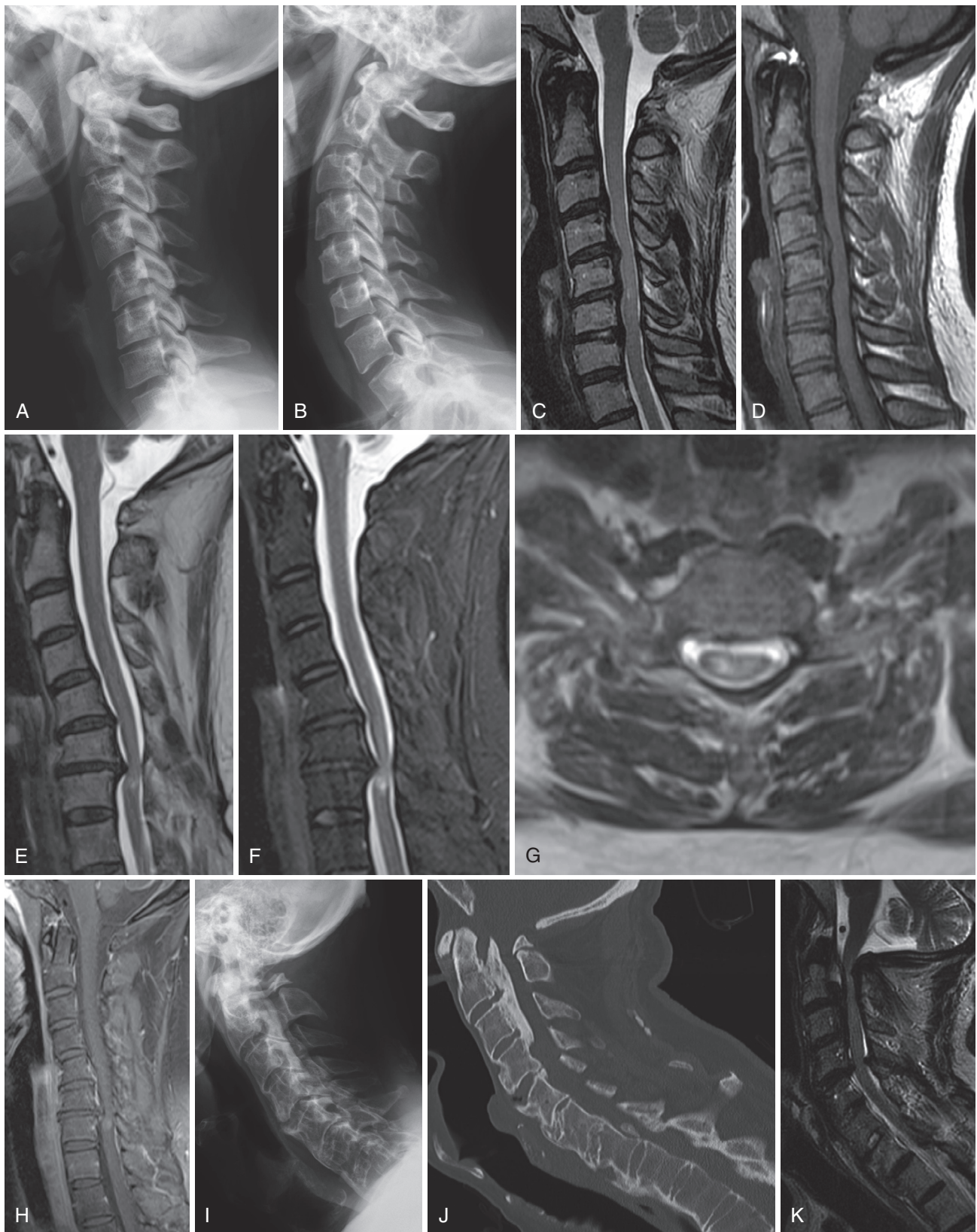


Figure 15.21 Cervical central canal compromise manifest as cervical spondylotic myelopathy (CSM). A 36-year-old female presents with very subtle bilateral hand incoordination, neck pain, and left arm symptoms. Her lateral radiograph (A) shows no lamina posterior to the articular pillar. Compare to a normal lateral radiograph (B). Sagittal T2 (C) and T1 (D) images show effacement of CSF and cord compression from the C4-C6 interspaces with subtle T2 hyperintensity in the cord at the C5-6 interspace level. Note that no dorsal epidural fat is visible above the C7-T1 level, a typical finding.

A 48-year-old female had intractable upper extremity pain and dysesthesia involving the right lateral forearm. There were also long tract signs. Sagittal T2 (E) and T2 with fat saturation (F) demonstrate cord deformity at the C6-C7 interspace level, with focal T2 hyperintensity in the right side of the cord, as seen on the axial FSE image (G). Postgadolinium sagittal T1-weighted image with fat saturation (H) shows enhancement at the site of T2 hyperintensity, a negative prognostic sign.

A 77-year-old Caucasian male has slowly progressive myelopathy on clinical examination. Lateral radiograph (I) demonstrates OPLL in the upper cervical spine; note the coexistent manifestations of DISH. CT sagittal reconstruction (J) and sagittal T2 (K) images better depict the severe cord deformity at C2.

IMAGING SPECIFICITY

The significant prevalence of asymptomatic cervical central canal stenosis was noted earlier in this chapter. When a population of patients with a clinical diagnosis of CSM is studied, the correlations appear more favorable. The transverse area of the spinal cord as measured by MRI correlates well with the severity of myelopathy and the pathologic changes observed in the cord in CSM.²⁰⁹ The physiologic parameters of T2 hyperintensity or T1 hypointensity have provided further insight into the evolution of CSM. The several studies addressing these correlates are explored in a review.²¹⁰ From these studies we can conclude the following:

1. Intramedullary T2 hyperintensity represents a range of reversible (edema) and irreversible (demyelination, gliosis, cystic necrosis) pathology.
2. Faint and indistinct T2 hyperintensity is more likely to reflect reversible edema.
3. Very intense and well-defined T2 hyperintensity more likely represents fixed gliosis or cystic necrotic change.
4. Intramedullary T1 hypointensity represents irreversible necrosis and myelomalacia.

A 2010 study by Ozawa²¹¹ and a 2011 study by Cho²¹² compared CSM patients who exhibited gadolinium enhancement with a nonenhancing control group. The zone of enhancement was always within and smaller than a zone of T2 hyperintensity at the site of maximal compression, with extension caudally. It was typically observed in the posterior or posterolateral cord. There was no correlation of enhancement with preoperative clinical symptoms. Enhancement disappeared in most patients within 1 year of surgical decompression; patients who exhibited preoperative enhancement had a poorer postoperative prognosis than those who did not. Floeth studied 20 CSM patients with FDG-PET in the setting of a single level stenosis at C3/C4 or C4/C5.²¹³ All the CSM patients showed a significant decrease in 18F-FDG uptake in the lower cord below the stenosis, relative to normal controls. A cohort of these patients also exhibited increased uptake at the level of the stenosis. The patients with increased 18F-FDG uptake at the stenosis had a significantly shorter duration of symptoms, a more precipitous decline in function in the 3 months prior to decompression, and ultimately exhibited significant improvement after decompression. Patients without increased uptake at the stenotic zone did not recover neurologic function after decompression.

Early reports suggest that diffusion tensor imaging may offer greater accuracy in the identification of symptomatic cord compromise than T2 hyperintensity or T1 hypointensity. The measured parameters are fractional anisotropy (FA), mean diffusivity (MD), or apparent diffusion coefficient (ADC). The ADC or MD values reflect overall diffusivity in the tissue irrespective of directional dependence. Anisotropy (directional dependence) of diffusion in white matter tracts results from oriented membrane structure (i.e., axons and myelin). Diminished FA values may reflect loss of directionally oriented membrane structures, increased extracellular edema, or both. Several studies²¹⁰ suggest diminished FA is more sensitive in the detection of early cord injury than intramedullary T2 hyperintensity and is better correlated with symptoms. This may assist in the

Box 15.7 Cervical Spondylotic Myelopathy: Prognostic Factors for Surgical Decompression

1. Intramedullary T2 hyperintensity diminishes prognosis relative to normal signal.
 - a. Intense, focal T2 hyperintensity is a more negative prognostic sign than ill-defined hyperintensity.
 - b. Multilevel T2 hyperintensity is a more negative prognostic sign than single level change.
 - c. Resolution of T2 hyperintensity postoperatively improves prognosis.
 - d. Expansion of T2 hyperintensity postoperatively diminishes prognosis.
2. Intramedullary T1 hypointensity greatly diminishes prognosis.
 - a. Evolution of T1 hypointensity postoperatively diminishes prognosis.
3. Intramedullary gadolinium enhancement greatly diminishes prognosis.
4. Increased metabolic activity at the site of compression on 18F-FDG PET improves prognosis over no increased activity.
5. Postoperative residual compression and failure of re-expansion of the cord cross section are negative prognostic signs.

From Maus TP. Imaging of spinal stenosis: neurogenic intermittent claudication and cervical spondylotic myelopathy. *Radiol Clin North Am.* 2012;50:651-679.

selection of patients for surgical decompression, although additional work remains to be done.

IMAGING CORRELATES WITH DECOMPRESSION PROGNOSIS

The ultimate goal of imaging must be to improve the clinical outcomes of patients. In the CSM population, this currently implies the timely and appropriate selection of patients for therapeutic interventions, primarily surgical decompression. There is a large body of literature²¹⁰ that has examined the role of imaging in predicting clinical response to surgical decompression; imaging parameters under consideration include the cross-sectional area of the cord, intramedullary T2 hyperintensity, including its degree of intensity and multifocality, intramedullary T1 hypointensity, change or stability of intramedullary signal after decompression, recovery of cord cross-sectional area after decompression, and intramedullary gadolinium enhancement. These are summarized in Box 15.7. Utilization of these findings should assist in the selection and counseling of CSM patients regarding surgical decompression.

OSSIFICATION OF THE POSTERIOR LONGITUDINAL LIGAMENT (OPLL)

Ossification of the posterior longitudinal ligament (OPLL) is a multifactorial disease, whose genetic basis is a defect in the nucleotide pyrophosphatase (NPPS) gene.²⁰¹ The prevalence is 1.9 to 4.3% of the Japanese population and approximately 3% of the populations of Korea and Taiwan. It is

implicated in up to 25% of North American and Japanese cases of CSM. It has a significant association (up to 50%) with DISH, and some consider it a subtype of DISH. Like age-related causes of structural central canal narrowing, it is often asymptomatic. The ossification is most common in the cervical region, where it causes static narrowing of the canal; repeated impact of the ventral cord on the bony mass contributes to myelopathic injury. Patients may present in their 40s and 50s with pain, chronic myelopathy, or acute neurologic injury after modest trauma. The natural history of the ossification is progression. Close clinical follow-up is warranted.

The ligamentous ossification may be identified on radiographs, CT, and MRI. On lateral radiographs, reduction of the sagittal canal diameter available for the cord by > 60% correlates strongly with myelopathy.²¹³ The ossification is located from C2-4 in 70% of cases, T1-4 in 15%, and L1-3 in 15%.²¹⁴ On CT, the ossification may be classified as segmental (posterior to individual vertebrae, 39%), continuous (bridging across vertebra, 27%), mixed type (29%), and other (ossification posterior to disks, variable sagittal extension, 5%).²¹⁵ In addition to documenting the degree of central canal compromise, the CT characteristics of OPLL can suggest dural penetration. CSF leaks are a significant risk in anterior decompression surgery, particularly when the dura is ossified or inseparable from the bony ligamentous mass. On MRI, mature ligamentous ossification is of diminished signal intensity on all sequences; early OPLL may have inhomogeneous signal and exhibit slight enhancement.²¹⁵ When mature, there is no enhancement, allowing differentiation from epidural fibrosis. The secondary signal alterations in the cord were described earlier in the chapter.

SYSTEMIC DISEASE CAUSAL OF SPINE/LIMB PAIN

In the context of the very low prevalence of systemic disease as causal of spine or limb pain, this chapter has focused on the mechanical and inflammatory processes involving the articulations of the spine that most commonly provoke axial or radicular pain syndromes and syndromes of neurologic dysfunction. It must be remembered, however, that detection of undiagnosed systemic disease—including stress fractures, infection, spondyloarthropathy, neoplasm, and dural fistula—is the primary role of spine imaging.

STRESS FRACTURES

Stress fractures encompass fatigue fractures, in which normal osseous architecture is subjected to sustained supraphysiologic loads, and insufficiency fractures, in which deficient osseous structure fails under normal load conditions. Insufficiency (osteoporotic) fractures are the most common manifestation of systemic disease to present as back pain. In 2005, an estimated 2 million osteoporotic fractures occurred in the United States in patients > 50 years of age; 27% were vertebral body fractures.²¹⁶ This is an underestimate of prevalence, as many vertebral fractures remain asymptomatic. Each vertebral wedge configuration fracture accentuates load on the anterior aspect or adjacent vertebra and increases the annual risk of additional fractures fivefold.²¹⁷

Imaging of vertebral compression fractures begins with weight-bearing radiographs, which provide a low-cost means of assessing change over time with serial images but are relatively insensitive in fracture detection. Radiographic findings include a wedge deformity, most commonly of the superior end plate, which may be accompanied by increased density in the involved end plate in the acute or subacute phase. Chronic deformities often demonstrate remodeled osteophytes. MRI or bone scan are much more sensitive in fracture detection and can better assess acuity. The presence and extent of a marrow edema pattern (T1 hypointense, T2 hyperintense, most conspicuous on STIR or fat-saturated images) can provide an estimate of acuity. The signal abnormality in the marrow tends to be bandlike, paralleling the involved end plate; it may be traversed by a low signal line, adding further confidence to the diagnosis of fracture.

A primary role of imaging in this setting is the characterization of a vertebral fracture as benign or malignant. Malignant lesions are much more likely to exhibit diminished T1 signal throughout the vertebral body. Extension of diminished T1 signal to the vertebral pedicles or posterior elements is relatively specific for malignancy. Paravertebral or epidural mass associated with a fracture is more common in malignant lesions. Posterior bowing of the vertebral body strongly suggests malignancy. Gadolinium enhancement to a level greater than that noted in normal marrow suggests a malignant lesion. Associated disk rupture and retropulsion of a bony fragment without bowing of the posterior margin of the vertebral body suggest a benign lesion. Discrete linear zones of T2 hyperintensity similar to CSF adjacent to the fractured end plate (the fluid sign) are visible in 40% of osteoporotic compression fractures and are a finding of high specificity for a benign fracture.²¹⁸ Advanced MRI techniques, such as diffusion sequences or chemical shift imaging, may play a problem-solving role.²¹⁹

In the non-MRI compatible patient, CT can aid in characterization of fractures but is less sensitive to marrow abnormality than MRI. Trabecular preservation within the vertebral body outside the fracture zone suggests a benign process. The ability of CT to display cortical or trabecular destruction or an adjacent soft tissue mass can aid in the diagnosis of a malignant lesion. The fluid sign noted earlier is occasionally visible as a vacuum cleft containing gas under the fractured end plate, marking a benign osteoporotic compression. Bone scans are highly sensitive in fracture detection, but they are of poor specificity in characterization.

Pelvic insufficiency fractures are increasingly recognized as a cause of axial and somatic referred pain experienced in the low back, pelvis, groin, and proximal lower extremities. Postmenopausal osteoporosis is the dominant risk factor, along with pelvic radiation, corticosteroid use, rheumatoid arthritis, and osteomalacia. The role of osteoporosis is emphasized by the marked female predominance of these lesions, with a reported female-to-male ratio of 9:1.²²⁰ Patients are typically in their sixth decade or older. There is often significant morbidity associated with insufficiency fractures. Taillandier and colleagues²²⁰ noted that 50% of their patients did not recover their former level of independence, and in 25% the insufficiency fracture precipitated institutionalization in their elderly study population. Sacral insufficiency fractures are the most common expression of this

condition; pubic ramus fractures, parasymphseal fractures, and para-acetabular fractures have also been described.

Sacral insufficiency fractures were first described by Lourie in 1982.²²¹ Plain radiographs of the pelvis are relatively insensitive. The most common radiographic finding is a vertical sclerotic band in the sacral ala paralleling the SI joint, representing trabecular compression and callous formation.

Less commonly one may see cortical disruption at the superior or inferior margins of the sacrum or directly visualize a fracture line. These are difficult findings to appreciate in the setting of osteoporotic bone and overlying bowel gas. In Grangier's²²² series, only 25% of patients had typical plain film findings. CT is more sensitive in detecting cortical disruption and the sclerotic margins of the fracture. Axial CT demonstrates the vertical component of the fracture. There is often a horizontal fracture line extending through the sacral body; this may be missed on axial images and will be better identified on coronal CT images. A vacuum phenomenon may also be observed within the fracture.

Technetium bone scan also represents a sensitive means of insufficiency fracture detection. The classic finding is the so-called Honda sign. Increased metabolic activity in bilateral vertical sacral ala fracture lines are bridged by a horizontal line representing a fracture through the sacral body, resulting in a representation of the letter *H*. In Fujii's²²³ series, 63% of patients with sacral insufficiency fractures exhibited this sign in toto, with 35% showing a variant thereof such as two vertical lines without a crossbar or a single vertical and horizontal line. In this series, the Honda sign taken with its variants had a 96% sensitivity and 92% positive predictive value for sacral insufficiency fracture.

MRI is more sensitive than CT in the early detection of insufficiency fractures; it will reveal marrow edema (low T1, high T2 signal with gadolinium enhancement) in a pattern typical of insufficiency fracture (Honda sign) before sclerosis or a fracture line can be visualized with CT.²¹⁹ Imaging in the coronal plane is preferred; fat-saturated or STIR sequences are mandatory. In Grangier's series, marrow edema was observed in all cases as early as 18 days after symptom onset.²²² Over time, the fracture line will become visible within the zone of marrow edema as a line of diminished signal. Fluid (very high, homogeneous T2 signal) may be detected within insufficiency fractures. The confidence in the diagnosis of sacral insufficiency fracture will be increased by the presence of similar bone lesions in the pubic rami, immediately about the pubic symphysis, and in the para-acetabular region, also typical sites of insufficiency fracture.

SPONDYLOLYSIS

Spondylolysis, or isthmic spondylolisthesis, describes a defect in the pars interarticularis, which may be unilateral or bilateral. It is considered a fatigue fracture occurring within a vulnerable pars; the vulnerability may be related to the distribution of ossification centers within the posterior neural arch, not a deficit in bone quality. Spondylolysis has a familial predisposition. There is a 2-4:1 male-to-female predominance. The incidence of spondylolysis has been estimated at 7% in the U.S. population.²²⁴ Spondylolysis is frequently asymptomatic, but it is a particular clinical issue in adolescent athletes. A retrospective study of lumbar radiographs

in more than 4000 athletes demonstrated a 13.9% rate of spondylolysis with concomitant spondylolisthesis in 47%.²²⁴ Spondylolysis occurs most commonly at the L5 level (67%), followed by the L4 level (15% to 20%), and L3 (1% to 2%). It is unusual in the cervical region, where it most often occurs at the C6 level. Spondylolysis is extremely rare in the infant population but appears to develop in childhood or adolescence, with no significant change in its incidence beyond age 20.

Although considered a fatigue fracture, it is unusual in that there is seldom an effective healing response, and the bony defect is persistent. The pars defect is frequently a synovial-lined pseudoarthrosis. Shipley demonstrated that injection of the facet immediately superior to a pars defect showed communication with the pars defect cavity in 30 of 32 facets, with communication to the next most inferior facet in 20 of 32 facets.²²⁵ The presence of synovial fluid in the defect likely contributes to its diminished capacity to heal.

Radiographic findings of spondylolysis are often evident on lateral plain films where a radiolucent band can be directly visualized across the pars interarticularis, with or without a sclerotic margin; there is no role for oblique radiographs. Spondylolisthesis refers to the anterior translation of the vertebral body bearing the spondylolytic defects in relation to the vertebral body below (Fig. 15.22). The degree of spondylolisthesis is graded from I to V based on the percentage of anterior translation relative to the anterior-posterior dimension of the vertebrae: grade I, 0% to 25%; grade II, 26% to 50%; grade III, 51% to 75%; grade IV, 76% to 100%; and grade V, > 100% (spondyloptosis).²¹⁹ Most cases of spondylolisthesis are of grade I. A trapezoidal appearance of L5 with a dome-shaped superior end plate of S1 can be observed in chronic spondylolysis with spondylolisthesis.

Computed tomography allows direct visualization of the pars defect interposed between the adjacent facet joints on axial images. Sagittal reconstructions make the defect more obvious. Care must be taken to distinguish between a true pars defect and severe facet arthrosis. CT will also help distinguish between a stress response (sclerosis, hypertrophy) in the contralateral pedicle or pars in a unilateral spondylolysis, and an osteoid osteoma. CT allows characterization of the process as a stress response (sclerosis), an incomplete fracture, or a completed fracture. Fujii and colleagues categorized these types as early, progressive, and terminal.²²⁶ The early stage consists of a narrow fissure with sharp margins; the progressive stage consists of a narrow fissure with less well-defined, rounder margins; and the terminal stage consists of a wide defect with rounded, sclerotic margins. Early stage lesions healed with conservative care, including bracing, more frequently than progressive lesions; no terminal stage lesions healed (see Fig. 15.22).²²⁶

The defect in the pars interarticularis can be directly visualized on sagittal MRI images. Several ancillary signs have been described on MRI including (1) an increase in the sagittal diameter of the central canal at the level of the pars defect, (2) reactive marrow changes (hypointense T1, hyperintense T2) within the adjacent pedicle, and (3) wedging of the posterior aspect of the associated vertebral body, usually L5.²²⁷ Reactive marrow changes in a vertebral pedicle are not specific for the presence of spondylolysis and may be observed in the presence of adjacent facet arthrosis or synovitis. Hollenberg and colleagues developed an MRI

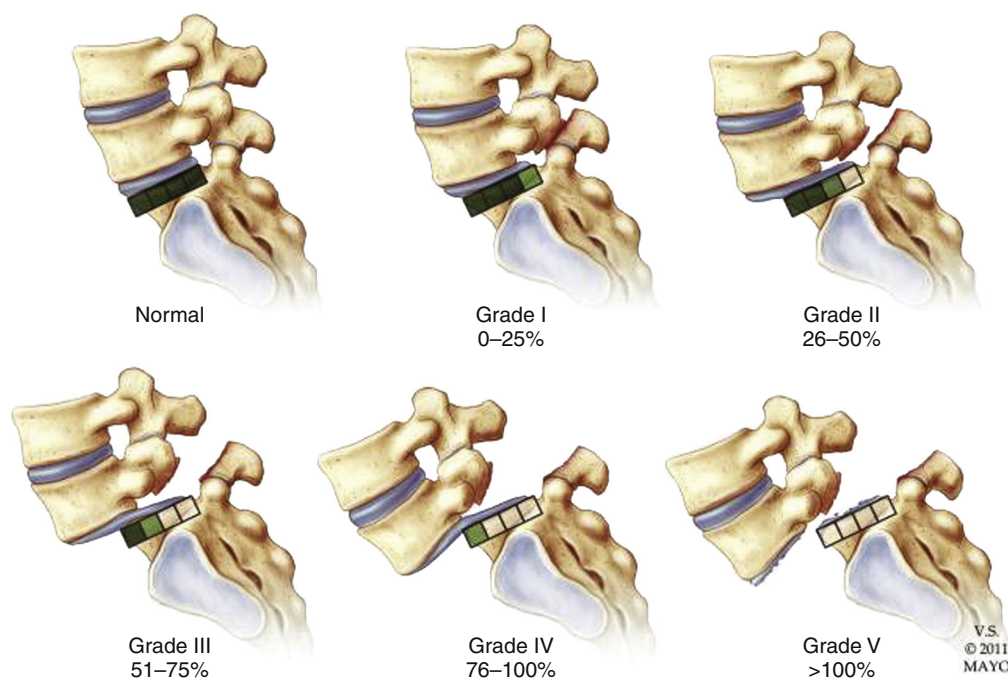


Figure 15.22 Spondylolisthesis, modified Meyerding classification. Modified Meyerding classification of spondylolisthesis: grade I, 0% to 25%; grade II, 26% to 50%; grade III, 51% to 75%; grade IV, 76% to 100%; grade V, greater than 100% (spondyloptosis [falling off]). (From Murthy NS. Imaging of stress fractures of the spine. *Radiol Clin North Am.* 2012;50:799-821.)

Table 15.8 MRI Classification of Spondylolysis

Grade	Description	MRI Features
0	Normal	Normal bone marrow signal No cortical disruption
1	Stress reaction	Bone marrow edema No cortical disruption
2	Incomplete fracture	Bone marrow edema Incomplete fracture through the pars interarticularis
3	Acute complete	Bone marrow edema Complete fracture through the pars interarticularis
4	Chronic complete	No bone marrow edema Complete fracture through the pars interarticularis

From Murthy NS. Imaging of stress fractures of the spine. *Radiol Clin North Am.* 2012;50:799-821, Table 1.

classification of spondylolysis (Table 15.8).²²⁸ A subsequent study comparing CT staging and MRI findings noted that CT-defined early stage lesions all exhibited T2 hyperintensity in the ipsilateral pedicle; terminal stage lesions never exhibited T2 hyperintensity in the pedicle.²²⁸ Nearly 80% of lesions with T2 hyperintensity in the pedicle healed with conservative care.²²⁹

Spondylolysis has also been assessed with SPECT/CT, although at the cost of radiation dose to a typically young population. Gregory and colleagues assessed the diagnostic value of combining SPECT with CT in the evaluation of spondylolysis.²³⁰ They described four categories of patients: group A: (+) SPECT and (+) CT findings for spondylolysis; group B: (+) SPECT and (-) CT findings for spondylolysis +/- sclerosis of the pars; group C: (-) SPECT and (+) CT

findings for spondylolysis; and group D: (-) SPECT and (-) CT findings for spondylolysis. Group A and B patients were felt to have a healing potential with early fatigue fractures or stress responses; group C patients had terminal lesions without healing potential, and group D patients had other pain generators, often the disk.²³⁰ Although adult spondylolysis is often asymptomatic, there is a tendency to develop significant disk failure at the level of the pars defect, which may result in late progression of the degree of vertebral displacement and neural element compromise resulting from foraminal stenosis, which is well demonstrated on sagittal MRI. Spondylolysis patients may then experience axial pain caused by the inflammatory change about the pars defect, diskogenic pain from the failed disk, and radicular pain from secondary foraminal compromise.

Characterization of pars defects sufficient for therapeutic planning requires assessment of both morphologic and physiologic parameters. A stress response in the pars, or an incomplete fracture, may respond to conservative therapy with healing; completed chronic fractures seldom heal and are often asymptomatic. Persistent symptoms in the face of a chronic completed fracture may reflect secondary phenomena of diskogenic pain or radicular pain from foraminal stenosis. The combined morphologic and physiologic characterization can be performed with SPECT/CT or MRI. The interested reader is referred to a far more complete review by Murthy.²¹⁹

SPINE INFECTION

Extradural spinal infections are primarily the result of arterial seeding. In children, the disk and end plate have a rich blood supply; infection occurs initially in the disk itself. In the adult, the disk is avascular; an infection develops in the anterior subchondral vertebral body with secondary spread to the disk, adjacent vertebrae, and subligamentous (deep to the anterior longitudinal ligament) space. Most disk space

infections involve two adjacent lumbar vertebrae. Spread from contiguous infection or direct inoculation of the disk (surgery, injections, diskography) is much less common.

Pyogenic disk space infection involves men much more commonly than women (2-3:1) in the fifth to seventh decades of life.²³¹ Infection is usually unimicrobial, *Staphylococcus aureus* is the most common pathogen, and urinary tract infections are the most common source of seeding.²³² Clinical symptoms may precede radiographic findings by 1 to 8 weeks. Clinical signs of elevated sedimentation rate, white cell count, and C-reactive protein are usually present. Plain films reveal early rarefaction of anterior subchondral bone, followed by a loss of disk space height (at 1 to 3 weeks) with subsequent destructive changes in the vertebral end plates. Late changes include variable amounts of sclerosis, kyphotic deformity from vertebral collapse, and ankylosis. CT in pyogenic diskitis shows early hypodensity in the disk, moth-eaten destruction of the vertebral end plates, inflammatory changes in paravertebral soft tissues, and epidural mass. Scattered gas formation may be observed as well. Extensive gas formation in the central portion of the disk is typical of noninfectious disk degeneration; the disappearance of such a vacuum disk sign may herald infection.

MRI is the preferred imaging modality for the evaluation of diskitis, with a greater than 90% sensitivity and specificity in disease detection.^{231,232} It also provides critical anatomic information. Early marrow changes are elevated T2 signal (best observed with fat saturation or STIR), diminished T1 signal, and gadolinium enhancement (Fig. 15.23). There is loss of the crisp dark cortical line of the vertebral end plate. Within the disk, the intranuclear cleft is lost and foci of elevated T2 signal and gadolinium enhancement develop. The paravertebral and epidural soft tissues show diffuse enhancement (phlegmon) or frank abscess formation with zones of hypo-enhancement and increased T2 signal where liquid purulent material is present. The imaging differential diagnosis consists of a Modic type I degenerative change, atypical cartilaginous (Schmorl's) nodes, adjacent metastatic lesions, osteomalacia secondary to osteodystrophy, and pseudoarthroses in patients with ankylosing spondylitis or a Charcot spine. Discrimination from a Modic type I end plate change can be particularly vexing; differential points are presented in Table 15.9. In challenging cases, image-guided biopsy and culture are appropriate.

MRI abnormalities lag behind the clinical syndrome. Imaging may be minimally abnormal early in the disease process and remain quite dramatic even after a gratifying clinical response to antibiotics. In following the short-term efficacy of antibiotic therapy, erythrocyte sedimentation rate (ESR), C-reactive protein (CRP), and white cell count will be more useful than repeated imaging. Follow-up imaging should be reserved for patients in whom there is a clinical concern for continued infection with central canal compromise. Persistently elevated or increasing ESR or CRP at week 4 of antibiotic therapy predicts treatment failure.²³³

Nuclear medicine scans using gallium-67 citrate and technetium-99m diphosphonate are complementary in the evaluation for suspected spondylodiscitis. A series by Hadjipavlou and colleagues demonstrated 100% sensitivity, specificity, and accuracy for the combination of gallium and technetium

scans when compared with surgical biopsy results.²³⁴ Gallium may be useful in following resolution of the infection. All nuclear medicine techniques lack anatomic information; they are unable to define the extent of epidural or paraspinal disease or central canal compromise.

Pyogenic epidural abscesses may arise from the contiguous spread of adjacent spondylodiscitis or facet joint infection, but they are most commonly primary, because of the hematogenous dissemination or direct inoculation of the epidural space. *S. aureus* is the most common pathogen; immune compromise, especially diabetes, is common.²³¹ Emergent MRI is the imaging modality of choice. This will demonstrate a T1 hypointense, T2 hyperintense epidural process with peripheral or heterogeneous enhancement, depending on the physical state of abscess versus phlegmon. The midline ventral epidural septum may be violated; most neoplasms respect this structure. Compression of the dural sac is common; severe compromise with neurologic deficit precipitates emergent decompression. Imaging resolution of an epidural abscess more closely parallels the clinical state than in spondylodiscitis.

Pyogenic facet joint infection is uncommon; it is usually the result of hematogenous dissemination, although direct inoculation caused by invasive procedures is reported. Clinical presentation may resemble spondylodiscitis, although most commonly with lateralizing symptoms; the lumbar spine segment is most frequently affected. Bilateral involvement may occur via the space of Okada.¹³⁰ CT will demonstrate an erosive process centered on the joint with inflammatory change in adjacent multifidus muscle. MRI will demonstrate marrow edema in the articular processes, a joint effusion, and edematous changes in the multifidus; enhancement in the joint with peripheral enhancement about an adjacent paraspinal or epidural abscess or uniform heterogeneous enhancement within a phlegmon may be noted.

Tuberculosis (TB) remains the most common cause of spinal infection worldwide, and it is of increasing incidence in industrialized societies. Clinical symptoms are usually insidious. Whereas 90% to 100% of patients will have back pain, only 50% will have constitutional symptoms or fever. Tuberculous spondylitis (Pott's disease) arises from hematogenous (arterial) spread of tuberculous bacilli, usually from a pulmonary source. This initially lodges in the anterior subchondral bone. There is early anterior subligamentous extension and then spread to adjacent vertebrae, often multiple, as well as spread across the disk. Neurologic deficit occurs in a moderate number of patients due to epidural extension. Posterior elements tend to be spared. Extensive anterior column destruction with gibbus deformity is characteristic.

Tuberculous spondylitis with diskitis shows disk space narrowing, vertebral osteolysis with collapse, and gibbus deformity on plain films. The thoracolumbar junction is most frequently affected, with less frequent involvement as one ascends the thoracic or descends the lumbar spine.²³¹ Plain films may not be abnormal until 2 to 5 months after the onset of infection. Paraspinal soft tissue masses caused by subligamentous spread, particularly with calcification, are characteristic. CT will demonstrate the osteolytic changes of spinal tuberculosis earlier than plain films will. It more readily demonstrates epidural involvement, particularly when

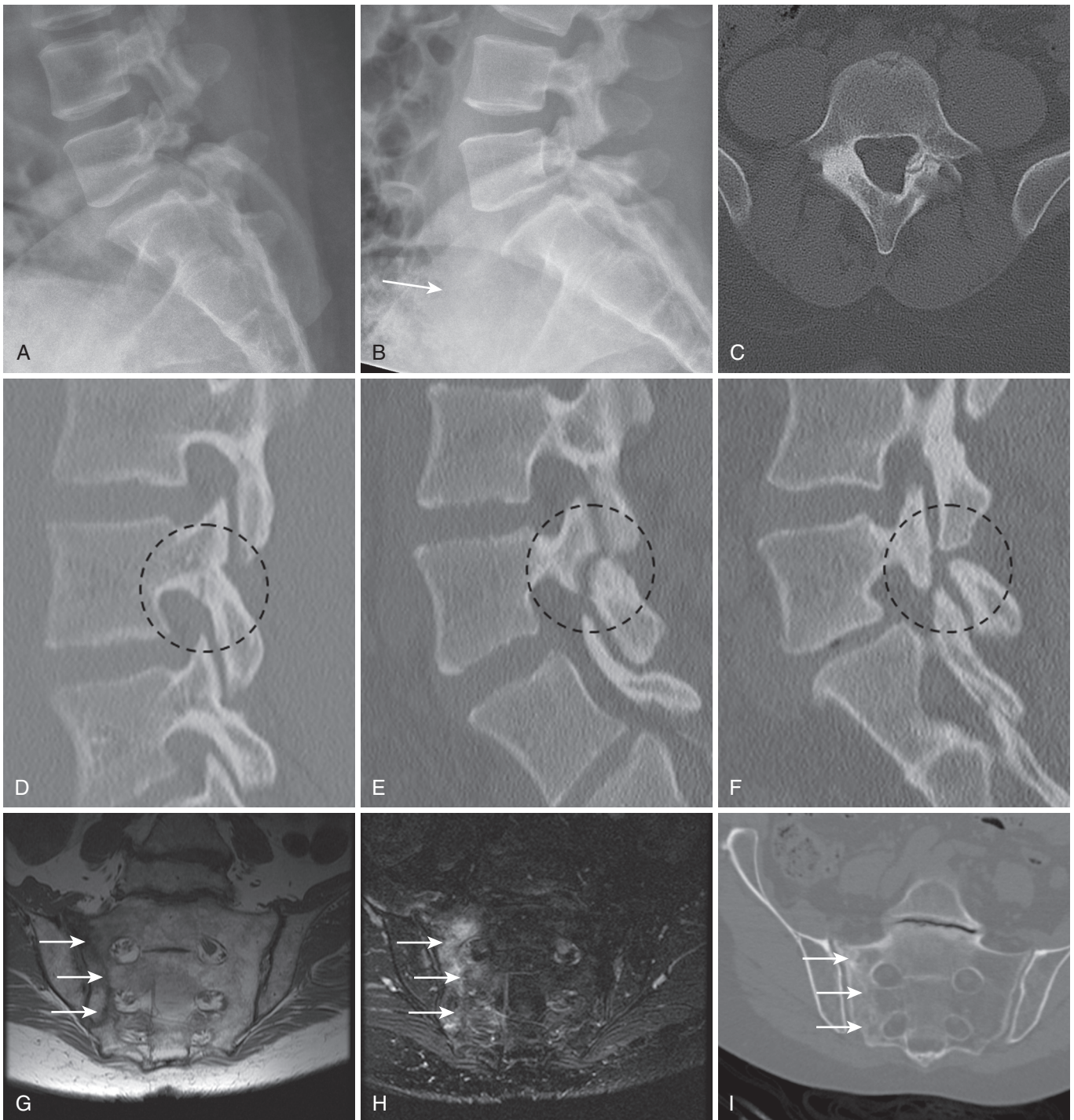


Figure 15.23 Stress fractures. Spondylolysis at L5 is visible on flexion (**A**) and extension (**B**) radiographs. Although there is no translation of L5 on S1, the degree of rotation (12 degrees) qualifies this as unstable. In unilateral spondylolysis, the contralateral pars often shows hypertrophy and sclerosis (**C**). CT can be used to stage pars fractures as early stage (**D**) with a narrow, sharply margined fissure; progressive stage (**E**) with a narrow fissure having slightly rounded margins; and terminal stage (**F**) with a wide fissure with rounded margins and sclerosis. Typical sacral stress fracture (*arrows*) demonstrates a low signal fracture line on a coronal T1 image (**G**), a linear zone of T2 hyperintensity on a STIR image (**H**), whereas CT demonstrates a linear zone of sclerosis (**I**). The integrity of the neural foramina is better defined on CT. (From Murthy NS. Imaging of stress fractures of the spine. *Radiol Clin North Am.* 2012;50:799-821.)

calcification or bone fragments are visible in the epidural space. Paraspinal involvement is also well demonstrated.

MRI is the primary imaging procedure for the detection of spinal TB. Early changes of tuberculous spondylitis with diskitis are very similar to pyogenic disk space infection, with marrow

and disk inflammatory changes consisting of elevated T2 signal, diminished T1 signal, and enhancement. Extensive subligamentous spread of disease suggests TB. Paraspinal abscesses, granulomas, and epidural involvement are common. Epidural involvement may be observed in 60% to 80% of cases.²³¹

Table 15.9 Differentiating Spondylodiscitis from Modic Type I End Plate Changes

	Favoring Spondylodiscitis	Favoring Modic Type I End Plate Changes	Pitfall/Comments
Disk Space Signal	T2 hyperintensity	T2 hypointensity or lack of T2 hyperintensity	Severely degenerated disks rarely can be T2 hyperintense (even fluid signal)
Disk Space Enhancement	Present	Absent	Rarely absent in infection; rarely present in Modic I
Disk Space Vacuum Sign	Absent, or only scattered	Often present; large amount of confluent gas on radiographs virtually exclude infection	Gas may be present early in infection, in rare gas-forming bacterial infection, or in rare fistulas with the gastrointestinal tract
Vertebral Body End Plates	End plate destruction	Lack of end plate destruction	Modic I can have end plate irregularity; <i>CT is very useful here</i>
Paraspinal, Epidural Spaces	Inflammation or abscess	Absent	Peripherally enhancing disk herniation can be confused for abscess
Location	Anteriorly eccentric	Laterally eccentric: at point of biomechanical stress (e.g., inner aspect of curve)	Both spondylodiscitis and Modic I are often along entire end plate
Fever, Elevated Inflammatory Markers	Present	Absent	Fever is only variably present in spondylodiscitis; inflammatory markers are nonspecific
Short-Term Follow-up	Progression	Stability	If <i>remote</i> comparison images are available, even Modic I can show significant progression

From Diehn FE. Imaging of spine infection. *Radiol Clin North Am.* 2012;50:777-798.

A second pattern of tuberculous infection is spondylitis without diskitis (see Fig. 15.23).²³⁵ This describes lytic lesions in the central portions of the vertebral bodies, often multiple, without disk involvement. This pattern of involvement was present in approximately 50% of patients in one large series.²³⁴ Imaging findings consist of discrete, destructive vertebral body lesions. Plain films show well-defined lytic lesions, often multifocal, and with more frequent posterior element and cervical involvement than is observed in tuberculous diskitis. Lytic lesions may exhibit marginal sclerosis on CT, indicating a more indolent lesion than a typical metastatic deposit. These lesions typically enhance peripherally on MRI, often with a cystic central cavity. There may be cortical destruction with an adjacent paravertebral abscess. Because of the greater frequency of multiple lesions, this entity must be distinguished from metastasis, myeloma, or lymphoma.

MRI has significantly advanced the diagnosis of spinal infection, allowing this to be suggested as a likely diagnosis before destructive changes have evolved. The MRI findings remain nonspecific, however, and accurate diagnosis and therapy require tissue sampling for histology and culture. Image-guided percutaneous aspiration/biopsy with large caliber bone cutting needles can provide minimally invasive tissue sampling.

INFLAMMATORY SPONDYLOARTHROPATHY

Noninfectious inflammatory disease of the spine includes rheumatoid arthritis (RA) and the seronegative spondyloarthropathies (SpA), of which ankylosing spondylitis is the prototype. These diverse entities have spine involvement in common and may present with axial spine pain.

Rheumatoid arthritis is most common in the cervical spine, sometimes referred to as the fifth limb in RA patients. Symptoms and signs of cervical spine involvement are present in 60% to 80% of RA patients.²³⁶ The most frequent site of involvement is the atlantoaxial articulation. Inflammatory pannus may be seen on MRI as a low T1, high T2 signal-enhancing mass posterior to the dens. This may cause compression of the cervicomedullary junction. The inflammatory change may destroy the transverse and alar ligaments, resulting in atlantoaxial instability in 20% to 25% of RA patients. A distance of greater than 4 mm between the posterior arch of C1 and the cortical surface of the dens on radiographs is abnormal and is most evident in flexion views. The destruction of supporting structures at the craniocervical junction may also result in cranial settling, a vertical migration of the dens into the foramen magnum, with possible compression of the C1 and C2 cranial nerves, the medulla, and vertebral arteries.

The cervical spine below the C1-2 articulations demonstrates erosive arthritis in the uncovertebral and facet joints in RA patients. The inflammatory change can be demonstrated on MRI as increased T2 signal on STIR sequences and gadolinium enhancement on fat-saturated T1 sequences. This results in multilevel instability, with anterior subluxation of successive vertebral bodies in flexion, the so-called step ladder cervical spine, noted in up to 30% of RA patients.²³⁶ Disk space narrowing and end plate sclerosis are common, but this may be a secondary phenomenon to the posterior element instability.

Involvement of the thoracic and lumbar spine in RA is uncommon. Synovitis and erosive change may be present in the facet and costovertebral joints but is inconstant and not well demonstrated. Discovertebral changes may be present,



Figure 15.24 Spondylodiscitis. A lateral radiograph (A) demonstrates early pyogenic spondylodiscitis manifest as subtle destruction of the anterior inferior aspect of the L3 vertebrae. In another patient, a sagittal CT reconstruction (B), sagittal T1-unenanced (C) and enhanced (D) and axial T1-enhanced MRI images (E) of a patient with L2-3 pyogenic diskitis. Note loss of disk space height, end plate destruction, low T1 signal and extensive vertebral, epidural, and paraspinal enhancement.

Sagittal T2-weighted MRI (F) of a back pain patient without myelopathy demonstrates vertebral destruction with kyphotic deformity; this is tuberculous spondylodiscitis. Coronal T1-enhanced MRI (G) in the same patient demonstrates the extensive paraspinal disease typical of Pott's disease. A sagittal T2-weighted MRI (H) in another patient with tuberculous spondylodiscitis; note the multiple vertebral lesions with sparing of the disks. This can be confused with metastatic disease. Tissue sampling is essential. (From Maus T. Imaging the back pain patient. *Phys Med Rehabil Clin N Am.* 2010;21:725-766.)

but it is again unclear if these are primary inflammatory lesions or a response to facet instability. The sacroiliac joints may show inflammatory change, but with much less frequency and severity than in ankylosing spondylitis patients.

The seronegative spondyloarthropathies are a group of rheumatoid factor negative inflammatory disease processes affecting the spine and sacroiliac joints, with a unique predilection for entheses. Historically these have included ankylosing spondylitis, psoriatic arthritis, reactive arthritis (formerly known as Reiter's syndrome), and the arthritis associated with inflammatory bowel disease. The categorization of these diseases has evolved, most recently in 2009 with the designation of axial spondylarthritis for the spectrum of disease with axial, as opposed to peripheral,

dominance.²³⁷ Axial spondylarthritis requires active sacroiliitis on MRI plus one or more features of spondylarthritis, or human leukocyte antigen B27 (HLA-B27) positivity with two or more features of spondylarthritis. This discussion only encompasses the axial imaging features of the classically defined processes (Fig. 15.24).

MRI is the necessary imaging modality for the assessment of disease activity in the SI joints and spine articulations. MRI or CT can demonstrate the aftermath of disease: joint space narrowing, subchondral erosions, reactive sclerosis, or periarticular fat deposition (a Modic II analog); only MRI can assess active inflammation with T2 hyperintensity (STIR or fat-saturated images) and gadolinium enhancement on fat-saturated T1 images.

Ankylosing spondylitis (AS) is the prototypical seronegative spondyloarthropathy; active disease in the SI joints by MRI criteria is integral to its diagnosis. AS has a prevalence of up to 0.1% in the general population; a very high percentage will be HLA B27 positive. Males dominate by 4:1. The disease involves synovial and cartilaginous joints and entheses (ligament and tendon insertions on bone) with a strong predilection for the axial skeleton. The most common presentation is low back pain with inflammatory features (Calin criteria, 4 out of 5 of insidious onset, age < 40, 3 months persistence, morning stiffness, and pain improved by exercise). Radiating pain mimicking sciatica may be observed in up to 50% of patients.

Imaging findings in AS include sacroiliitis, ultimately bilaterally symmetric and multiple manifestations of spondylitis (see Fig. 15.24). Sacroiliitis is the uniform initial imaging finding. Early plain film findings of sacroiliitis are blurring of the subchondral cortex by small erosions, predominantly on the iliac side of the joint. As the erosions coalesce, the joint space appears widened and ill defined; sclerotic reaction develops in the trabecular bone about both sides of the joint. Over time the joint undergoes ankylosis via direct bony bridging; the joint space is no longer visible and the sclerosis resolves.²³⁸ MRI can detect inflammation in the SI joint in symptomatic patients with normal plain films. Inflammation can be reliably identified with low interobserver variability as high T2 signal on STIR sequences or gadolinium enhancement on fat-saturated T1 images.²³⁹ In patients with recent onset axial low back pain with inflammatory clinical characteristics, SI joint inflammation may be detected by MRI in one third of patients and structural changes in one sixth of patients.²³⁹ Inflammation is initially observed in the iliac side of the joint at its caudal and dorsal aspects, and in the adjacent dorsal entheses.

Spine findings in AS are present in 50% of patients and include osteitis, syndesmophyte formation, discovertebral lesions, and inflammation leading to ankylosis of facet and costovertebral joints.²³⁸ Osteitis is observed at the anterior margins of the discovertebral junction, termed the *Romanus lesion*. On plain films, sclerosis at these sites leads to increased density of the anterior corners of the vertebra, termed the *shiny corners sign*.²³⁸ Remodeling of the anterior margin of the vertebral body as a result of osteitis straightens the normally concave anterior vertebral margin, referred to as “squaring” of the vertebra. These findings are most evident in the lumbar region. MRI is more sensitive to the early detection of osteitis, recognized as diminished T1 and increased T2 signal and enhancement at the anterior vertebral corners.²³⁸ Osteitis at the margins of the discovertebral junctions leads to reactive bone formation in the outer annulus fibrosis, which ultimately bridges the margins of adjacent vertebrae. These vertically oriented bony struts are syndesmophytes. They are distinguished from osteophytes by their vertical orientation and gracile nature; osteophytes are oriented in the horizontal plane and are bulkier. Syndesmophytes are most common at the anterior and lateral aspects of the vertebral body; when long standing, the ossification may involve the anterior longitudinal ligament.

Erosions at the discovertebral junction are termed *Anderson lesions*; this inflammatory destruction of the vertebral end plate with intravertebral disk displacement can progress to pseudarthrosis. End plate destruction is visible on plain films;

MRI demonstrates structural and inflammatory change. The inflammatory change will undergo evolution reminiscent of the progression from Modic type 1 to Modic type 2. Over time there is sclerosis and transdiscal ossification leading to ankylosis. The facet and costovertebral joints show similar findings, with initial periarticular erosions followed by sclerosis and ankylosis. Enthesitis of the posterior interspinous and supraspinous ligament attachments ultimately leads to ossification of these structures, visible as a vertical midline bony band on frontal radiographs, the so-called dagger sign. The inflammatory spinal lesions are most common in the mid-thoracic spine (T7-T8) and in the midlumbar region (L2-3).

AS may also produce changes at the atlanto-axial articulation. Synovitis may result in erosive changes in the dens, although the extent of inflammatory change seldom reaches that noted in RA. Atlanto-axial subluxation may be present. The extensive ankylosis observed in patients with long-standing AS leads to flattening of the lumbar lordosis and exaggeration of the thoracic kyphosis. The rigidity places these patients at risk for catastrophic fracture-dislocations with modest trauma, most commonly with a hyperextension mechanism. The cervical spine is most frequently involved; neurologic deficits are common. Plain film evaluation is difficult because of the osteopenia typical of these patients; the three-column nature of these fractures is best appreciated with CT or MRI. The threshold for use of advanced imaging in the AS patient with trauma should be low. Three-column fractures that do not cause acute neurologic injury or go undetected may be a cause of chronic focal pain as a pseudarthrosis. MRI will show a linear zone of inflammatory change, often through a disk space with extension through the posterior elements. The cortical disruption may be best appreciated on CT. Finally, some AS patients will have findings of dural ectasia (see Fig. 15.24). The thecal sac will be abnormally capacious with diverticular-like outpouchings; there is associated bony erosion in the posterior elements, medial margins of the pedicles, and the posterior vertebral body. These patients may present with a cauda equina syndrome, perhaps related to arachnoiditis.

Psoriatic arthritis (PA) is far less common than AS; it affects 7% of patients with cutaneous psoriasis.²³⁸ Approximately 10% to 25% of patients with moderate to severe skin disease will have abnormal SI joint radiographs. Spondylitis is present in a roughly similar proportion but may or may not coexist with sacroiliitis. Males and females are equally affected.²³⁸ The sacroiliitis is usually bilateral but asymmetric, with a lesser tendency to progress to bony ankylosis. Erosions and foci of reactive sclerosis tend to be larger and more discrete than in AS. The spondylitis in psoriatic arthritis is characterized by asymmetric, coarse paravertebral ossification more resembling osteophytes than syndesmophytes. Vertebral squaring and shiny corners are absent. Facet involvement is infrequent.

Reactive spondylarthritis describes an inflammatory arthropathy, preferentially affecting the heel and large peripheral joints.²³⁸ Sacroiliitis is very common, affecting up to 45% of patients. It is more commonly unilateral or asymmetric than in AS; ankylosis is rare. Spine involvement may be identical to that of PA but more common; the lumbar spine is involved in 30% of RS patients.²³⁸ In the setting of a triggering infection (often chlamydia) and the triad of urethritis, uveitis, and arthritis, the term *Reiter's syndrome* may be applied.

Enteropathic arthritis may also be observed in association with ulcerative colitis or Crohn's disease. The initial presentation of back pain may precede symptoms of gastrointestinal disease. The spondylitis and sacroiliitis noted in association with these conditions are indistinguishable from classic ankylosing spondylitis. Sacroiliitis is usually bilaterally symmetric progressing to ankylosis; spondylitic findings of vertebral squaring, discovertebral lesions, syndesmophytes, and involvement of the facet joints are typical.

SPINE NEOPLASM

Spinal neoplasms are classified by the anatomic compartment from which they arise: extradural, intradural-extramedullary, or intramedullary. Extradural neoplasms arise from the vertebral bodies, within the paravertebral soft tissues, or within the epidural space. These include metastatic lesions, hematologic malignancies, and primary osseous or cartilaginous tumors. Intradural-extramedullary lesions arise within the dural tube but are extrinsic to the spinal cord itself. Lesions in this category include meningiomas, Schwannomas, neurofibromas, and leptomeningeal metastatic disease. Intramedullary lesions are those that arise primarily from the spinal cord or filum terminale. Astrocytomas, ependymomas, and hemangioblastomas make up the majority of these lesions.

Extradural neoplasms are common. MRI provides the best combination of lesion detection, morphologic characterization, and assessment of neural compromise. Nuclear medicine techniques such as technetium bone scan and PET scanning provide high sensitivity to lesion detection and excellent body wide assessment of tumor burden (Fig. 15.25). Nuclear medicine studies will not provide anatomic information regarding compression of neural elements. CT is less sensitive than MRI in lesion detection; plain films are far less sensitive.

Extradural neoplasms may narrow the subarachnoid space (cerebrospinal fluid) as they extrinsically intrude into the spinal canal. They exhibit diminished T1 signal, elevated T2 signal, and gadolinium enhancement on MRI. The unenhanced T1 image is the mainstay of lesion detection; normal adult marrow should be brighter than the intervertebral disks. Fat-saturated T2-weighted images and STIR images provide high sensitivity to lesion detection. Fat-saturated postgadolinium images will also display extradural neoplasm with high sensitivity. On axial images, compression of the thecal sac or exiting nerve roots can be directly displayed. CT and plain films play a role in characterizing primary bone and cartilaginous tumors including malignant lesions such as osteosarcoma, chondrosarcoma, chordoma, and the benign tumors, including hemangioma, osteoid osteoma, giant cell tumor, and aneurysmal bone cyst.

Metastases are the most common extradural spine tumor, and the spinal column is the most common site of osseous metastases. An overwhelming majority of spine metastases are due to prostate, lung, and breast cancer. The thoracic spine is most commonly involved (70%), followed by the lumbar and cervical segments. Involvement of the vertebral body is most common (85%), with less frequent spread to the paravertebral tissues or epidural space. The disks, dura, and the anterior longitudinal ligament are resistant to invasion by metastatic tumor; the posterior longitudinal ligament is more readily involved, as it is penetrated by

numerous venous channels. Vertebral body metastases may be blastic (bone forming), lytic (destructive), or mixed. Blastic lesions are observed as ill-defined areas of increased density on plain films or CT; on MRI, blastic lesions will have low T1 and T2 signal with enhancement. Common primary tumors are prostate, carcinoid, or bladder cancer. Lytic metastases show destruction on plain films and CT, and low T1 and variable T2 signal with enhancement on MRI. Lytic metastases are most commonly produced by breast, lung, renal, and thyroid neoplasms. Mixed lytic and blastic lesions are visible in lung, breast, cervical, and ovarian primaries.

Hemangiomas are the most common spine tumor, present in up to 10% to 12% of adults. They are frequently multiple. Typical hemangiomas are benign and of no clinical significance; they are identified by their fatty content on MRI (high T1 and T2 signal) and a corduroy appearance on plain films or CT. This is due to sparse, thickened trabeculae surrounded by fat; on axial images this results in a polka dot appearance.

Osteoid osteomas occur in patients under the age of 30, and they typically present with pain, often nocturnal. Aspirin or nonsteroidal anti-inflammatory drugs (NSAIDs) can usually relieve pain. The lesion consists of a small nidus, less than 1.5 cm in diameter, surrounded by a larger zone of sclerotic reaction or soft tissue inflammation, visible on plain films or CT. The nidus is intensely enhancing on CT, MRI, or bone scan. Ten percent of osteoid osteomas occur in the spine, almost exclusively in the posterior neural arch. The lumbar spine is involved in 59% of spinal osteoid osteomas, the cervical region in 27%, and the thoracic spine in 12%. Lesions larger than 1.5 cm are considered osteoblastomas.

Myeloma is the most common malignant primary tumor of bone; it presents with bone pain in 75% of patients. It is often widespread at presentation. Its imaging appearance can range from discrete destructive lesions to diffuse loss of bone density indistinguishable from osteoporosis on plain films. CT is better able to resolve the discrete destructive lesions in trabecular or cortical bone. The MRI appearance is variable, with diminished T1 marrow signal and gadolinium enhancement in a multifocal or diffuse pattern. Compression fractures are common and they may be indistinguishable from benign osteoporotic fractures. Single focal lesions (plasmacytomas) are expansile and lytic on imaging.

Leukemia may present with spine pain in the setting of diffuse marrow involvement and associated compression fractures. The most common imaging finding is that of diffuse marrow replacement, with osteopenia on plain films and CT, and generalized loss of the normal T1 marrow signal. Normal marrow should always be brighter than disk signal on T1 images. Focal extra-osseous soft tissue masses of leukemic tissue may be present and are termed *chloromas*.

Lymphoma is the great mimic. It can present in the spine as vertebral lesions indistinguishable from metastases, as an epidural soft tissue mass without bone involvement, as a diffuse leptomeningeal process, and as a primary intramedullary lesion.

Intradural-extramedullary neoplasms are situated within the dural sac, widening the subarachnoid space as they displace the cord or cauda equina. Meningiomas typically exhibit a broad base against the dural surface and enhance uniformly. Schwannomas and neurofibromas are indistinguishable on imaging. They may enhance uniformly

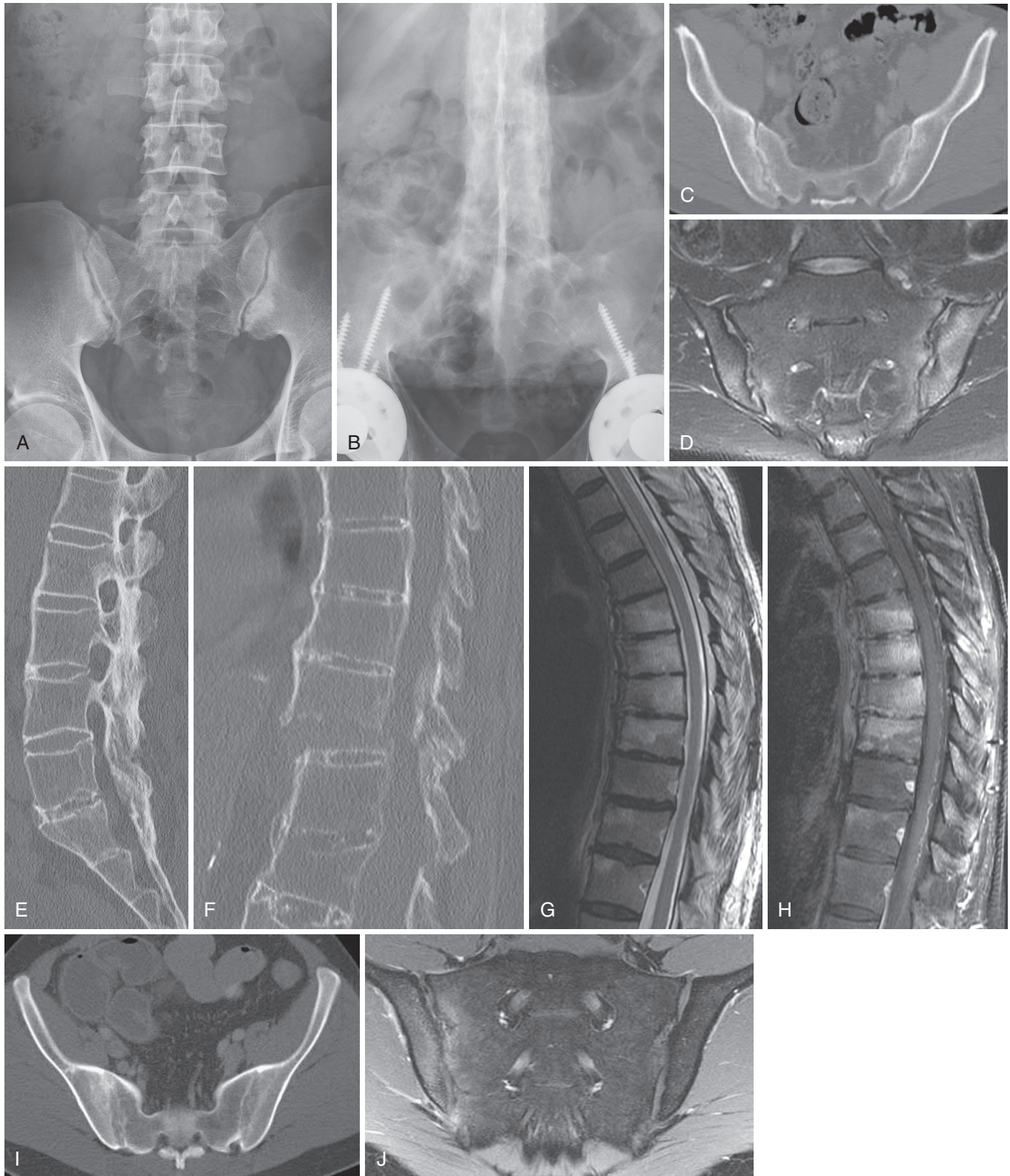


Figure 15.25 Spondyloarthropathy. Changes of sacroiliitis are detectable on radiographs (**A**) as irregularity, erosions, and sclerosis, dominant on the iliac side of the joint. In the end stage of ankylosing spondylitis (AS), the sacroiliac joints are fused and the sclerosis resolves (**B**); this radiograph also depicts the dagger sign, as the fused spinous processes make a continuous sclerotic structure in the midline. CT (**C**) is more sensitive in the detection of erosions and early sclerotic reaction in AS; this structural change may simply reflect prior disease. Only MRI can detect disease activity (**D**) as demonstrated by the T2 hyperintensity in and about both SI joints in this AS patient. The gracile vertical syndesmophytes bridging lumbar vertebrae and the fused posterior elements are well seen on CT (**E**); the spine in AS is rendered vulnerable to three-column unstable fractures with modest trauma (**F**). These situations deserve CT imaging. The spondyloarthropathy of inflammatory bowel disease may present as back pain (T2 sagittal [**G**] and enhanced T1 fat-saturated sagittal [**H**]) with evidence of multifocal inflammatory spondyloarthropathy. The differential diagnosis here is multilevel spondylodiscitis, especially Pott's disease (tuberculosis). Changes of sacroiliitis in inflammatory bowel disease (**I**) may be indistinguishable from AS. Asymmetric sacroiliitis (T1-enhanced, fat-saturated coronal MRI [**J**]) is typical of reactive spondylarthritis (formerly Reiter's syndrome).

or show central zones of cystic degeneration. The classic “dumb-bell” neurofibroma may issue through and widen a neural foramen. They may also occur entirely within the dural sac or in a paravertebral location. Leptomeningeal metastatic disease is most typically seen as enhancement on the surface of the cord or within the roots of the cauda equina. In some cases more discrete small masses may be observed within the cauda equina. CSF cytology remains more sensitive than MRI in the detection of leptomeningeal metastatic disease.

Intramedullary neoplasms are rare entities, but they may present with pain or dysfunction that can mimic degenerative disease. Ependymomas arise from the ependymal cells lining the central canal of the cord. Ependymomas are the most common intramedullary tumor in adults; they are most frequently located in the conus medullaris and filum terminale (myxopapillary ependymoma). Because of their slow growth, they may cause bony erosion and scalloped enlargement of the central canal. MRI demonstrates an enlarged cord or filum terminale with an elevated T2 signal and heterogenous enhancement. Small cysts or hemorrhage are frequent. Astrocytomas are typically low-grade neoplasms, more commonly noted in young patients and in the cervical region. They typically extend over multiple vertebral segments within the cord with poorly defined margins. The cord is enlarged with heterogenous enhancement. The entire cross section of the cord is typically involved. Considerable edema within the white matter of the cord extends cephalad and caudal to the enhancing neoplasm itself. Peritumoral cysts may be present. Hemangioblastomas are rare lesions that typically occur in the cervical and thoracic spine. An intensely enhancing vascular nodule adjacent to the pial surface, often associated with an intramedullary cyst, is typical. About one third of patients with hemangioblastomas will have Von Hippel Lindau syndrome.

SPINAL DURAL ARTERIOVENOUS FISTULA (AVF)

Spinal dural AVFs are the most common form of vascular malformation involving the spine. This lesion merits description in that it may present with pain and progressive neurologic deficit, mimicking neurogenic intermittent claudication; it frequently remains undiagnosed for prolonged periods. In Atkinson’s series, the mean delay from symptom onset to diagnosis was 23 months.²⁴⁰ Patients are frequently subjected to misdirected interventions, including decompressive surgery. When diagnosed, it is treatable with arrest of the progressive neurologic deficit.

Spinal dural AVFs are an acquired lesion, with a fistulous communication within the dura of a root sleeve and intrathecal venous drainage to the venous plexus surrounding the cord. This results in venous hypertension within the cord and ultimately cord dysfunction. The fistula is most commonly in the low thoracic or lumbar spine. It is a lesion of elderly males. Gilbertson’s series²⁴¹ had a mean age of 62, with a range from 37 to 81; Atkinson’s series²⁴⁰ reported a 4:1 male predominance. Pain was a reported symptom in 53% of patients; many of these patients described a burning, dysesthetic pain in the lower extremities; 15% had low back pain when erect, which worsened with use of the lower extremities. This is typically accompanied by

a slowly progressive or stepwise worsening myelopathy, manifest as lower extremity fatigue and weakness. Atkinson’s series²⁴⁰ reported that 69% of patients had upper and lower motor neuron signs; 30% had only lower motor neuron signs.

Imaging findings of dural AVFs have been well described.²⁴² On CT myelography, abnormally prominent tortuous vessels are present in 100% of cases; this may give the cauda equina a beaded appearance. On MRI, there will be T2 hyperintensity in the cord in nearly 100% of cases (Fig. 15.26). This typically extends over multiple vertebral segments and may be accompanied by cord enlargement in 45% of cases. There may be patchy cord enhancement; these findings may raise a concern for tumor. A differentiating finding is the presence of prominent flow voids or intravascular enhancement caused by the dilated veins, particularly on the dorsal surface of the cord. The T2 hyperintensity in the cord usually involves the low thoracic cord and conus; this does not predict the site of the fistula. Magnetic resonance angiography (MRA) is useful in predicting the site of the fistula (Fig. 15.27)²⁴² and reducing the scope of spinal angiography, which provides the definite diagnosis. The fistula then may be disconnected surgically or by an endovascular approach.

The goal of diagnosis and therapy is primarily to arrest the progression of the neurologic deficit and possibly improve the current disability. After successful occlusion of the fistula, either surgically or by endovascular embolic techniques, gait improvement was noted in 67% to 80% of patients.²⁴² Bowel/bladder dysfunction or pain is relieved in only a minority of patients. Worsening of motor symptoms should prompt an imaging investigation for recanalization of the fistula.²⁴² After successful fistula occlusion, cord enlargement, enhancement, and T2 hyperintensity and the prominent veins about the conus will slowly resolve; T2 hyperintensity and enhancement may persist for up to a year.

CONCLUSION

As a synopsis of the imaging assessment of the patient with spine or limb pain, this chapter has ranged widely over large swaths of pathology and imaging technology. There are enduring themes. The primary role of imaging is to detect systemic disease causal of the patient’s pain or neurologic dysfunction; such disease is uncommon. Imaging is currently overutilized to the detriment of patients and society. It has no value in the initial presentation of the patient in the absence of red flag features suggesting systemic disease. The decision to begin imaging should be a reasoned one, considering benefits of improved outcomes versus real risks and harms. The ACR and the ACP have promulgated evidence-based guidelines for imaging use; they should be respected. When imaging occurs, it must be done with a full appreciation of its inherent specificity and sensitivity faults. There is a high prevalence of asymptomatic, age-related change evident on all types of spine imaging; loss of T2 signal in the disk nucleus, anterior and lateral vertebral osteophytes, disk protrusions, and facet and sacroiliac joint arthrosis do not correlate with pain. Imaging performed without axial load and physiologic posture may be insensitive to dynamic lesions.

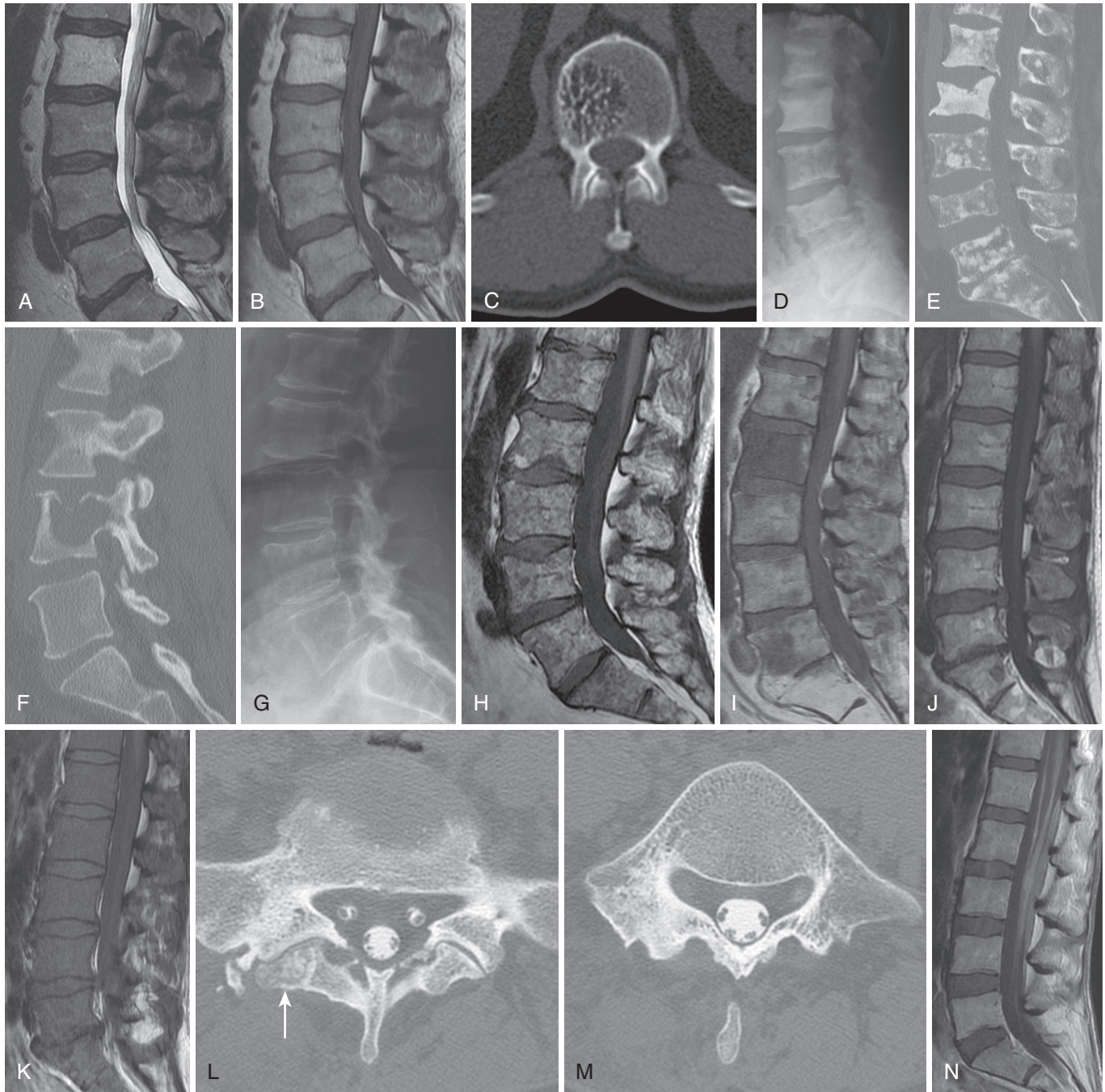


Figure 15.26 Spine neoplasm. Sagittal T2 (A) and T1 (B) images show a lesion in the L2 vertebral body characterized by increased signal intensity on both sequences, typical of hemangioma, the most common benign spinal extradural neoplasm. A CT image in another patient (C) demonstrates the classic CT features of hemangioma: thickened trabeculae surrounding increased marrow fat, resulting in a polka dot appearance. Blastic metastases (D) have increased bone density; CT is more sensitive than radiographs (E), particularly in the detection of lytic metastases (F). Myeloma can be challenging to detect on radiographs, mimicking osteoporosis (G); MRI in the same patient (H) identifies the myriad of tiny destructive lesions. The MRI T1 sagittal sequence (I) typically reveals metastatic disease as focal hypointense lesions, as in this patient with prostate cancer, as the bright signal of normal marrow fat is replaced. When marrow replacement is diffuse, this can be difficult to detect. Normal marrow should always be brighter than adjacent disks. Note that normal marrow in (J) is completely replaced 2 years later by leukemia (K) when this patient presented with back pain. Osteoid osteoma is a posterior element benign neoplasm causal of pain, often nocturnal and relieved by salicylates. It is visible as a small nidus (arrow in [L]) with surrounding sclerotic reaction (M). Leptomeningeal metastases or lymphoma may be imaged as diffuse enhancing tissue coating the cord and cauda equina (N).

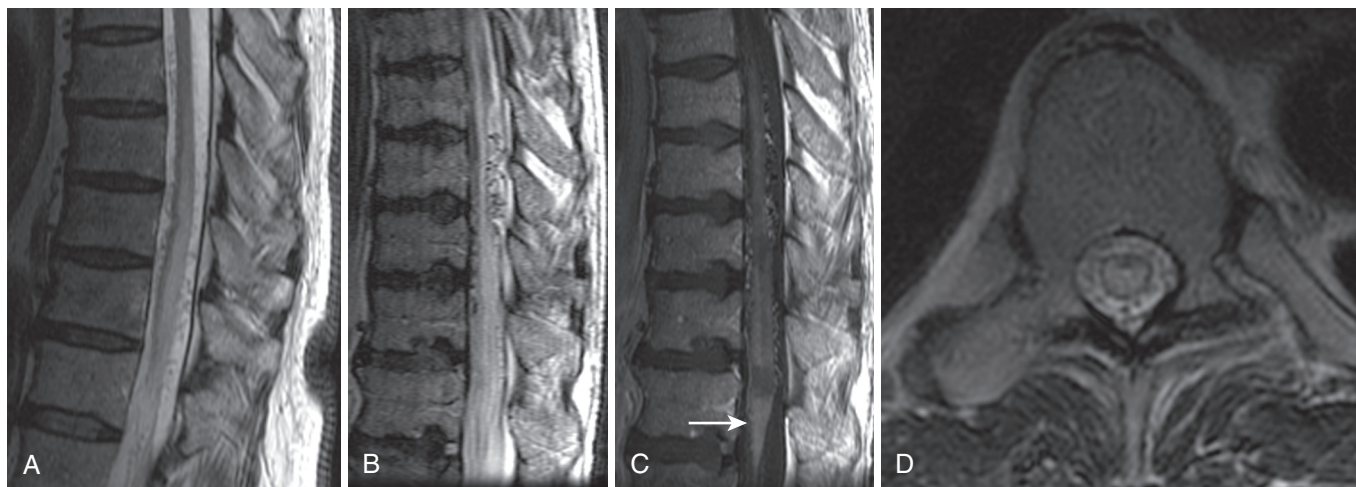


Figure 15.27 Dural arteriovenous fistulae. T2 sagittal MRI images in two patients, **(A)** and **(B)**, both demonstrate enlargement of the conus with multisegmental T2 hyperintensity. Postgadolinium T1 sagittal MRI **(C)**, same patient as **(B)** shows intravascular enhancement in the enlarged perimedullary veins and patchy parenchymal enhancement in the conus (arrow). Axial T2 image through the lower thoracic cord **(D)** demonstrates increased T2 signal throughout the substance of the cord, with a dark border of diminished T2 signal at the periphery of the cord. (From Morris JM. Imaging of dural arteriovenous fistula. *Radiol Clin North Am.* 2012;50:823-839.)

Structural alterations detected by imaging are of less significance than physiologic parameters of edema, hyperemia, disruption of blood-nerve barrier, or accelerated metabolism noted with T2 hyperintensity (STIR or fat-saturated images), gadolinium enhancement, or nuclear medicine techniques. Always treat the patient, not the images.

KEY POINTS

- The primary role of imaging is to identify systemic disease; no imaging is indicated in the acute presentation of back or limb pain without “red flag” features.
- All spine imaging has a significant specificity fault: a high prevalence of asymptomatic age-related findings, including disk “degeneration” and facet arthrosis.
- Spine imaging performed without physiologic positioning and axial load may be insensitive to dynamic lesions.
- Imaging correlates poorly with clinical presentation and course.
- Meticulous enumeration of spine segmentation from the skull base caudally is necessary to avoid wrong segment procedures.
- Magnetic resonance imaging (MRI) findings can reasonably predict positive lumbar diskography; the high intensity zone and significant expression of Modic end plate change have high specificity but low sensitivity.
- Imaging cannot identify cervical diskogenic pain.
- Findings of structural arthrosis of the facet or sacroiliac joints (osteophytes, joint space narrowing, sclerosis) have no relationship to pain; physiologic findings (positive bone scan, MRI T2 hyperintensity) may predict pain but have not been tested against an appropriate reference standard.

KEY POINTS—cont’d

- Radicular pain requires both neural compression and an inflammatory response; standard imaging detects only the neural compression.
- There is no relationship among the size, type, or change in disk herniations over time and patient outcomes.
- The imaging natural history of disk herniation is resolution.
- Neurogenic intermittent claudication requires compression at multiple segmental levels or in multiple compartments (central, lateral recess, foraminal) for clinical expression.
- MRI signal changes in the cervical cord can provide prognostic guidance for decompression in the cervical spondylotic myelopathy patient.

SELECTED READINGS

- Amrami KA. Imaging of the seronegative spondylarthropathies. *Radiol Clin North Am.* 2012;50:841-854.
- Baptiste DC, Fehlings MG. Pathophysiology of cervical myelography. *Spine J.* 2006;6(suppl 6):190S-197S.
- Bogduk N, ed. *Practice Guidelines for Spinal Diagnostic Procedures.* San Francisco: International Spine Intervention Society; 2004.
- Bogduk N. *Clinical and Radiologic Anatomy of the Lumbar Spine.* 5th ed. Churchill Livingstone Elsevier; San Francisco, USA, 2012.
- Carrino JA, Campbell PD Jr, Lin DC, et al. Effect of spinal segment variants on numbering vertebral levels at lumbar MR imaging. *Radiology.* 2011;259:196-202.
- Chou R, Fu R, Carrino JA, et al. Imaging strategies for low-back pain: systematic review and meta-analysis. *Lancet.* 2009;373:463-472.
- Chou R, Loeser J, Owens D, et al. Interventional therapies, surgery, and interdisciplinary rehabilitation for low back pain: evidence based clinical practice guidelines from the American Pain Society. *Spine.* 2009;34:1066-1077.
- Chou R, Qaseem A, Owens DK, et al. Diagnostic imaging for low back pain: advice for high-value health care from the American College of Physicians. *Ann Intern Med.* 2011;154:181-189.
- Chou R, Deyo RA, Jarvik JG. Appropriate use of lumbar imaging for evaluation of low back pain. *Radiol Clin North Am.* 2012;50:569-585.

- Diehn FE. Imaging of spine infection. *Radiol Clin North Am.* 2012;50:777-798.
- Fardon DF, Milette PC. Combined Task Forces of the North American Spine Society, American Society of Spine Radiology, and American Society of Neuroradiology. Nomenclature and classification of lumbar disk pathology: recommendations of the combined task forces of the North American Spine Society, American Society of Spine Radiology, and American Society of Neuroradiology. *Spine.* 2001;26:E93-E113.
- Jarvik JG, Deyo R. Diagnostic evaluation of low back pain with emphasis on imaging. *Ann Intern Med.* 2002;137:586-597.
- Maus TP. Imaging of spinal stenosis: neurogenic intermittent claudication and cervical spondylotic myelopathy. *Radiol Clin North Am.* 2012;50:651-679.
- Maus TP, Aprill CN. Lumbar discogenic pain, provocation diskography, and imaging correlates. *Radiol Clin North Am.* 2012;50:681-704.
- Maus TP, Martin DP. Imaging for discogenic pain. In: Kapural L, Kim P, Deer T, eds. *Diagnosis, Management and Treatment of Discogenic Pain.* Philadelphia: Elsevier/Saunders; 2012: 38.
- Morris JM. Imaging of dural arteriovenous fistula. *Radiol Clin North Am.* 2012;50:823-839.
- Mulleman D, Mammou S, Griffoul I, et al. Pathophysiology of disk-related sciatica, I: evidence supporting a chemical component. *Joint Bone Spine.* 2006;73:151-158.
- Mulleman D, Mammou S, Griffoul I, et al. Pathophysiology of disk-related low back pain and sciatica, II: evidence supporting treatment with TNF-alpha antagonists. *Joint Bone Spine.* 2006;73:270-277.
- Murthy NS. Imaging of stress fractures of the spine. *Radiol Clin North Am.* 2012;50:799-821.
- North American Spine Society. *Evidence-Based Clinical Guidelines for Multidisciplinary Spine Care, Diagnosis and Treatment of Degenerative Lumbar Spinal Stenosis.* Burr Ridge, Ill: North American Spine Society; 2011.

The references for this chapter can be found at www.expertconsult.com.

REFERENCES

- Deyo RA, Mirza SK, Martin BI. Back pain prevalence and visit rates. *Spine*. 2006;31:2724-2727.
- Hart LG, Deyo RA, Cherkin DC. Physician office visits for low back pain: frequency, clinical evaluation, and treatment patterns from a U.S. national survey. *Spine*. 1995;20:11-19.
- Koes BW, van Tulder MW, Thomas S. Diagnosis and treatment of low back pain. *BMJ*. 2006;332(7555):1430-1434.
- Deyo RA, Mirza SK, Turner JA, et al. Overtreating chronic back pain: time to back off? *J Am Board Fam Med*. 2009;22:62-68.
- Ivanova JI, Birnbaum HG, Schiller M, et al. Real-world practice patterns, health-care utilization, and costs in patients with low back pain: the long road to guideline-concordant care. *Spine J*. 2011;11:622-632.
- Pham HH, Landon BE, Reschovsky JD, et al. Rapidity and modality of imaging for acute low back pain in elderly patients. *Arch Intern Med*. 2009;169:972-981.
- Friedman BW, Chilstrom M, Bijur PE, et al. Diagnostic testing and treatment of low back pain in United States emergency departments. *Spine*. 2010;35:E1406-E1411.
- U.S. Department of Health and Human Services. Hospital Compare. 2011. Available at www.hospitalcompare.hhs.gov/hospital-search.aspx.
- Martin BI, Deyo RA, Mirza SK, et al. Expenditures and health status among adults with back and neck problems. *JAMA*. 2008;299:656-664.
- Freburger JK, Holmes GM, Agans RP, et al. The rising prevalence of chronic low back pain. *Arch Intern Med*. 2009;169:251-258.
- Chou R, Deyo RA, Jarvik JG. Appropriate use of lumbar imaging for evaluation of low back pain. *Radiol Clin North Am*. 2012;50:569-585.
- Jarvik JG, Deyo R. Diagnostic evaluation of low back pain with emphasis on imaging. *Ann Intern Med*. 2002;137:586-597.
- Nathan H. Osteophytes of the vertebral column: an anatomical study of their development according to age, race, and sex, with consideration as to their etiology and significance. *J Bone Joint Surg Am*. 1962;44:243-268.
- Hult L. The Munkfors investigation. *Acta Orthop Scand Suppl*. 1954;16:1-76.
- Hult L. Cervical, dorsal and lumbar spinal syndromes. *Acta Orthop Scand Suppl*. 1954;17:1-102.
- Hitselberger WE, Witten RM. Abnormal myelograms in asymptomatic patients. *J Neurosurg*. 1968;28:204-206.
- Wiesel SW, Tsourmas N, Feffer HL, et al. A study of computer-assisted tomography, I: the incidence of positive CAT scans in an asymptomatic group of patients. *Spine*. 1984;9:549-551.
- Boden SD, Davis DO, Dina TS, et al. Abnormal magnetic-resonance scans of the lumbar spine in asymptomatic subjects: a prospective investigation. *J Bone Joint Surg Am*. 1990;72:403-408.
- Jarvik JJ, Hollingworth W, Heagerty P, et al. The Longitudinal Assessment of Imaging and Disability of the Back (LAID Back) study. *Spine*. 2001;26:1158-1166.
- Hellstrom M, Jacobsson B, Sward L, et al. Radiologic abnormalities of the thoraco-lumbar spine in athletes. *Acta Radiol*. 1990;31:127-132.
- Weinreb JC, Wolbarsht LB, Cohen JM, et al. Prevalence of lumbosacral intervertebral disk abnormalities on MR images in pregnant and asymptomatic nonpregnant women. *Radiology*. 1989;170:125-128.
- Jensen MC, Brant-Zawadzki MN, Obuchowski N, et al. Magnetic resonance imaging of the lumbar spine in people without back pain. *N Engl J Med*. 1994;331:69-73.
- Boos N, Rieder R, Schade V, et al. 1995 Volvo Award in clinical sciences: the diagnostic accuracy of magnetic resonance imaging, work perception, and psychosocial factors in identifying symptomatic disc herniation. *Spine*. 1995;20:2613-2625.
- Stadnik TW, Lee RR, Coen HL, et al. Annular tears and disk herniation: prevalence and contrast enhancement on MR images in the absence of low back pain or sciatica. *Radiology*. 1998;206:49-55.
- Weishaupt D, Zanetti M, Hodler J, et al. MR Imaging of the lumbar spine: prevalence of intervertebral disc extrusion and sequestration, nerve root compression, end plate abnormalities, and osteoarthritis of the facet joint in asymptomatic volunteers. *Radiology*. 1998;209:661-666.
- Kanayama M, Togawa D, Takahashi C, et al. Cross-sectional magnetic resonance imaging study of lumbar disc degeneration in 200 healthy individuals. *J Neurosurg Spine*. 2009;11:501-507.
- Kjaer P, Leboeuf-Yde C, Sorensen JS, et al. An epidemiologic study of MRI and low back pain in 13-year-old children. *Spine*. 2005;30:798-806.
- Salminen JJ, Erkintalo MO, Pentti J, et al. Recurrent low back pain and early disc degeneration in the young. *Spine*. 1999;24:1316-1321.
- Takatalo J, Karppinen J, Niinimäki J, et al. Prevalence of degenerative imaging findings in lumbar magnetic resonance imaging among young adults. *Spine*. 2009;34:1716-1721.
- Matsumoto M, Fujimura Y, Suzuki N, et al. MRI of cervical intervertebral discs in asymptomatic subjects. *J Bone Joint Surg Br*. 1998;80:19-24.
- Boden SD, McCowin PR, Davis DO, et al. Abnormal magnetic-resonance scans of the cervical spine in asymptomatic subjects: a prospective investigation. *J Bone Joint Surg Am*. 1990;72:1178-1184.
- Teresi LM, Lufin RB, Reicher MA, et al. Asymptomatic degenerative disc disease and spondylolysis of the cervical spine: MR imaging. *Radiology*. 1987;164:82-88.
- Wood KB, Garvey TA, Gundry C, et al. Magnetic resonance imaging of the thoracic spine: evaluation of asymptomatic individuals. *J Bone Joint Surg Am*. 1995;77:1631-1638.
- Nachemson AL. Disc pressure measurements. *Spine*. 1981;6:93-97.
- Inufusa A, An HS, Lim TH, et al. Anatomic changes of the spinal canal and intervertebral foramen associated with flexion-extension movement. *Spine*. 1996;21:2412-2420.
- Fujiwara A, An HS, Lim TH, et al. Morphologic changes in the lumbar intervertebral foramen due to flexion-extension, lateral bending, and axial rotation: an in vitro anatomic and biomechanical study. *Spine*. 2001;26:876-882.
- Schmid MR, Stucki G, Duewelle S, et al. Changes in cross-sectional measurements of the spinal canal and intervertebral foramina as a function of body position: in vivo studies on an open-configuration MR system. *AJR Am J Roentgenol*. 1999;172:1095-1102.
- Danielson B, Willén J. Axially loaded magnetic resonance image of the lumbar spine in asymptomatic individuals. *Spine*. 2001;26:2601-2606.
- Hansson T, Suzuki N, Hebelka H, et al. The narrowing of the lumbar spinal canal during loaded MRI: the effects of the disc and ligamentum flavum. *Eur Spine J*. 2009;18:679-686.
- Madsen R, Jensen TS, Pope M, et al. The effect of body position and axial load on spinal canal morphology: an MRI study of central spinal stenosis. *Spine*. 2008;33:617.
- Weishaupt D, Schmid MR, Zanetti M, et al. Positional MR imaging of the lumbar spine: does it demonstrate nerve root compromise not visible at conventional MR imaging? *Radiology*. 2000;215:247-253.
- Zamani AA, Moriarty T, Hsu L, et al. Functional MRI of the lumbar spine in erect position in a superconducting open-configuration MR system: preliminary results. *J Magn Reson Imaging*. 1998;8:1329-1333.
- Chen IH, Vasavada A, Panjabi M. Kinematics of the cervical spine canal: changes with sagittal plane loads. *J Spinal Disord*. 1994;7:93-101.
- Muhle C, Weinert D, Falliner A, et al. Dynamic changes of the spinal canal in patients with cervical spondylosis at flexion and extension using magnetic resonance imaging. *Invest Radiol*. 1998;33:444-449.
- Zhang L, Zeitoun D, Rangel A, et al. Preoperative evaluation of the cervical spondylotic myelopathy with flexion-extension magnetic resonance imaging: about a prospective study of fifty patients. *Spine*. 2011;36:E1134-E1139.
- Kitagawa T, Fujiwara A, Kobayashi N, et al. Morphologic changes in the cervical neural foramen due to flexion and extension: in vivo imaging study. *Spine*. 2004;29:2821-2825.
- Torgerson WR, Dotter WE. Comparative roentgenographic study of the asymptomatic and symptomatic lumbar spine. *J Bone Joint Surg Am*. 1976;58:850-853.
- White AP, Biswas D, Smart LR, et al. Utility of flexion-extension radiographs in evaluating the degenerative cervical spine. *Spine*. 2007;32:975-979.
- Willén J, Danielson B, Gaulitz A, et al. Dynamic effects on the lumbar spinal canal: axially loaded CT-myelography and MRI in patients with sciatica and/or neurogenic claudication. *Spine*. 1997;22:2968-2976.
- North American Spine Society. *Evidence-based clinical guidelines for multidisciplinary spine care, diagnosis and treatment of degenerative lumbar spinal stenosis*. Burr Ridge, Ill: North American Spine Society; 2011.

51. Willén J, Wessberg PJ, Danielsson B. Surgical results in hidden lumbar spinal stenosis detected by axial loaded computed tomography and magnetic resonance imaging: an outcome study. *Spine*. 2008;33:E109-E115.
52. Chou R, Fu R, Carrino JA, et al. Imaging strategies for low-back pain: systematic review and meta-analysis. *Lancet*. 2009;373(9662):463-472.
53. Carragee E, Alamin T, Cheng I, et al. Are first-time episodes of serious LBP associated with new MRI findings? *Spine J*. 2006;6:624-635.
54. Modic MT, Obuchowski NA, Ross JS, et al. Acute low back pain and radiculopathy: MR imaging findings and their prognostic role and effect on outcome. *Radiology*. 2005;237:597-604.
55. Mettler FA, Huda W, Yoshizumi T, et al. Effective doses in radiology and diagnostic nuclear medicine: a catalog. *Radiology*. 2008;48:254-263.
56. Berrington de Gonzalez A, Mahesh M, Kim KP, et al. Projected cancer risks from computed tomographic scans performed in the United States in 2007. *Arch Intern Med*. 2009;169:2071-2077.
57. Fazel R, Krumholz HM, Wang Y, et al. Exposure to low-dose ionizing radiation from medical imaging procedures. *N Engl J Med*. 2009;361:849-857.
58. E-publication Centers for Medicare & Medicaid Services. Available at www.cms.hhs.gov. Accessed on May 29, 2012.
59. Kendrick D, Fielding K, Bentley E, et al. Radiography of the lumbar spine in primary care patients with low back pain: randomised controlled trial. *BMJ*. 2001;322:400-405.
60. Jarvik JG, Hollingworth W, Martin B, et al. Rapid magnetic resonance imaging vs radiographs for patients with low back pain. *JAMA*. 2003;289:2810-2818.
61. Lurie JD, Birkmeyer NJ, Weinstein JN. Rates of advanced spinal imaging and spine surgery. *Spine*. 2003;28:616-620.
62. Webster BS, Cifuentes M. Relationship of early magnetic resonance imaging for work-related acute low back pain with disability and medical utilization outcomes. *J Occup Environ Med*. 2010;52:900-907.
63. Agency for Health Care Policy and Research. Acute low back problems in adults: assessment and treatment. *AHCPR Clinical Practice Guidelines*. 1994;14:iii-iv, 1-25.
64. Davis PC, Wippold II FJ, Brunberg JA, et al. ACR appropriateness criteria on low back pain. *J Am Coll Radiol*. 2009;6:401-407.
65. Chou R, Qaseem A, Snow V, et al. Diagnosis and treatment of low back pain: a joint clinical practice guideline from the American College of Physicians and the American Pain Society. *Ann Intern Med*. 2007;147:478-491.
66. Chou R, Qaseem A, Owens DK, et al. Diagnostic imaging for low back pain: advice for high-value health care from the American College of Physicians. *Ann Intern Med*. 2011;154:181-189.
67. Suarez-Almazor ME, Belseck E, Russell AS, et al. Use of lumbar radiographs for the early diagnosis of low back pain. *JAMA*. 1997;277:1782-1786.
68. Deyo R, Diehl A. Cancer as a cause of back pain: frequency, clinical presentation, and diagnostic strategies. *J Gen Intern Med*. 1988;3:230-238.
69. van Tulder MW, Assendelft WJ, Koes BW, et al. Spinal radiographic findings and nonspecific low back pain: a systematic review of observational studies. *Spine*. 1997;22:427-434.
70. Carrino JA, Campbell PD Jr, Lin DC, et al. Effect of spinal segment variants on numbering vertebral levels at lumbar MR imaging. *Radiology*. 2011;259:196-202.
71. Akbar JJ, Weiss KL, Saafir MA, et al. Rapid MRI detection of vertebral numeric variation. *AJR Am J Roentgenol*. 2010;195:465-466.
72. Thawait GV, Chhabra A, Carrino JA. Spine segmentation and enumeration and normal variants. *Radiol Clin North Am*. 2012;50:587-598.
73. Castellvi AE, Goldstein LA, Chan DP. Lumbosacral transitional vertebrae and their relationship with lumbar extradural defects. *Spine*. 1984;9:493-495.
74. Wood KB, Kos P, Schendel M, et al. Effect of patient position on the sagittal-plane profile of the thoracolumbar spine. *J Spinal Disord*. 1996;9:165-169.
75. Hall FM. Back pain and the radiologist. *Radiology*. 1980;137:861-863.
76. DePalma MJ, Ketchum JM, Saullo T. What is the source of chronic low back pain and does age play a role? *Pain Med*. 2011;12:224-233.
77. Maus TP, Aprill CN. Lumbar discogenic pain, provocation diskography, and imaging correlates. *Radiol Clin North Am*. 2012;50:681-704.
78. Depalma MJ, Ketchum JM, Saullo TR. Multivariable analyses of the relationships between age, gender, and body mass index and the source of chronic low back pain. *Pain Med*. 2012;13:498-506.
79. Schwarzer AC, Aprill CN, Derby R, et al. Clinical features of patients with pain stemming from the lumbar zygapophysial joints. Is the lumbar facet syndrome a clinical entity? *Spine*. 1994;19:1132-1137.
80. Schwarzer A, Wang SC, Bogduk N, et al. Prevalence and clinical features of lumbar z joint pain: a study in an Australian population w/chronic low back pain. *Ann Rheum Dis*. 1995;54:100-106.
81. Bogduk N, ed. Practice guidelines for spinal diagnostic procedures. San Francisco: International Spine Intervention Society; 2004.
82. Guyer R, Ohnmeiss D. Lumbar discography. *Spine J*. 2003;3(suppl 3):11S-27S.
83. Manchikanti L, Glaser S, Wolfer L, et al. Systematic review of lumbar discography as a diagnostic test for chronic low back pain. *Pain Physician*. 2009;2:541-559.
84. Chou R, Loeser J, Owens D, et al. Interventional therapies, surgery, and interdisciplinary rehabilitation for low back pain: evidence based clinical practice guidelines from the American Pain Society. *Spine*. 2009;34:1066-1077.
85. Cohen SP, Larkin TM, Barna SA, et al. Lumbar discography: a comprehensive review of outcome studies, diagnostic accuracy, and principles. *Reg Anesth Pain Med*. 2005;30:163-183.
86. Walsh TR, Weinstein JN, Spratt KF, et al. Lumbar discography in normal subjects: a controlled, prospective study. *J Bone Joint Surg Am*. 1990;72:1081-1088.
87. Korecki C, Costi J, Iatridis J. Needle puncture injury affects intervertebral disc mechanics and biology in an organ culture model. *Spine*. 2008;33:235-241.
88. Carragee E, Don A, Hurwitz E, et al. Does discography cause accelerated progression of degenerative changes in the lumbar disc: a ten-year matched cohort study. *Spine*. 2009;34:2338-2345.
89. Hancock M, Maher C, Latimer, et al. Systematic review of tests to identify the disc, SJJ or facet joint as the source of low back pain. *Eur Spine J*. 2007;16:1539-1550.
90. Maus TP, Martin DP. Imaging for discogenic pain. In: Kapural L, Kim P, Deer T, eds. *Diagnosis, Management and Treatment of Discogenic Pain*. Philadelphia: Elsevier/Saunders; 2012: 38.
91. Ito M, Incorvaia K, Yu S, et al. Predictive signs of discogenic lumbar pain on magnetic resonance imaging with discography correlation. *Spine*. 1998;23:1252-1258.
92. Lim C, Jee W, Son B, et al. Discogenic lumbar pain: association with MRI imaging and CT discography. *Eur J Radiol*. 2005;54:431-437.
93. O'Neill C, Kurgansky M, Kaiser J, et al. Accuracy of MRI for diagnosis of discogenic pain. *Pain Physician*. 2008;11:311-326.
94. Kang C, Kim Y, Lee S, et al. Can magnetic resonance imaging accurately predict concordant pain provocation during provocative disc injection? *Skeletal Radiol*. 2009;38:877-885.
95. Osti O, Fraser R. MRI and discography of annular tears and intervertebral disc degeneration. *J Bone Joint Surg Br*. 1992;74:431-435.
96. Horton C, Daftari T. Which disc visualized by magnetic resonance imaging is actually a source of pain? *Spine*. 1992;17(suppl 6):S164-S171.
97. Weishaupt D, Zanetti M, Hodler J, et al. Painful lumbar disk derangement: relevance of endplate abnormalities at MR imaging. *Radiology*. 2001;218:420-427.
98. Lei D, Rege A, Koti M, et al. Painful disc lesion: can modern biplanar magnetic resonance imaging replace discography. *J Spinal Disord Tech*. 2008;21:430-435.
99. Pearce RH, Thompson JP, Bebault GM, et al. Magnetic resonance imaging reflects the chemical changes of aging degeneration in the human intervertebral disk. *J Rheumatol Suppl*. 1991;27:42-43.
100. Pfirrmann CW, Metzendorf A, Zanetti M, et al. Magnetic resonance classification of lumbar intervertebral disc degeneration. *Spine*. 2001;26:1873-1878.
101. Modic MT, Steinberg PM, Ross JS, et al. Degenerative disk disease: assessment of changes in vertebral body marrow with MR imaging. *Radiology*. 1988;166(1 Pt 1):193-199.
102. Ohtori S, Inoue G, Ito T, et al. Tumor necrosis factor-immunoreactive cells and PGP 9.5-immunoreactive nerve fibers in vertebral endplates of patients with discogenic low back pain and Modic type 1 or type 2 changes on MRI. *Spine*. 2006;31:1026-1031.

103. Toyone T, Takahashi K, Kitahara H, et al. Vertebral bone-marrow changes in degenerative lumbar disc disease: an MRI study of 74 patients with low back pain. *J Bone Joint Surg Br.* 1994;76:757-764.
104. Albert HB, Manniche C. Modic changes following lumbar disc herniation. *Eur Spine J.* 2007;16:977-982.
105. Braithwaite IJ, White J, Saifuddin A, et al. Vertebral end-plate (Modic) changes on lumbar spine MRI: correlation with pain reproduction at lumbar discography. *Eur Spine J.* 1998;7:363-368.
106. Kokkonen S, Kurunlahti M, Tervonen O, et al. Endplate degeneration observed on magnetic resonance imaging of the lumbar spine. *Spine.* 2002;27:2274-2278.
107. Aprill C, Bogduk N. High-intensity zone: a diagnostic sign of painful lumbar disc on magnetic resonance imaging. *Br J Radiol.* 1992;65:361-369.
108. Schellhas K, Pollei S, Gundry C, et al. Lumbar disk high-intensity zone: correlation of magnetic resonance imaging and discography. *Spine.* 1996;21:79-86.
109. Ricketson R, Simmons J, Hauser W. The prolapsed intervertebral disc: the high intensity zone with discography correlation. *Spine.* 1996;21:2758-2762.
110. Saifuddin A, Braithwaite I, White J, et al. The value of magnetic resonance imaging in the demonstration of annular tears. *Spine.* 1998;23:453-457.
111. Smith B, Hurwitz E, Solsberg D, et al. Interobserver reliability of detecting lumbar intervertebral disc high-intensity zone on magnetic resonance imaging and association of high-intensity zone with pain and annular disruption. *Spine.* 1998;23:2074-2080.
112. Carragee E, Paragioudakis S, Khurana S. Lumbar high-intensity zone and discography in subjects without low back problems. *Spine.* 2000;25:2987-2992.
113. Peng B, Hou S, Wu W. The pathogenesis and clinical significance of a high-intensity zone (HIZ) of lumbar intervertebral disc on MRI imaging in the patient with discogenic low back pain. *Eur Spine J.* 2006;15:583-587.
114. Bogduk N. Point of view: predictive signs of discogenic lumbar pain on magnetic resonance imaging with discography correlation. *Spine.* 1998;23:1259-1260.
115. Okada E, Matsumoto M, Fujiwara H, et al. Disc degeneration of cervical spine on MRI in patients with lumbar disc herniation: comparison study with asymptomatic volunteers. *Eur Spine J.* 2011;20:585-591.
116. Parfenchuck TA, Janssen ME. A correlation of cervical magnetic resonance imaging and discography/computed tomographic discograms. *Spine.* 1994;19:2819-2825.
117. Schellhas KP, Smith MD, Gundry CR, et al. Cervical discogenic pain: prospective correlation of magnetic resonance imaging and discography in asymptomatic subjects and pain sufferers. *Spine.* 1996;21:300-311.
118. Zheng Y, Liew SM, Simmons ED. Value of magnetic resonance imaging and discography in determining the level of cervical discectomy and fusion. *Spine.* 2004;29:2140-2145, discussion 2146.
119. Ashton IK, Ashton BA, Gibson SJ, et al. Morphological basis for back pain: the demonstration of nerve fibers and neuropeptides in the lumbar facet joint capsule but not in ligamentum flavum. *J Orthop Res.* 1992;1:72-79.
120. Igarashi A, Kikuchi S, Konno S, et al. Inflammatory cytokines released from the facet joint tissue in degenerative lumbar spinal disorders. *Spine.* 2004;29:2091-2095.
121. Schwarzer AC, Wang SC, O'Driscoll D, et al. The ability of computed tomography to identify a painful zygapophysial joint in patients with chronic low back pain. *Spine.* 1995;20:907-912.
122. Cohen SP, Bajwa ZH, Kraemer JJ, et al. Factors predicting success and failure for cervical facet radiofrequency denervation: a multicenter analysis. *Reg Anesth Pain Med.* 2007;32:495-503.
123. Wybier M. Imaging of lumbar degenerative changes involving structures other than disk space. *Radiol Clin North Am.* 2001;39:101-114.
124. Dolan AL, Ryan PJ, Arden NK, et al. The value of SPECT scans in identifying back pain likely to benefit from facet joint injection. *Br J Rheumatol.* 1996;35:1269-1273.
125. Holder LE, Machin JL, Asdourian PL, et al. Planar and high-resolution SPECT bone imaging in the diagnosis of facet syndrome. *J Nucl Med.* 1995;36:37-44.
126. Pneumaticos SG, Chatziioannou SN, Hipp JA, et al. Low back pain: prediction of short-term outcome of facet joint injection with bone scintigraphy. *Radiology.* 2006;238:693-698.
127. McDonald M, Cooper R, Wang MY. Use of computed tomography-single-photon emission computed tomography fusion for diagnosing painful facet arthropathy: technical note. *Neurosurg Focus.* 2007;22:E2.
128. Kim KA, Wang MY. MRI-based morphological predictors of SPECT positive facet arthropathy in patients with axial back pain. *Neurosurgery.* 2006;59:147-156.
129. Czervionke LF, Fenton DS. Fat-saturated MR imaging in the detection of inflammatory facet arthropathy (facet synovitis) in the lumbar spine. *Pain Med.* 2008;9:400-406.
130. Okada K. Studies on the cervical facet joints using arthrography of the cervical facet joint. *Nippon Seikeigeka Gakkai Zasshi.* 1981;55:563-580.
131. Murthy NS, Maus TP, Aprill C. The retrodural space of Okada. *AJR Am J Roentgenol.* 2011;196:W784-W789.
132. Fortin JD, Washington WJ, Falco FJ. Three pathways between the sacroiliac joint and neural structures. *AJNR Am J Neuroradiol.* 1999;20:1429-1434.
133. Fortin JD, Tolchin RB. Sacroiliac arthrograms and post-arthrography computerized tomography. *Pain Physician.* 2003;6:287-290.
134. Dreyfuss P, Dreyer SJ, Cole A, et al. Sacroiliac joint pain. *J Am Acad Orthop Surg.* 2004;12:255-265.
135. Cohen SP. Sacroiliac joint pain: a comprehensive review of anatomy, diagnosis, and treatment. *Anesth Analg.* 2005;101:1440-1453.
136. Schwarzer AC, Aprill CN, Bogduk N. The sacroiliac joint in chronic low back pain. *Spine.* 1995;20:31-37.
137. Maigne JY, Alivaliklis A, Pfefer F. Results of sacroiliac joint double block and value of sacroiliac pain provocation tests in 54 patients with low back pain. *Spine.* 1996;21:1889-1892.
138. Elgafy H, Semaan HB, Ebraheim NA, et al. Computed tomography findings in patients with sacroiliac pain. *Clin Orthop.* 201;382:112-118.
139. Maigne JY, Boulahdour H, Chatellier G. Value of quantitative radionuclide bone scanning in the diagnosis of sacroiliac joint syndrome in 32 patients with low back pain. *Eur Spine J.* 1998;7:328-331.
140. Slipman CW, Sterefeld EB, Chou LH, et al. The value of radionuclide imaging the diagnosis of sacroiliac joint syndrome. *Spine.* 1996;21:2251-2254.
141. Bywaters EG, Evans S. The lumbar interspinous bursae and Bastrup's syndrome: an autopsy study. *Rheumatol Int.* 1982;2:87-96.
142. Kwong Y, Rao N, Latief K. MDCT Findings in Bastrup's disease: disease or normal feature of the aging spine? *Am J Roentgenol.* 2011;196:1156-1159.
143. Maes R, Morrison WB, Parker L, et al. Lumbar interspinous bursitis (Baastrup's disease) in a symptomatic population: prevalence on magnetic resonance imaging. *Spine.* 2008;33:E211-E215.
144. Tini PG, Wieser C, Zinn WM. The transitional vertebra of the lumbosacral spine: its radiological classification, incidence, prevalence, and clinical significance. *Rheumatol Rehabil.* 1977;16:180-185.
145. Jonsson B, Stromqvist B, Egund N. Anomalous lumbosacral articulations and low back pain: evaluation and treatment. *Spine.* 1989;14:831-834.
146. Brault JS, Smith J, Currier BL. Partial lumbosacral transitional vertebra resection for contralateral facetogenic pain. *Spine.* 2001;26:226-229.
147. DeAndres J, Chaves S. Coccygodynia: a proposal for an algorithm for treatment. *J Pain.* 2003;4:257-266.
148. Maigne JY, Lagauche D, Doursounian L. Instability of the coccyx in coccydynia. *J Bone Joint Surg.* 2000;82-B:1038-1041.
149. Etmann M, Girardi FP, Khan SN, et al. Revision strategies for lumbar pseudoarthrosis. *Orthop Clin North Am.* 2002;33:381-392.
150. Deckey JE, Court C, Bradford DS. Loss of sagittal plane correction after removal of spinal implant. *Spine.* 2000;25:2453-2460.
151. Ray CD. Threaded fusion cages for lumbar interbody fusions: an economic comparison with 360-degree fusions. *Spine.* 1997;22:681-685.
152. Gates GF, McDonald RJ. Bone SPECT of the back after lumbar surgery. *Clin Nucl Med.* 1999;24:395-403.
153. Ghiselli G, Wang JC, Bhatia NN, et al. Adjacent segment degeneration in the lumbar spine. *J Bone Joint Surg Am.* 2004;86A:1497-1503.
154. Waguespack A, Schofferman J, Slosar P, et al. Etiology of long-term failures of lumbar spine surgery. *Pain Med.* 2002;18-22.
155. Slipman CW, Shin CH, Patel RK, et al. Etiologies of failed back surgery syndrome. *Pain Med.* 2002;3:200-214, discussion 214-217.
156. Mulleman D, Mammou S, Griffoul I, et al. Pathophysiology of disk-related sciatica, I: evidence supporting a chemical component. *Joint Bone Spine.* 2006;73:151-158.

157. Mulleman D, Mammou S, Griffoul I, et al. Pathophysiology of disk-related low back pain and sciatica, II: evidence supporting treatment with TNF-alpha antagonists. *Joint Bone Spine*. 2006;73:270-277.
158. Fardon DF, Milette PC. Combined Task Forces of the North American Spine Society, American Society of Spine Radiology, and American Society of Neuroradiology. Nomenclature and classification of lumbar disc pathology: recommendations of the combined task forces of the North American Spine Society, American Society of Spine Radiology, and American Society of Neuroradiology. *Spine*. 2001;26:E93-E113.
159. Lurie JD, Tosteson AN, Tosteson TD, et al. Reliability of magnetic resonance imaging readings for lumbar disc herniation in the Spine Patient Outcomes Research Trial (SPORT). *Spine*. 2008;33:991-998.
160. Pfirrmann CW, Dora C, Schmid MR, et al. MR image-based grading of lumbar nerve root compromise due to disk herniation: reliability study with surgical correlation. *Radiology*. 2004;230:583-588.
161. Chiba K, Toyama Y, Matsumoto M, et al. Intraspinous cyst communicating with the intervertebral disc in the lumbar spine: discal cyst. *Spine*. 2001;26:2112-2118.
162. Peng B, Wu W, Li Z, et al. Chemical radiculitis. *Pain*. 2007;127:11-16.
163. Ross JS. MR imaging of the postoperative lumbar spine. *MRI Clin North Am*. 1999;7:513-524.
164. Ross JS, Robertson JT, Frederickson RC, et al. Association between peridural scar and recurrent radicular pain after lumbar discectomy: magnetic resonance evaluation. ADCON-L European Study Group. *Neurosurgery*. 1996;38:855-861, discussion 861-863.
165. Saal JA, Saal JS, Herzog RJ. The natural history of lumbar intervertebral disc extrusions treated nonoperatively. *Spine*. 1990;15:683-686.
166. Maigne JY, Rime B, Deligne B. Computed tomographic follow-up study of forty-eight cases of nonoperatively treated lumbar intervertebral disk herniation. *Spine*. 1992;17:1071-1074.
167. Bush K, Cowan N, Katz DE, et al. The natural history of sciatica associated with disc pathology: a prospective study with clinical and independent radiologic follow-up. *Spine*. 1992;17:1205-1212.
168. Jensen TS, Albert HB, Soerensen JS, et al. Natural course of disc morphology in patients with sciatica: an MRI study using a standardized qualitative classification system. *Spine*. 2006;31:1605-1612, discussion 1613.
169. Masui T, Yukawa Y, Nakamura S, et al. Natural history of patients with lumbar disc herniation observed by magnetic resonance imaging for minimum 7 years. *J Spinal Disord Tech*. 2005;18:121-126.
170. Willén J, Danielson B. The diagnostic effect from axial loading of the lumbar spine during computed tomography and magnetic resonance imaging in patients with degenerative disorders. *Spine*. 2001;26:2607-2614.
171. Steurer J, Roner S, Gnannt R, et al. Quantitative radiologic criteria for the diagnosis of lumbar spinal stenosis: a symptomatic literature review. *BMC Musculoskeletal Disord*. 2011;12:175.
172. Doyle AJ, Merrilees M. Synovial cysts of the lumbar facet joints in a symptomatic population. *Spine*. 2004;29:874-878.
173. Metellus P, Fuentes S, Adetchessi T, et al. Retrospective study of 77 patients harbouring lumbar synovial cysts: functional and neurological outcome. *Acta Neurochir*. 2005. doi 10.1007/s00701-005-0650-z
174. Apostolaki E, Davies AM, Evans N, et al. MR imaging of lumbar facet joint synovial cyst. *Eur Radiol*. 2000;10:615-623.
175. Lyons MK, Atkinson JLD, Wharen RE, et al. Surgical evaluation and management of lumbar synovial cysts: the Mayo Clinic experience. *J Neurosurg*. 2000;93:53-57.
176. Sabers SR, Ross SR, Grogg BE. Procedure-based nonsurgical management of lumbar zygapophysial joint cyst induced radicular pain. *Arch Phys Med Rehabil*. 2005;86:1767-1771.
177. Martha JF, Swaim B, Wang DA, et al. Outcome of percutaneous rupture of lumbar synovial cysts: a case series of 101 patients. *Spine J*. 2009;9:899-904.
178. Radhakrishnan K, Litchy WJ, O'Fallon WM, et al. Epidemiology of cervical radiculopathy: a population-based study from Rochester, Minnesota, 1976 through 1990. *Brain*. 1994;117(Pt 2):325-335.
179. Levi N, Gjerris F, Dons K. Thoracic disc herniation: unilateral transpedicular approach in 35 consecutive patients. *J Neurosurg Sci*. 1999;43:37-42.
180. Stillerman CB, Chen TC, Douldwell WE, et al. Experience in the surgical management of 82 symptomatic herniated thoracic discs and review of the literature. *J Neurosurg*. 1998;88:623-633.
181. Kauppila LI, Eustace S, Kiel D, et al. Degenerative displacement of lumbar vertebrae: a 25-year follow-up study in Framingham. *Spine*. 1998;23:1868-1873.
182. Deyo RA. Treatment of lumbar spinal stenosis: a balancing act. *Spine J*. 2010;19:625-627.
183. Amundsen T, Weber H, Lilleås F, et al. Lumbar spinal stenosis: clinical and radiologic features. *Spine*. 1995;20:1178-1186.
184. Kalichman L, Cole R, Kim D, et al. Spinal stenosis prevalence and association with symptoms: the Framingham Study. *Spine J*. 2009;9:545-550.
185. North American Spine Society. Evidence-Based Clinical Guidelines for Multidisciplinary Spine Care, Diagnosis and Treatment of Degenerative Lumbar Spinal Stenosis. Burr Ridge, Ill: North American Spine Society; 2011.
186. Verbiest H. A radicular symptom from developmental narrowing of the lumbar vertebral canal. *J Bone Joint Surg Br*. 1954;36:230-237.
187. Takahashi K, Olmarker K, Porter RW, et al. Double level cauda equina compression: an experimental study with continuous monitoring of intraneural blood flow in the porcine cauda equina. *J Orthop Res*. 1993;11:104-109.
188. Olmarker K, Rydevik B. Single-level versus double-level nerve root compression: an experimental study on the porcine cauda equina with analysis of nerve impulse conduction properties. *Clin Orthop*. 1992;279:35-39.
189. Kobayashi S, Uchida K, Takeno K, et al. Imaging of cauda equina edema in lumbar canal stenosis by using gadolinium-enhanced MR imaging experimental constriction injury. *AJNR Am J Neuroradiol*. 2006;27:346-353.
190. Sato K, Kikuchi S. Clinical analysis of two-level compression of the cauda equina and the nerve roots in lumbar spinal canal stenosis. *Spine*. 1997;16:1898-1904.
191. Porter RW, Ward D. Cauda equina dysfunction: the significance of two-level pathology. *Spine*. 1992;17:19-15.
192. Morishita Y, Hida S, Naito M, et al. Measurement of the local pressure of intervertebral foramen and the electrophysiological values of the spinal nerve roots in the vertebral foramen. *Spine*. 2006;31:3076-3080.
193. Singh K, Samartzis D, Vaccaro AR, et al. Congenital lumbar spinal stenosis: a prospective control-matched, cohort radiographic analysis. *Spine J*. 2005;5:615-622.
194. Siebert E, Prüss H, Klingebiel R, et al. Lumbar spinal stenosis: syndrome, diagnostics and treatments. *Nat Rev Neurol*. 2009;5:392-403.
195. Lurie JD, Tosteson AN, Tosteson TD, et al. Reliability of readings of magnetic resonance imaging features of lumbar spinal stenosis. *Spine*. 2008;33:1605-1610.
196. Min JH, Jang JS, Lee SH. Clinical significance of redundant nerve roots of the cauda equina in lumbar spinal stenosis. *Clin Neurol Neurosurg*. 2008;110:14-18.
197. Barz T, Melloh M, Staub LP, et al. Nerve root sedimentation sign: evaluation of a new radiological sign in lumbar spinal stenosis. *Spine*. 2010;5:8927.
198. Jinkins R. Gd-DTPA enhanced MR of the lumbar spinal canal in patients with claudication. *J Comput Assist Tomogr*. 1993;17:555-562.
199. Hamanishi C, Matukura N, Fujita M, et al. Cross-sectional area of the stenotic lumbar dural tube measured from the transverse views of magnetic resonance imaging. *J Spinal Disord*. 1994;7:388-393.
200. Sirvanci M, Bhatia M, Ganiyusufoglu KA, et al. Degenerative lumbar spinal stenosis: correlation with Oswestry Disability Index and MR imaging. *Eur Spine J*. 2008;17:679-685.
201. Baptiste DC, Fehlings MG. Pathophysiology of cervical myelography. *Spine J*. 2006;6(suppl 6):190S-197S.
202. Stookey B. Compression of the spinal cord due to ventral extradural cervical chondromas. *Arch Neurol Psychiatry*. 1928;20:275-291.
203. Edwards WC, LaRocca H. The developmental segmental sagittal diameter of the cervical spinal patients with cervical spondylosis. *Spine*. 1983;8:20-27.
204. Morishita Y, Naito M, Hymanson H, et al. The relationship between the cervical spinal canal diameter and the pathological changes in the cervical spine. *Eur Spine J*. 2009;18:877-883.
205. Morio Y, Teshima R, Nagashima H, et al. Correlation between operative outcomes of cervical compression myelography and MRI of the spinal cord. *Spine*. 2001;26:123.

206. Yu WR, Liu T, Kiehl TG, Fehlings MG. Human neuropathological and animal model evidence supporting a role for Fas-mediated apoptosis and inflammation in cervical spondylotic myelopathy. *Brain*. 2011;134(pt 5):1277-1292.
207. Naganawa T, Miyamoto K, Ogura H, et al. Comparison of magnetic resonance imaging and computed tomogram-myelography for evaluation of cross sections of cervical spine morphology. *Spine*. 2011;36:50-56.
208. Song KJ, Choi BW, Kim GH, et al. Clinical usefulness of CT-myelogram comparing with the MRI in degenerative cervical spinal disorders: is CTM still useful for primary diagnostic tool? *J Spinal Disord Tech*. 2009;22:353-357.
209. Okada Y, Ikata T, Katoh S, et al. Morphologic analysis of the cervical spinal cord, dural tube, and spinal canal by magnetic resonance imaging in normal adults and patients with cervical spondylotic myelopathy. *Spine*. 1994;19:2331-2335.
210. Maus TP. Imaging of spinal stenosis: neurogenic intermittent claudication and cervical spondylotic myelopathy. *Radiol Clin North Am*. 2012;50:651-679.
211. Ozawa H, Sato T, Hyodo H, et al. Clinical significance of intramedullary Gd-DTPA enhancement in cervical myelopathy. *Spinal Cord*. 2010;48:415-422.
212. Cho YE, Shin JJ, Kim K, et al. The relevance of intramedullary high signal intensity and gadolinium (Gd-DTPA) enhancement to the clinical outcome in cervical compressive myelography. *Eur Spine J*. 2011;20:2267-2274.
213. Floeth FW, Stoffels G, Herdmann J, et al. Prognostic value of 18F-FDG PET in monosegmental stenosis and myelopathy of the cervical spinal cord. *J Nucl Med*. 2011;52:1385-1391.
214. Matsumoto S, Nakamura K, Seichi A, et al. Radiographic predictors for the development of myelopathy in patients with ossification of the posterior longitudinal ligament: a multicenter cohort study. *Spine*. 2008;33:2648-2650.
215. Epstein N. Ossification of the cervical posterior longitudinal ligament: a review. *Neurosurg Focus*. 2002;13:ECP1.
216. Burge R, Dawson-Hughes B, Solomon DH, et al. Incidence and economic burden of osteoporosis-related fractures in the United States, 2005-2025. *J Bone Miner Res*. 2007;22:465-475.
217. Lindsay R, Silverman SL, Cooper C, et al. Risk of new vertebral fracture in the year following a fracture. *JAMA*. 2001;285:320-323.
218. Baur A, Stabler A, Arbogast S, et al. Acute osteoporotic and neoplastic vertebral compression fractures: fluid sign at MR imaging. *Radiology*. 2002;225:730-735.
219. Murthy NS. Imaging of stress fractures of the spine. *Radiol Clin North Am*. 2012;50:799-821.
220. Taillandier J, Langue F, Alemanni M, et al. Mortality and functional outcomes of pelvic insufficiency fractures in older patients. *Joint Bone Spine*. 2003;70:287-289.
221. Lourie H. Spontaneous osteoporotic fracture of the sacrum: an unrecognized syndrome of the elderly. *JAMA*. 1982;13(248):715-717.
222. Grangier C, Garcia J, Howarth N, et al. Role of MRI in the diagnosis of insufficiency fractures of the sacrum and acetabular roof. *Skeletal Radiol*. 1997;26:517-524.
223. Fujii M, Abe K, Hayashi K, et al. Honda sign and variants in patients suspected of having a sacral insufficiency fracture. *Clin Nucl Med*. 2005;30:165-169.
224. Rossi F, Dragoni S. The prevalence of spondylolysis and spondylolisthesis in symptomatic elite athletes: radiographic findings. *Radiology*. 2001;7:37-42.
225. Shipley JA, Beukes CA. The nature of the spondylolytic defect: demonstration of a communicating synovial pseudarthrosis in the pars interarticularis. *J Bone Joint Surg Br*. 1998;80:662-664.
226. Fujii K, Katoh S, Sairyo K, et al. Union of defects in the pars interarticularis of the lumbar spine in children and adolescents: the radiological outcome after conservative treatment. *J Bone Joint Surg Br*. 2004;86-B:225-231.
227. Ulmer JL, Mathews VP, Elster AD, et al. MR imaging of lumbar spondylolysis: the importance of ancillary observations. *AJR*. 1997;169:233-239.
228. Hollenberg GM, Beattie PF, Meyers SP, et al. Stress reactions of the lumbar pars interarticularis: the development of a new MRI classification system. *Spine*. 2002;27:181-186.
229. Sakai T, Sairyo K, Mima S, et al. Significance of magnetic resonance imaging signal change in the pedicle in the management of pediatric lumbar spondylolysis. *Spine*. 2010;35:E641-E645.
230. Gregory PL, Batt ME, Kerslake RW, et al. The value of combining single photon emission computerised tomography and computerised tomography in the investigation of spondylolysis. *Eur Spine J*. 2004;13:503-509.
231. Diehn FE. Imaging of spine infection. *Radiol Clin North Am*. 2012;50:777-798.
232. Maiuri F, Iaconetta G, Gallicchio B, et al. Spondylodiscitis: clinical and magnetic resonance diagnosis. *Spine*. 1997;22:1741-1746.
233. Yoon SH, Chung SK, Kim KJ, et al. Pyogenic vertebral osteomyelitis: identification of microorganism and laboratory markers used to predict clinical outcome. *Eur Spine J*. 2010;19:575-582.
234. Hadjipavlou AG, Cesani-Vazquez F, Villaneuva-Meyer J. The effectiveness of gallium citrate Ga 67 radionuclide imaging in vertebral osteomyelitis revisited. *Am J Orthop*. 1998;27:179-183.
235. Pertuiset E, Beaudreuil J, Liote F. Spinal tuberculosis in adults: a study of 103 cases in a developed country, 1980-1994. *Medicine (Baltimore)*. 1999;78:309-320.
236. Hermann K, Bollow M. Magnetic resonance imaging of the axial skeleton in rheumatoid disease. *Best Pract Res Clin Rheumatol*. 2004;18:881-907.
237. Rudwaleit M, van der Heijde D, Landewé R, et al. The development of assessment of SpondyloArthritis International Society classification criteria for axial spondylarthritis (part II): validation and final selection. *Ann Rheum Dis*. 2009;68:777-783.
238. Amrami KA. Imaging of the seronegative spondylarthropathies. *Radiol Clin North Am*. 2012;50:841-854.
239. Heuft-Dorenbosch L, Weijers R, Landewe R, et al. Magnetic resonance imaging changes of sacroiliac joints in patient with recent-onset inflammatory back pain: inter-reader reliability and prevalence of abnormalities. *Arthritis Res Ther*. 2006;9:R11.
240. Atkinson JLD, Miller GM, Krauss WE, et al. Clinical and radiographic features of dural arteriovenous fistula, a treatable cause of myelopathy. *Mayo Clin Proc*. 2001;76:1120-1130.
241. Gilbertson JR, Miller GM, Goldman MS, et al. Spinal dural arteriovenous fistulas: MRI and myelographic findings. *AJNR Am J Neuroradiol*. 1995;16:2049-2057.
242. Morris JM. Imaging of dural arteriovenous fistula. *Radiol Clin North Am*. 2012;50:823-839.